

University of Windsor

## Scholarship at UWindsor

---

Electronic Theses and Dissertations

Theses, Dissertations, and Major Papers

---

7-17-1969

### Non-isothermal flow of air in a vertical pipe.

Jai Krishan Lal Bajaj  
*University of Windsor*

Follow this and additional works at: <https://scholar.uwindsor.ca/etd>

---

#### Recommended Citation

Bajaj, Jai Krishan Lal, "Non-isothermal flow of air in a vertical pipe." (1969). *Electronic Theses and Dissertations*. 6552.

<https://scholar.uwindsor.ca/etd/6552>

This online database contains the full-text of PhD dissertations and Masters' theses of University of Windsor students from 1954 forward. These documents are made available for personal study and research purposes only, in accordance with the Canadian Copyright Act and the Creative Commons license—CC BY-NC-ND (Attribution, Non-Commercial, No Derivative Works). Under this license, works must always be attributed to the copyright holder (original author), cannot be used for any commercial purposes, and may not be altered. Any other use would require the permission of the copyright holder. Students may inquire about withdrawing their dissertation and/or thesis from this database. For additional inquiries, please contact the repository administrator via email ([scholarship@uwindsor.ca](mailto:scholarship@uwindsor.ca)) or by telephone at 519-253-3000ext. 3208.

## INFORMATION TO USERS

This manuscript has been reproduced from the microfilm master. UMI films the text directly from the original or copy submitted. Thus, some thesis and dissertation copies are in typewriter face, while others may be from any type of computer printer.

**The quality of this reproduction is dependent upon the quality of the copy submitted.** Broken or indistinct print, colored or poor quality illustrations and photographs, print bleedthrough, substandard margins, and improper alignment can adversely affect reproduction.

In the unlikely event that the author did not send UMI a complete manuscript and there are missing pages, these will be noted. Also, if unauthorized copyright material had to be removed, a note will indicate the deletion.

Oversize materials (e.g., maps, drawings, charts) are reproduced by sectioning the original, beginning at the upper left-hand corner and continuing from left to right in equal sections with small overlaps.

ProQuest Information and Learning  
300 North Zeeb Road, Ann Arbor, MI 48106-1346 USA  
800-521-0600

**UMI<sup>®</sup>**



NON-ISOTHERMAL FLOW OF AIR  
IN A VERTICAL PIPE

A Thesis  
Submitted to the Faculty of Graduate Studies through the  
Department of Mechanical Engineering in Partial  
Fulfillment of the Requirements for the  
Degree of Master of Applied Science  
at the University of Windsor

by

JAI KRISHAN LAL BAJAJ  
B.TECH(HONS)., I.I.T. KHARAGPUR(INDIA), 1962.

Windsor, Ontario, Canada

1969

UMI Number:EC52734

UMI<sup>®</sup>

---

UMI Microform EC52734  
Copyright 2007 by ProQuest Information and Learning Company.  
All rights reserved. This microform edition is protected against  
unauthorized copying under Title 17, United States Code.

---

ProQuest Information and Learning Company  
789 East Eisenhower Parkway  
P.O. Box 1346  
Ann Arbor, MI 48106-1346

PT-13380

APPROVED BY:

M. G. Colburne

S. di Eran.

J. T. Foster.

247610

## ABSTRACT

The object of this research was to experimentally investigate the non-isothermal flow of air in a vertical pipe in a constant temperature environment. This investigation was mainly concerned with the heat transfer characteristics, the development of velocity profile, and the wall temperature variation. The experiments were conducted at various flow rates ( $N_{Rei} < 4000$ ) and various inlet temperatures ( $t_i < 700^\circ\text{F}$ ). The major part of the investigation was for low flow rates ( $N_{Rei} < 2000$ ) and low inlet temperatures ( $t_i < 200^\circ\text{F}$ ). The effect on the flow of small temperature differences ( $t_i - t_o$ ) was also studied and it was found that even a few degrees difference between inside and ambient would result in a form of turbulent flow at Reynolds numbers as low as 1000. The non-isothermal velocity ratio ( $u_{\max}/\bar{U}$ ) was studied for Reynolds numbers between 1000-4000. The buoyancy effects tended to elongate the velocity profile and in some cases the velocity ratio was found to exceed the parabolic isothermal ratio of 2.0 in the range  $N_{Rei} < 2000$ . The wall temperature was a function of  $t_i$ ,  $t_o$ ,  $N_{Rei}$ ,  $L$  and  $D$ . A correlation between  $t_w$  and these five variables was determined. Local Nusselt number decreased as  $L/D$  ratio increased as expected, and increased with  $t_m/t_w$  in the range of Reynolds numbers tested. The mean and the local Nusselt numbers were found to be higher than the values given by Kays, Graetz, Hausen and others.

## ACKNOWLEDGEMENTS

The author acknowledges with deep gratitude the help, guidance and encouragement of Prof.W.G.Colborne during various stages of this experimental study. He is grateful to Dr.K.Sridhar for his critical comments and advice. Thanks are due to Messers O.Brudy, R.Myers, L.Cory and B.Gordon for their technical assistance in making the probes, setting and checking up the equipment.

The financial assistance from the National Research Council of Canada is gratefully acknowledged.

## TABLE OF CONTENTS

	PAGE
ABSTRACT	iii
ACKNOWLEDGEMENTS	iv
TABLE OF CONTENTS	v
LIST OF FIGURES	vii
NOTATION	x
 CHAPTER	
1. INTRODUCTION	1
2. LITERATURE SURVEY	4
2.1 Graetz Analysis	4
2.2 Effect of Variable Fluid Properties.	5
2.3 Combined Forced and Free Convection.	9
2.4 Simultaneous Development of Temperature and velocity Profiles.	13
2.5 Cooling.	16
3. APPARATUS AND INSTRUMENTATION	
3.1 Basic Description	20
3.2 Flow Meters	20
3.3 Furnace	21
3.4 Test Section	21
3.5 Leakage	22
3.6 Velocity Measurement	22
3.7 Temperature Measurement	24
3.8 Pressure Measurement	25
3.9 Traversing Mechanism	25
4. PROCEDURE AND EXPERIMENTAL RESULTS	26
4.1 Procedure	26
4.2 Heat Transfer and Wall Temperature Results	27
4.3 Velocity Profiles	28
5. DISCUSSION	63
5.1 Axial Variation of Temperature	63

	Page
5.2 Heat Transfer Characteristics	66
5.3 Velocity Ratio $u_{\max}/\bar{U}$	71
5.4 Type of flow	72
5.5 Error Analysis	73
6. CONCLUSIONS	76
BIBLIOGRAPHY	78
APPENDIX A	82
APPENDIX B	87
APPENDIX C	107
APPENDIX D	120
APPENDIX E	123
APPENDIX F	124
VITA AUCTORIS	132

## LIST OF FIGURES

### Figure

- 1 TYPICAL TEMPERATURE BOUNDARY CONDITIONS SHOWING AXIAL VARIATION OF MEAN AND WALL TEMPERATURES
- 2 SCHEMATIC LAYOUT OF EQUIPMENT
- 3 DIMENSIONS OF THE BELL MOUTH AND TEST PIPE
- 4 VARIATION OF  $I/I_0$  WITH  $V$  FOR TWO RESISTANCE RATIOS
- 5 HOT WIRE AND THERMOCOUPLE PROBES
- 6 AXIAL VARIATION OF MEAN AND WALL TEMPERATURES FOR  $N_{Rei} \approx 1500$
- 7 AXIAL VARIATION OF MEAN AND WALL TEMPERATURES FOR  $N_{Rei} \approx 2000$
- 8 AXIAL VARIATION OF MEAN AND WALL TEMPERATURES AT HIGH INLET TEMPERATURES ( $t_i > 600^\circ\text{F}$ )
- 9 AXIAL VARIATION OF WALL TEMPERATURE FOR  $N_{Rei} \approx 600$
- 10 AXIAL VARIATION OF WALL TEMPERATURE FOR  $N_{Rei} \approx 3000$
- 11 AXIAL VARIATION OF WALL TEMPERATURE FOR  $N_{Rei} \approx 4000$
- 12 VARIATION OF  $(t_w - t_o)$  WITH  $(t_i - t_o)$  FOR  $N_{Rei} \approx 600$
- 13 VARIATION OF  $(t_w - t_o)$  WITH  $(t_i - t_o)$  FOR  $N_{Rei} \approx 1000$
- 14 VARIATION OF  $(t_w - t_o)$  WITH  $(t_i - t_o)$  FOR  $N_{Rei} \approx 1500$
- 15 VARIATION OF  $(t_w - t_o)$  WITH  $(t_i - t_o)$  FOR  $N_{Rei} \approx 4000$
- 16 VARIATION OF THE SLOPE  $m$ , ( $m = (t_w - t_o)/(t_i - t_o)$ ) WITH  $N_{Rei}$  AT LOW INLET TEMPERATURES ( $t_i < 200^\circ\text{F}$ )
- 17 VARIATION OF THE SLOPE  $m$ , ( $m = (t_w - t_o)/(t_i - t_o)$ ) WITH  $N_{Rei}$  AT HIGH INLET TEMPERATURES ( $t_i > 600^\circ\text{F}$ )

- 18      EMPIRICAL RELATION FOR WALL TEMPERATURE
- 19      AXIAL VARIATION OF LOCAL NUSSELT NUMBER FOR  $N_{Rei} \approx 600$
- 20      AXIAL VARIATION OF LOCAL NUSSELT NUMBER FOR  
 $N_{Rei} \approx 1000$
- 21      AXIAL VARIATION OF LOCAL NUSSELT NUMBER FOR  
 $N_{Rei} \approx 1500$
- 22      AXIAL VARIATION OF LOCAL NUSSELT NUMBER FOR  
 $N_{Rei} \approx 2000$
- 23      AXIAL VARIATION OF LOCAL NUSSELT NUMBER FOR  
 $N_{Rei} \approx 3000$
- 24      VARIATION OF  $u_{max}/\bar{U}$  AND LOCAL NUSSELT NUMBER WITH  
L/D FOR NON-ISOTHERMAL FLOW AT  $N_{Rei} = 3886$
- 25      AXIAL VARIATION OF LOCAL NUSSELT NUMBER AT HIGH  
INLET TEMPERATURES ( $t_i > 600^\circ\text{F}$ )
- 26      AXIAL VARIATION OF LOCAL NUSSELT NUMBER AT HIGH  
INLET TEMPERATURES ( $t_i > 600^\circ\text{F}$ ) FOR BAJAJ, VISSERS,  
& DROBITCH
- 27      VARIATION OF LOCAL NUSSELT NUMBER WITH GRAETZ  
NUMBER
- 28      VARIATION OF MEAN NUSSELT NUMBER WITH GRAETZ  
NUMBER
- 29      VARIATION OF LOCAL NUSSELT NUMBER WITH  $t_m/t_w$  FOR  
 $N_{Rei} \approx 600, 1000, \& 1500$  AT  $L/D = 24.5$
- 30      VARIATION OF LOCAL NUSSELT NUMBER WITH  $t_m/t_w$  FOR  
 $N_{Rei} \approx 2000, 3000, \& 4000$  AT  $L/D = 24.5$

- 31 VARIATION OF  $u_{\max}/\bar{U}$  WITH L/D FOR NON-ISOTHERMAL FLOW AT  $N_{\text{Rei}} \approx 1000$
- 32 VARIATION OF  $u_{\max}/\bar{U}$  WITH L/D FOR NON ISOTHERMAL FLOW AT  $N_{\text{Rei}} \approx 1500$ .
- 33 VARIATION OF  $u_{\max}/\bar{U}$  WITH L/D FOR NON-ISOTHERMAL FLOW AT  $N_{\text{Rei}} \approx 2000$
- 34 VARIATION OF  $u_{\max}/\bar{U}$  WITH L/D FOR NON-ISOTHERMAL FLOW AT  $N_{\text{Rei}} \approx 3000$

## PHOTOGRAPHS

- F-1 HOT WIRE ANEMOMETER
- F-2 ROTAMETERS
- F-3 TRAVERSING MECHANISM WITH THERMOCOUPLE IN POSITION
- F-4 TRAVERSING MECHANISM ON THE PIPE SHOWING THE PROBE OUT SIDE THE SLOT
- F-5 TRAVERSING MECHANISM ON THE PIPE SHOWING THE PROBE INSIDE THE SLOT

## NOTATION

A	Surface area of pipe, $L^2$
C	Calibration constant for hot-wire
$C_p$	Specific heat at constant pressure, $L^2/\theta^2 t$
$C_v$	Specific heat at constant volume, $L^2/\theta^2 t$
d	Sectional position measured from the wall of the pipe, L
D	Diameter of pipe, L
f	Functional relation
g	Acceleration due to gravity, $L/\theta^2$
h	Film coefficient, $M/\theta^3 t$
$I_0$	Current in hot wire, milliamperes (velocity = 0 f.p.s.)
I	Current in hot wire, milliamperes (velocity = u f.p.s.)
K	Thermal conductivity of air, $M L/\theta^3 t$
L	Length of pipe, L
P	Pressure per unit area, $M/L\theta^2$ .
q	Rate of heat transfer to or from the pipe wall, $M/L^2\theta^3$
r	Radial distance measured from centre of the pipe, L
R	Radius of pipe, L
$R'$	Perfect gas constant, $L^2/t^2\theta$
u	Axial velocity component, $L/\theta$
U	Average velocity, $L/\theta$
t	Temperature in degrees Fahrenheit, t
T	Temperature in degrees absolute

W	Mass flow rate, M/θ
X	Axial distance measured from entrance of the pipe, L
$N_{Gr}$	Grashof number = $\frac{\rho^2 \cdot D^3 \cdot g \cdot \beta \cdot \Delta T}{\mu^2}$
$N_{Gz}$	Graetz number = $\frac{W C_p}{K L} = \frac{\mu^2}{K} N_{Re} \cdot N_{Pr} \cdot \frac{D}{L}$
$N_{Nu}$	Nusselt number = $\frac{h D}{K}$
$N_{Pe}$	Peclet number = $N_{Re} \cdot N_{Pr}$
$N_{Pr}$	Prandtl number = $\frac{C_p \mu}{K}$
$N_{Re}$	Reynolds number = $\frac{\bar{U} D \rho}{\mu}$
$\beta$	Coefficient of thermal expansion = $\frac{1}{T_0}, \frac{1}{t}$
$\mu$	Absolute viscosity, M/Lθ
$\nu$	Kinematic viscosity, L <sup>2</sup> /θ
$\Delta t$	Difference between the bulk mean and wall temperatures
$\rho$	Density, mass per unit volume, M/L <sup>3</sup>
L	Length, feet
M	Mass, pounds
t	Temperature, fahrenheit degrees
θ	Time, seconds

## Subscripts.

b	Bulk mean, Evaluated at bulk mean temperature
D	Based on diameter
i	at inlet or Entrance
L	Distance L from the entrance
m	Mean
O	Ambient

r	Condition at radius r
w	Condition at wall
x	Condition at distance x from the entrance
mb	Properties to be evaluated at the arithmetic mean of the bulk mean temperatures at inlet and exit of the pipe
lm	based on log mean temperature difference
C.L	Centre line

Number within brackets indicate the reference

## CHAPTER 1

### INTRODUCTION

Attempts have been made in the past to study the heat transfer between the inner surface of a pipe and a gas flowing through it under steady state conditions. Most of the theoretical and experimental work done so far can be grouped under the following thermal boundary conditions and/or assumptions.

1. Uniform wall temperature.
2. Linear variation of wall temperature with length.
3. Uniform wall heat flux.
4. Prescribed wall heat flux.
5. Constant fluid to wall temperature difference.

These thermal boundary conditions have been studied with the following flow conditions.

- a. Fully developed velocity profile at the entrance of the heat transfer section.
- b. Simultaneous development of velocity and temperature profiles.

These thermal and flow conditions have been further studied assuming (i) constant fluid properties, i.e., fluid properties not varying with temperature (ii) variable fluid properties.

The variation of fluid and wall temperature with  $L/D$  ratio for typical thermal boundary conditions, namely, constant wall temperature, constant heat flux per unit length

of tube and constant fluid to wall temperature difference are shown in figure 1.

The present investigation was undertaken to study the non-isothermal flow of air in a vertical pipe. Air was heated before entering the pipe and was cooled as it flowed upward losing its heat to the pipe wall and to the ambient air. The ambient air surrounding the pipe was assumed to be at a constant and uniform temperature for a given test.

The following were investigated:

1. the velocity profile development
2. the wall temperature variation
3. the inside film coefficient of heat transfer

This problem involved combined forced and free convection where the entering temperature and velocity profiles were flat. For air ( $N_{Pr} \approx 0.7$ ) the temperature and velocity profiles develop at nearly the same rate (16).

The true boundary condition for internal flow in a pipe is the temperature of the wall. Since constant ambient temperature was chosen as the reference it was used as a secondary boundary condition. In the earlier work sufficient data were not available to develop an empirical correlation for determining wall temperature. The results of this work along with the results of the previous investigators have made possible the derivation of an expression for wall temperature which is the true boundary condition. It is now possible to predict the wall temperature of a vertical pipe with air being cooled as it flows upwards in constant temperature surroundings.

No theoretical analysis of the present problem is yet available. The heat flux and wall temperature decrease as  $L/D$  ratio increases. At large values of  $L/D$  the fluid temperature, the wall temperature, and the ambient temperature tend to become equal.

Interest in the study of laminar flow heat transfer has arisen mainly in connection with heat exchanger applications involving oil. More recently this study has gained additional importance because of its utility in atomic reactors, boilers etc., where natural convection affects the circulation of coolants. Many situations can be conceived where a tube or pipe carries a hot gas through an essentially constant temperature environment. The specific practical application which initiated this study was the flow of hot gases up a chimney. For a realistic design, the heat transfer data and the flow behaviour must be known. This heat transfer information is also essential where heat recovery is desirable as for example in vertical stacks.

## CHAPTER 2

### LITERATURE SURVEY

The problems associated with the study of heat transfer, development of temperature and velocity profiles and the effect of other factors on fluid flow have been treated in numerous publications over the past 100 years. Although much research has been done for non-isothermal flow of air in vertical pipes, the boundary conditions varied considerably and very little information is available for up-flow with cooling. The common conditions under which analytical and experimental investigations have been made are given in Chapter 1. Due to the many variables to be considered there does not seem to be one solution to cover this complex problem.

The purpose of this chapter is to present and discuss the results of some previous investigations which are related to the present work.

#### 2.1 GRAETZ ANALYSIS

Graetz (14) in 1885 predicted analytically for the first time the heat transfer characteristics for a laminar flow of a fluid in a tube. He obtained the temperature profile and the heat transfer coefficients for the constant and uniform wall temperature case. The results were in the form of an infinite series the first three terms of which were evaluated. His calculations were based on the following assumptions:-

1. The temperature and the velocity profiles of the fluid were symmetric about the tube axis.
2. The velocity profile was fully developed i.e., parabolic, at the entrance and throughout the test section.
3. The physical properties of the fluid remained constant throughout the test section.
4. The temperature of the inside surface of the tube was constant for the heating or the cooling of the fluid.
5. Heat transfer occurred entirely by heat conduction.

This pioneering work has been looked at very minutely by the later authors and some of the theoretical assumptions made by Graetz have either been modified or discarded.

Hausen (7) suggested the following equation as an empirical representation of the Graetz solution for constant wall temperature and a parabolic velocity profile:

$$N_{\text{Num}} = 3.66 + \frac{0.0668 + \left[ \frac{N_{\text{Re}} \cdot N_{\text{Pr}}}{L/D} \right]}{1 + 0.045 \left[ \frac{N_{\text{Re}} \cdot N_{\text{Pr}}}{L/D} \right]^{2/3}} \quad \text{---(1)}$$

The fluid properties were evaluated at bulk mean temperature.  $N_{\text{Num}}$  approached a limiting value as  $L/D$  became large.

## 2.2 EFFECT OF VARIABLE FLUID PROPERTIES

Keevil and McAdams (17) after an experimental study involving laminar flow of oil found that viscosity was

an important factor when the fluid was being heated or cooled. They concluded that in the presence of heat transfer the velocity profile was distorted because of the changes in viscosity.

Taking into consideration the change of viscosity with temperature, Seider and Tate (25) suggested the following empirical equation for both cooling and heating of viscous liquids.

$$(N_{\text{Num}})_{\text{mb}} = 1.86 (N_{\text{Pe}})^{1/3} (D/L) \left( \frac{\mu_{\text{mb}}}{\mu_{\text{w}}} \right)^{0.14} \quad -(2)$$

$$= 2.02 (N_{\text{Gz}})^{1/3} \left( \frac{\mu_{\text{mb}}}{\mu_{\text{w}}} \right)^{0.14} \quad -(3)$$

Equation (2) gave results close to those of the Graetz solution. Their analysis was for constant wall temperature using oil as a fluid but natural convection effects were neglected.

Yamagata (30) considered variable properties when he published his analytical study on gases and found that the distortion of the parabolic velocity profile was reversed from that of the liquid when the gas was heated or cooled, due to the variation of viscosity with temperature.

The correction factor for viscosity change in equation (3) is mainly for liquid at moderate temperature differences between  $t_{\text{w}}$  and  $t_{\text{mb}}$ . For gases, Kays and London (14) have used another correction factor  $(T_{\text{mb}}/T_{\text{w}})^n$ , where  $n=0.08$  for cooling inside a tube and  $n=0.25$  for heating.

Deissler (3.4) analytically investigated fully developed laminar and turbulent flow of gases and of liquid metal in tubes with heat transfer considering fluid properties as variable along the radius. Natural convection was not considered. Relations were obtained to predict the radial velocity and temperature distributions. These relations were applicable to both heating and cooling of the fluid. Laminar Nusselt number was found to be independent of the Reynolds and Prandtl numbers, whereas turbulent Nusselt number was dependent on both. The effect of  $T_w/T_b$  on Nusselt number was eliminated by evaluating the fluid properties at various temperatures in the fluid. For turbulent flow he suggested  $T_{0.5}$  and for laminar flow  $T_{-0.27}$  as the temperatures at which the properties should be evaluated. These are given by:

$$T_{-0.27} = -0.27 (T_w - T_b) + T_b. \quad \text{--- (LAMINAR)} \quad \text{--- (4)}$$

$$T_{-0.5} = -0.5 (T_w - T_b) + T_b. \quad \text{--- (TURBULENT)} \quad \text{--- (5)}$$

He also stated that variation of viscosity across the tubes for laminar flow of gases caused a sharpening of the peak of the velocity and temperature profiles at the centre of the tube for heat addition to the gas, and flattening of these profiles for heat extraction. This was confirmed by Pigford (23).

Deissler (5) analysed, numerically, developing laminar flow with heat transfer for Helium gas. Both axial and radial property variations were considered. The heat flux at the wall was assumed to be constant. The initial velocity and temperature profiles were assumed to be flat. The Nusselt number  $N_{Nub}$  was found to be a function of  $(L/D)/(N_{Reb})_{local}$ ,  $q'$ ,  $M_i$  and  $N_{Pri}$  where

$$q' = q_{rw}/T_i K_i \text{ and}$$

$$M = \bar{u}_i / \left( \frac{C_p}{C_v} \right) \cdot R' \cdot T_i)^{\frac{1}{2}} \quad \text{--- (6)}$$

He compared the results for this quasi developed region with those from a previous analysis which considered the radial variation of properties but neglected axial effects and radial flow. The comparison showed that axial effects and radial flow have but a slight effect on the heat transfer results.

Test (27) made an analytical and experimental investigation of laminar flow with heat transfer in a vertical pipe, considering temperature dependent viscosity. He found that for liquids, the effect of wall temperature on local Nusselt number was almost negligible for the case of heating but significant for the case of cooling. This indicated that a local Nusselt number correlation should be different for heating than for cooling. He suggested the following correlation for the local Nusselt number

$$(N_{Nux})_b \left( \frac{\mu_w}{\mu_b} \right)^n = 1.4 (N_{Reb} \cdot N_{Prb} \frac{D}{X})^{1/3} \quad \text{--- (7)}$$

where

$n = 0.05$  for heating

$n = 1/3$  for cooling

### 2.3 COMBINED FREE AND FORCED CONVECTION

The fluid velocities associated with laminar motion are small; the heat transfer characteristics may be substantially affected by the buoyancy forces and the resulting velocity fields. Under such conditions Grashof number enters into the problem. The effect of free convection on heat transfer has been taken into account by some of the authors mentioned below.

The literature pertaining to combined forced and free convection was of great interest because the present study involved forced and free convection in the range of low Reynolds numbers. Martinelli and Boelter (20) presented predictions for such a system. They analytically considered a uniform wall temperature case with fluids being heated flowing vertically upwards and fluids being cooled flowing vertically downwards. In both cases the velocity near the wall was increased by the buoyant forces owing to the difference in densities caused by the difference in temperatures. Density was taken as a linear function of temperature with other physical properties being considered constant. They arrived at the following dimensionless relation.

$$\begin{aligned}
 N_{Nua} &= (h_a D)/K \\
 &= 1.75 F_1 \left( \frac{w C_{pb}}{K_b} + 0.0722 F_2 (N_{Gr} \cdot N_{Pr} \cdot D/L)_w^n \right)^{\frac{1}{2}} \\
 &= 1.75 F_1 \left( N_{Gzb} + 0.0722 F_2 (N_{Gr} \cdot N_{Pr} \cdot D/L)_w^n \right)^{\frac{1}{2}} \quad \text{-- (8)}
 \end{aligned}$$

The Nusselt number  $N_{Nua}$  is determined in terms of the arithmetic mean temperature difference (the arithmetic average of initial and final values of  $\Delta t$ ). The factors  $F_1$  and  $F_2$  are functions of  $N_{Nua}/N_{Gzb}$  and the exponent  $n$  was computed to be 0.75.

Pigford (23) also analytically treated combined forced and free convection in a vertical tube, allowance being made for the effect of temperature on viscosity and density. He calculated the formulas which are valid for short tubes and high rates of flow when the centre line temperature does not change appreciably. Like Martinelli and Boelter, Pigford expressed the arithmetic average Nusselt number as a function of Graetz number, Grashof-Prandtl product and the ratio of fluid viscosity at the wall to that at the average bulk fluid temperature as an additional parameter.

Jackson, Harrison and Boteler (15) also studied the combined forced and free convection for a vertical heated tube (constant wall temperature). Their experimental

data was in disagreement with Martinelli's theoretical equation and they suggested

$$N_{\text{Num}} = 1.128 \left( N_{\text{Re}} \cdot N_{\text{Pr}} \cdot \frac{D}{X} + (3.02 (N_{\text{Gr}} \cdot N_{\text{Pr}} \cdot \frac{D}{L}) N_{\text{Pr}})^{0.4} \right)^{\frac{1}{2}} \quad \text{--- (9)}$$

where  $N_{\text{Re}} \cdot N_{\text{Pr}} \cdot \frac{D}{X}$  is evaluated for the length of the heated section considered and  $L$  is the length of the total heated section. Mean Nusselt number  $N_{\text{Num}}$  is based on the log-mean temperature difference ( $\Delta t_{\text{lm}}$ ). If the velocity profile is flat at the entrance and the free convection effects are negligible, the heat transfer equation is

$$N_{\text{Num}} = 1.27 (N_{\text{Gz}})^{\frac{1}{2}} \quad \text{--- (10)}$$

The authors also state that free convection forces are functions of the total tube length and the resistance to flow for the whole system, hence it should be calculated on the basis of the total tube length.

More recently Brown and Gauvin (1) studied in detail the heat transfer characteristics of air flowing upwards (buoyancy forces aiding the flow) and with air flowing downwards (buoyancy forces opposing the flow). The analysis was done for constant heat flux at the wall for a fully developed flow when the air was being heated. Constant physical properties except for the density in the buoyancy force term were assumed. For laminar aiding flow they were able to correlate the local Nusselt

number with  $(N_{Gr}/N_{Re})$  which is

$$N_{Nux} = 0.931 \left( (N_{Gr})_D / N_{Re} \right)^{0.389} \text{ --- (11)}$$

It agreed well with the laminar aiding data of Hallman (11,12) and Brown (2). For turbulent flow the local Nusselt number was correlated with Grashof number independently of the axial position.

Hallman (11,12) suggested the following equation to determine the point of transition to a fluctuating type of flow. The transition point was defined as that point at which the wall temperature in the test section began to show random fluctuations.

$$\left( (N_{Gr})_D (N_{Pr}) \right) = 9470 \left( (N_{Re})(N_{Pr}) / 2(L/D) \right)^{1.83} \text{ --- (12)}$$

He compared the equation with the observations of Scheele, Rosen and Hanratty (24) and found that their results indicated that turbulence would begin at lower values of  $(N_{Gr})_D (N_{Pr})$  than those predicted from this equation. On comparison of their own data alongwith those of other authors mentioned above, Brown and Gauvin concluded that the location of the point of transition is not well established. The largest variation is caused by the magnitude of the initial turbulence, either existing in the entering flow or initiated by wall roughness etc., but the transition point is definitely a function of Reynolds and Rayleigh numbers and length

to diameter ratio.

#### 2.4 SIMULTANEOUS DEVELOPMENT OF VELOCITY AND TEMPERATURE PROFILES.

Kays (16) provided a numerical solution for laminar flow heat transfer in circular tubes with both temperature and velocity profiles uniform at the entrance. The solution of Langhaar (7) was employed to provide the velocity profiles. All of the solutions and experimental data are presented in the form of either local or mean Nusselt number as a function of a modified Graetz number  $(N_{Re} \times N_{Pr})/(L/D)$ . The following equations were suggested for the Nusselt number based on  $(t_m - t_w)$ .

For constant wall temperature, and Langhaar velocity profiles

$$N_{Num} = 3.66 + \frac{0.014 \times \left(\frac{N_{Re} \cdot N_{Pr}}{L/D}\right)}{1 + 0.016 \times \left(\frac{N_{Re} \cdot N_{Pr}}{L/D}\right)} \quad \text{--- (13)}$$

For constant temperature difference, and Langhaar velocity profile

$$N_{Num} = 4.36 + \frac{0.10 \times \left(\frac{N_{Re} \cdot N_{Pr}}{L/D}\right)}{1 + 0.016 \times \left(\frac{N_{Re} \cdot N_{Pr}}{L/D}\right)^{0.8}} \quad \text{--- (14)}$$

For constant heat input, and Langhaar velocity profile

$$N_{Nux} + 4.36 + \frac{0.036 \times \left( \frac{N_{Re} \cdot N_{Pr}}{L/D} \right)}{1 + 0.0011 \times \left( \frac{N_{Re} \cdot N_{Pr}}{L/D} \right)} \quad \text{--- (15)}$$

Urichson and Schmitz (28) studied the simultaneous development of temperature and velocity profiles in laminar flow for the cases of constant heat flux and constant wall temperature. They included the radial component of velocity in the analysis in the entrance region and thus improved upon the earlier work by Kays. The inclusion of radial component of velocity caused a significant decrease in the local Nusselt number from that obtained by Kays.

Lawrence and Chato (19) investigated the heat transfer effects on the developing laminar flow inside vertical tubes. These experiments were conducted with water and a numerical method was developed for the cases of upflow or downflow and constant wall temperature and constant heat flux so as to predict the developing velocity and temperature profiles, the heat transfer characteristics, the pressure drop and the transition to turbulent flow. Nonlinear variation of both density and viscosity were considered. Their theoretical solutions verified by experimental measurements show that for uniform heating with a real fluid in a vertical tube velocity and temperature profiles never become fully developed. The experimental measurements suggest that the transition process depends upon the developing velocity profiles.

For a constant heat flux case transition from laminar to turbulent flow will always occur at some axial distance, if the tube is long enough. For a given entrance condition, the distance to the point of transition is fixed by the fluid flow rate and the wall heat flux.

McMordie and Emery (22) give a numerical method of calculating the local Nusselt number for laminar flow in circular tubes with axial conduction, radial convection and simultaneously developing thermal and velocity fields. The radial convection is important only in the entrance region where  $N_{Re} N_{Pr} D/X > 1000$ . Since for laminar flow  $N_{Re} < 2300$  we have that  $X/D < 2.3 N_{Pr}$ . For air radial convection is important only for the first few diameters from the entrance. Kays had neglected this term in his analysis and his results for the Nusselt numbers were lower by less than 5%. Axial conduction is important for fluids with high conductivities, which again implies low Prandtl number fluids (air=0.7). The analysis by McMordie and Emery is for constant heat flux at the wall. The local Nusselt numbers have lower values than the numerical values of Kays but coincide with the values given by Urichson and Schmitz (28), who had considered radial convection by using Langhaar's velocity profiles.

Equations (1) and (2) assumed that heat transfer in

the inlet region depends only on the product of  $N_{Re} N_{Pr}$  and is therefore independent of kinematic viscosity. If there is a simultaneous development of temperature and velocity profiles then  $\mu$  or  $N_{Pr}$  has to appear as an independent variable since in the inlet length, viscous and inertia forces are comparable. Taking the above facts into account Elser (7) in 1952 obtained the following expression for simultaneously developing profiles.

$$\begin{aligned} \text{Local Nusselt number} = N_{Nux} &= \frac{h D}{K} \\ &= 0.289 (N_{Re})^{0.5} (N_{Pr})^{1/3} (D/L)^{0.5} \quad \text{---(16)} \end{aligned}$$

Mean Nusselt number over a length  $L$  from the pipe inlet is given by

$$N_{Num} = \frac{h_m D}{K} = 0.578 (N_{Re})^{0.5} N_{Pr} (D/L)^{0.5} \quad \text{---(17)}$$

The heat transfer coefficient in these equations is based on the temperature difference between the wall and the core. The core is that region outside the thermal boundary layer where the temperature profile is unaffected by the developing boundary layer. Reynolds number is based on the mean fluid velocity.

## 2.5 COOLING

Very few authors have studied the heat transfer characteristics when the gas is being cooled. Zellnik and Churchill (31) are two, who evaluated the effect of

increasing air temperatures on the local heat transfer in the inlet region. A uniform wall temperature, turbulent flow and a flat velocity profile at the inlet were chosen as reference conditions. Air entered the tube with a flat velocity and temperature profile at temperatures from 480 to 2000° F and flow rates corresponding to Reynolds numbers 4500 to 22500. They found an increase of local Nusselt number with increase of  $(t_b/t_w)$  and suggested the use of bulk temperature for evaluating the properties.

Goresch (9) considered the problem of determining heat losses from a gas flowing turbulently in a poorly insulated pipe and exposed to a uniform temperature environment. The heat loss from the outer surface was by free convection and radiation. From the initial radial temperature distribution the mean gas temperature and wall temperature were found for various values of  $L/D$ . These were determined in terms of the inside film coefficient and the combined heat transfer coefficient on the outside. This combined coefficient included free convection and radiation.

Gulati (8) studied the effects of variable fluid properties. He assumed that a laminar parabolic profile would exist under isothermal conditions and used the measured temperature profile to determine the new velocity profile which was distorted by buoyancy effects. He showed that when air is cooled in upward flow, the buoyancy forces predominate, resulting in

an elongated velocity profile at the centre. He did not consider any radial velocity.

Drobitch (6) studied the non-isothermal flow of air in a vertical pipe. Using high entrance temperatures ( $t_i \simeq 700^\circ\text{F}$ ) and Reynolds numbers upto 8000; he concluded that:

1) A non-laminar flow existed for all non-isothermal runs, including those below a Reynolds number of 1000.

2) The velocity profiles were not affected by the heat loss for  $N_{Re} > 6000$ , and thus were similar to the velocity profiles obtained for isothermal flow.

3) The heat transfer characteristics for laminar flow ( $N_{Rei} < 2000$ ) showed agreement with the analytical results of Martenelli & Boelter (20) and Pigford (23). The Nusselt numbers were found to be higher than the values obtained by Graetz (14) for constant wall temperature and the results of Kays (16) for constant heat flux. The results gave the following relationship between mean Nusselt number and the inlet Reynolds number for  $N_{Rei} < 4000$ .

$$N_{Num} \simeq 4.4 (N_{Rei})^{0.2} \quad \text{--- (18)}$$

Vissers (29) studied in detail the isothermal and non-isothermal flow of air in a vertical pipe. His findings are in conformity with those of Drobitch. He concluded:

a) Four distinct regions are present in the non-isothermal flow;

1) entrance region, from entrance to maximum  $u_{\max}/\bar{U}$ .  
2) cooling region, where the velocity ratio decreases continuously due to the cooling.

3) isothermal developing region, when the effect of temperature difference has become negligible and the velocity profile is developing isothermally.

4) fully developed isothermal flow, which would continue if no disturbances are encountered.

b) Buoyancy forces had the effect of elongating the velocity profile. This effect decreased with increasing Reynolds number.

d) The mean Nusselt number variation with  $(X/d_w)/N_{Pe}$  was found to agree with the correlation of Hausen when the Grashof number was between  $10^4$ - $10^5$  but the Nusselt number increased with higher Grashof numbers.

The last three investigations are the only three available which apply directly to the present investigation.

## CHAPTER 3

### APPARATUS AND INSTRUMENTATION

#### 3.1 BASIC DESCRIPTION

The investigation was carried out in the experimental setup shown in figure 2. The air was supplied by a compressor. It was passed through a filter and pressure reducing valve combination from which it entered the flow-meters. The air was expanded into a diverging section before entering the furnace. After passing through a screen and over the heating elements, it passed through a second set of screens before entering the test pipe through a smooth, rounded bell mouth. The second set of screens minimized flow irregularities due to the presence of heaters etc., and the bell mouth assisted in giving a flat velocity profile at the entrance to the test pipe. The dimensions of the bell mouth, the test pipe, and the location of probing positions along the test pipe are shown in figure 3.

#### 3.2 FLOW METERS

The volume of air was controlled by valves and measured by means of two Brooks high accuracy flow meters. The accuracy was within one percent. The low range flowmeter was capable of measuring 0-3.18 S.C.F.M., and the high range from 1.0 to 10.5 S.C.F.M., at 14.7 p.s.i.a. and 70 °F. Chromel Constantan thermocouples were installed in each rotameter to determine the temperature of air for use in making corrections for density.

### 3.3 FURNACE

The furnace was built for previous investigations (6,8,29), but it was completely reconditioned and overhauled before being put into use for the present investigations by the author.

Air from the rotameters entered the furnace through a sheet metal transition. A wire mesh screen was installed below the heaters to distribute the air uniformly across the heating elements. The elements consisted of 3 Nichrome wire electric heaters two of which were 3000 watts each. The third, rated at 2000 watts was connected to a variac to allow fine control of the air temperature leaving the furnace. To reduce heat loss from the furnace which would cause nonuniform air temperature, the furnace and the unit containing the second set of screens were covered with glass wool, 2" thick Magnesia bricks and a special putty. Temperature and velocity profiles were found to be flat to within  $1/16$ " of the wall at the entrance to the test section.

### 3.4 TEST SECTION

An aluminum pipe 24' long, 0.87" I.D., and 1.0" O.D. was used as the test section. The test pipe was made up of two 12' lengths connected with removable clamps. The shape and location of the access slots are shown in figure 3. The measurement of temperatures and velocities were made at these stations.

### 3.5 LEAKAGE

The leakage of air between the rotameter exit and the entrance to the test section was reduced by sealing all the joints with Devcon steel cement. Checks for leakage were made using a soap solution.

The upper 12' pipe was disconnected and the flow at the end of lower 12' test pipe was measured with a pitot tube, hot wire anemometer, and wet test gas meter. All the values agreed with the values shown by the rotameter within 2%.

### 3.6 VELOCITY MEASUREMENT

The air velocity in the test pipe was measured by means of a hot wire anemometer. It is an instrument which measures the velocity in a fluid stream, through the streams cooling effect on a very thin, electrically heated wire filament. FLOW CORPORATION, MODEL HWB3, constant current hot wire anemometer used in the investigation is described in detail in reference (6).

The well-known King's equation given below does not agree with experimental results at low velocities (less than 2' per second), therefore each wire was calibrated individually between 0 and 15 feet per second.

$$u = C/P \left[ \left( I/I_0 \right)^2 - 1.0 \right]^2 \quad \text{-----}(19)$$

$I_0$  = The value of current in still air at a temperature  $t_0$

$I$  = The value of current at velocity  $u$  at a temperature  $t_0$

$C$  = The calibration constant

$P$  = Absolute static pressure

Vissers (29) had observed a distortion in the velocity profile which was considered due to the 'blockage effects' of the probe itself. As suggested by him, a special probe bent at right angles near the end was used for this investigation. The hot wire was made of platinum drawn by the woolastan process. The wire diameter was 0.0005 inch. To obtain the readings close to the wall, a third leg or needle was built into the probe. The distance between the wire and the tip of the third needle was measured very accurately. The third needle was part of an electrical circuit, which was completed when the extended tip established contact with the wall.

The hot wire was calibrated at two resistance ratios at a constant air temperature. The probe was so held that the wire axis was at right angles to the flow. The calibration was carried out in a low turbulence wind tunnel and in the test pipe over a range of velocities. For velocities less than 3' per sec. the calibration points were obtained from the known fully developed profile for laminar flow in the test pipe. For velocities more than 3' per sec. the hot wire and the pitot static probes were held in the same plane normal to the flow in the wind tunnel. Cold setting of the hot wire anemometer was done at each flow rate and the values of the current given by the anemometer at the two resistance ratios were recorded along with corresponding micromanometer readings. Figure 4 shows a typical calibration curve giving the relation between current and velocity at resistance ratios 1.2 and 1.4 for isothermal flow. The calibration curve thus obtained was checked and verified at the test pipe. The velocity profiles along two perpendicular directions were obtained by measuring the velocities by means

of hot wire anemometer. The mass flow rate as calculated from the velocity profiles was compared with the mass flow rate as calculated from the rotameter readings. The results were found to be within 2%. The centre line velocities at various flow rates measured by means of the hot wire anemometer were also compared with the measurements taken with the pitot static tube. The results were within 2%.

Current correction for temperature was applied according to the table reference (6).

Resistance Ratio	-----	1.2	1.4
Current Correction m.a./10°F	-----	0.209	0.302

### 3.7 TEMPERATURE MEASUREMENT

The temperature of the (1) ambient air (2) surface of the aluminum pipe (3) air leaving the rotameters (4) air at the entrance of the test section and (5) air at various stations mentioned earlier was measured. Chromel Constantan 24 gauge thermocouples were used for the measurement of the temperatures of the ambient air, surface of the aluminum pipe and the air leaving the rotameters. For the measurement of the temperature profiles when the temperatures were less than 200°F, Copper Constantan 30 gauge thermocouples were used. For the measurement of temperature profiles and the inlet temperature when the temperatures were higher than 500°F Chromel Constantan thermocouples were used. A 24 gauge Copper Constantan thermocouple was used for measuring the inlet temperatures when  $t_i < 200^\circ\text{F}$ .

For air temperature measurements in the test pipe the thermocouple wire was mounted in a stainless steel tube bent at right angles. The wires were sanded at the tips to reduce the diameter, bent and soldered for 30 gauge or fused for 24 gauge. The probe was designed with a contact point at a known distance from the thermocouple junction. This point completed an electric circuit when it touched the wall. This provided a reference point from which to start the traverse.

All the Chromel Constantan thermocouples were connected to a Thermovolt Instruments 24 point rotary switch. All the outputs were measured on a Leeds and Northrup potentiometer. The probes used are shown in figure 5.

### 3.8 PRESSURE MEASUREMENT

Barometric pressure was read on a laboratory barometer accurate to  $\pm 0.01$  "Hg. For the calibration of the hot wire and for checking the flow, Flow Corporation's model MM3 micromanometer was used. It was accurate to  $\pm 0.0002$  " of the liquid column (Butyl Alcohol) over a 2" range.

### 3.9 TRAVERSING MECHANISM

The traversing mechanism (Photograph No. (F-3, F-4, F-5)) consisted mainly of a threaded rod, probe holder and an indicating dial capable of positioning the probe with an accuracy of 0.008". The hot wire and the thermocouple probes could be aligned parallel to the pipe axis with the help of a pointer as shown in the figure 5. 247610

## CHAPTER 4

### EXPERIMENTAL PROCEDURE AND RESULTS

#### 4.1 PROCEDURE

This investigation was mainly concerned with the heat transfer coefficients, the velocity profile development and the wall temperature variation associated with non-isothermal flow of air in a vertical pipe in a constant temperature environment. The majority of the data was for low Reynolds numbers ( $N_{Rei} < 2000$ ) and for small differences between  $t_i$  and  $t_o$  ( $(t_i - t_o) < 100^\circ\text{F}$ ). Several runs were taken at higher Reynolds numbers ( $N_{Rei} \simeq 3000, 4000$ ) and larger differences between  $t_i$  and  $t_o$  ( $(t_i - t_o) \simeq 600^\circ\text{F}$ ) for the purpose of comparison with the readings taken by Drobitch (6), and Vissers (29). Small values of  $(t_i - t_o)$  were used along with low Reynolds numbers to investigate the point where thermally induced turbulence would occur. The air flow was selected to cover a range of entrance Reynolds numbers from 600 to 4000. For non-isothermal runs 6 to 8 hours were allowed for the system to reach a steady state. Readings were taken only when the ambient air temperature along the pipe varied by less than two degrees.

For each run the following measurements were recorded:

- (1) barometric Pressure
- (2) ambient air temperatures at 6' and 15' along the pipe length and about 1' away from the axis.
- (3) inlet air temperature
- (4) wall temperature at each measuring station

(5) Radial temperature profile at each measuring station

(Mean temperature was calculated from the temperature readings at equal area points along the diameter)

(6) mass flow rate of air in the pipe.

(7) centre line velocity at each measuring station

The readings listed above were taken periodically to check for the steady state condition.

#### 4.2 HEAT TRANSFER AND WALL TEMPERATURE RESULTS

The variation with  $L/D$  of mean air temperatures and wall temperatures for different inlet air temperatures and Reynolds numbers are shown in figures 6 to 11 inclusive. The variation of  $(t_w - t_o)$  with  $(t_i - t_o)$  at various values of  $N_{Rei}$  and  $L/D$  are shown in figures 12 to 15 inclusive. The slope of these curves is given by  $(t_w - t_o)/(t_i - t_o)$  and is designated as 'm'. In figures 16 and 17 the values of 'm' are shown for various values of  $L/D$  and  $N_{Rei}$ .

The variation of local Nusselt number ( $N_{Nux}$ ) with  $L/D$  for various values of  $N_{Rei}$  &  $t_i$  are shown in figures 19 to 25 inclusive. Figure 26 shows the variation of local Nusselt number with  $L/D$  for  $N_{Rei} = 2175$  &  $2720$  at  $t_i = 665.0$  and  $605.0$  °F respectively. The results of Drobitch (6) and Vissers (29) at about the same inlet temperatures are also shown on the same graph for comparison. The variation of local Nusselt number with Graetz number is shown in figure 27

along with the numerical solution given by Kays (16) for the constant temperature and constant heat flux boundary conditions. These results are for high inlet temperatures ( $t_i > 600^\circ\text{F}$ ) and for  $N_{\text{Rei}} < 2000$ . The variation of mean Nusselt number with Graetz number for  $N_{\text{Rei}} < 4000$  and  $t_i < 120^\circ\text{F}$  is shown in figure 28. Pigford's (23) analytical data for ( $\mu_w/\mu_{c,L} = 1.0$ ) is also shown on the same plot.

The variation of local Nusselt number with  $t_m/t_w$  for different Reynolds numbers is shown in figures 29 & 30. The local Nusselt number for these two plots was calculated by measurements at  $L/D = 15.9$  &  $33.1$ , thereby representing  $N_{\text{Nux}}$  at  $L/D = 24.5$ .

#### 4.3 VELOCITY RATIOS

Figures 24 & 31 to 34 inclusive show the variation of  $u_{\text{max}}/\bar{U}$  with  $L/D$  ratios for non-isothermal flow at different temperature differences ( $t_i - t_o$ ) and various Reynolds numbers ( $N_{\text{Rei}}$ ).

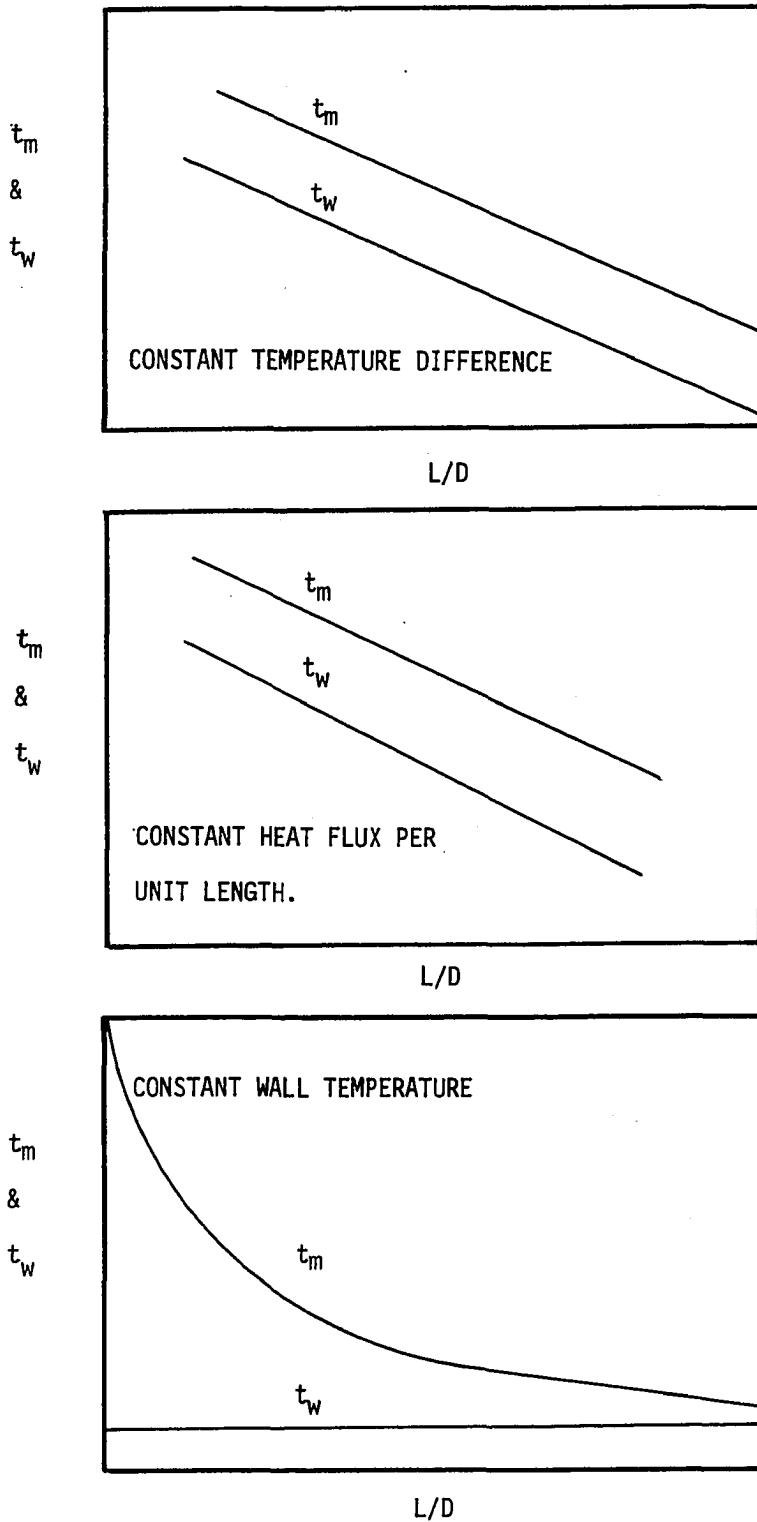


Fig.1 . Typical Temperature Boundary Conditions  
 Showing the Axial Variation of Mean & Wall Temperatures.

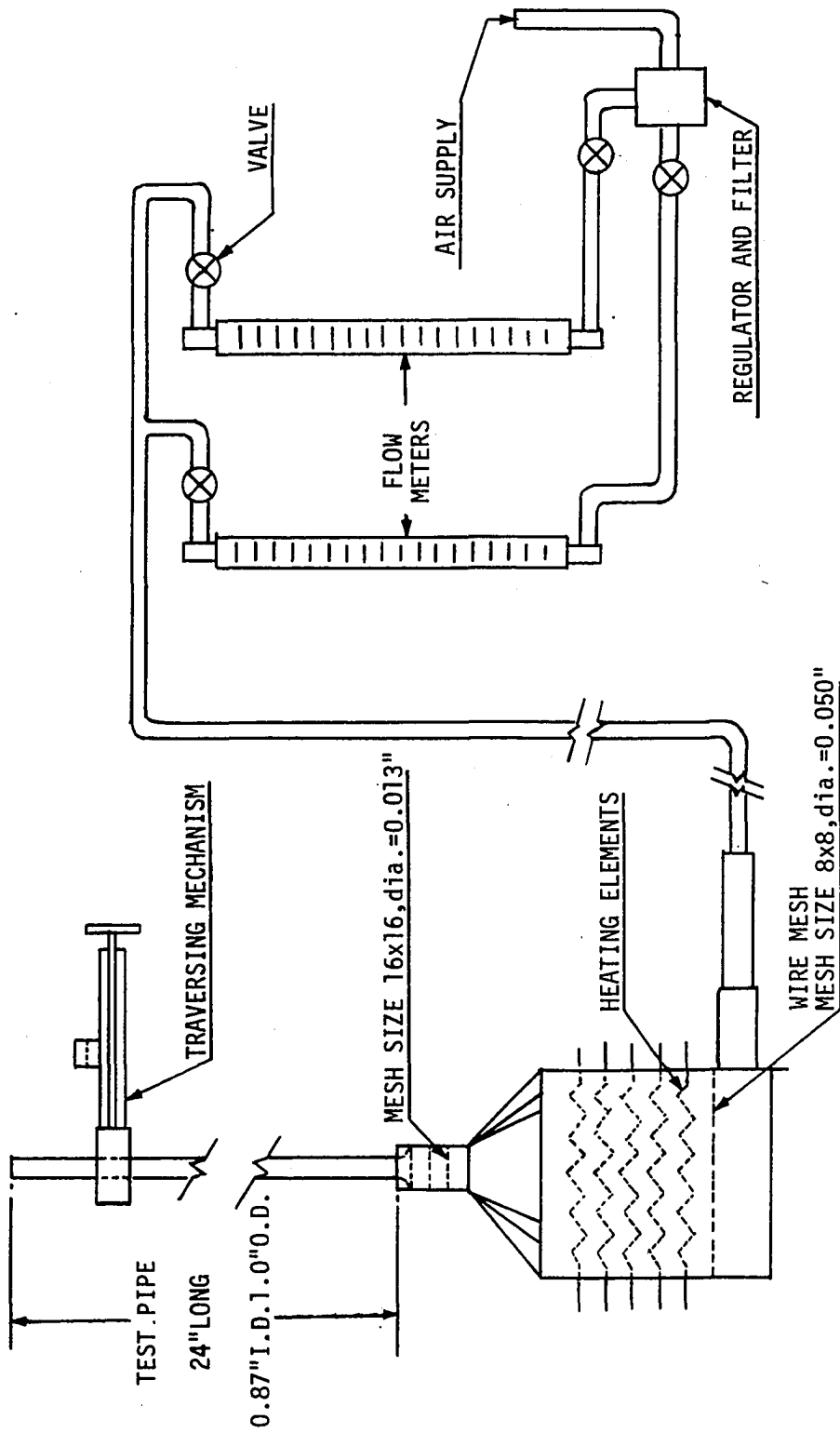


Fig. 2. Schematic Layout of Equipment.

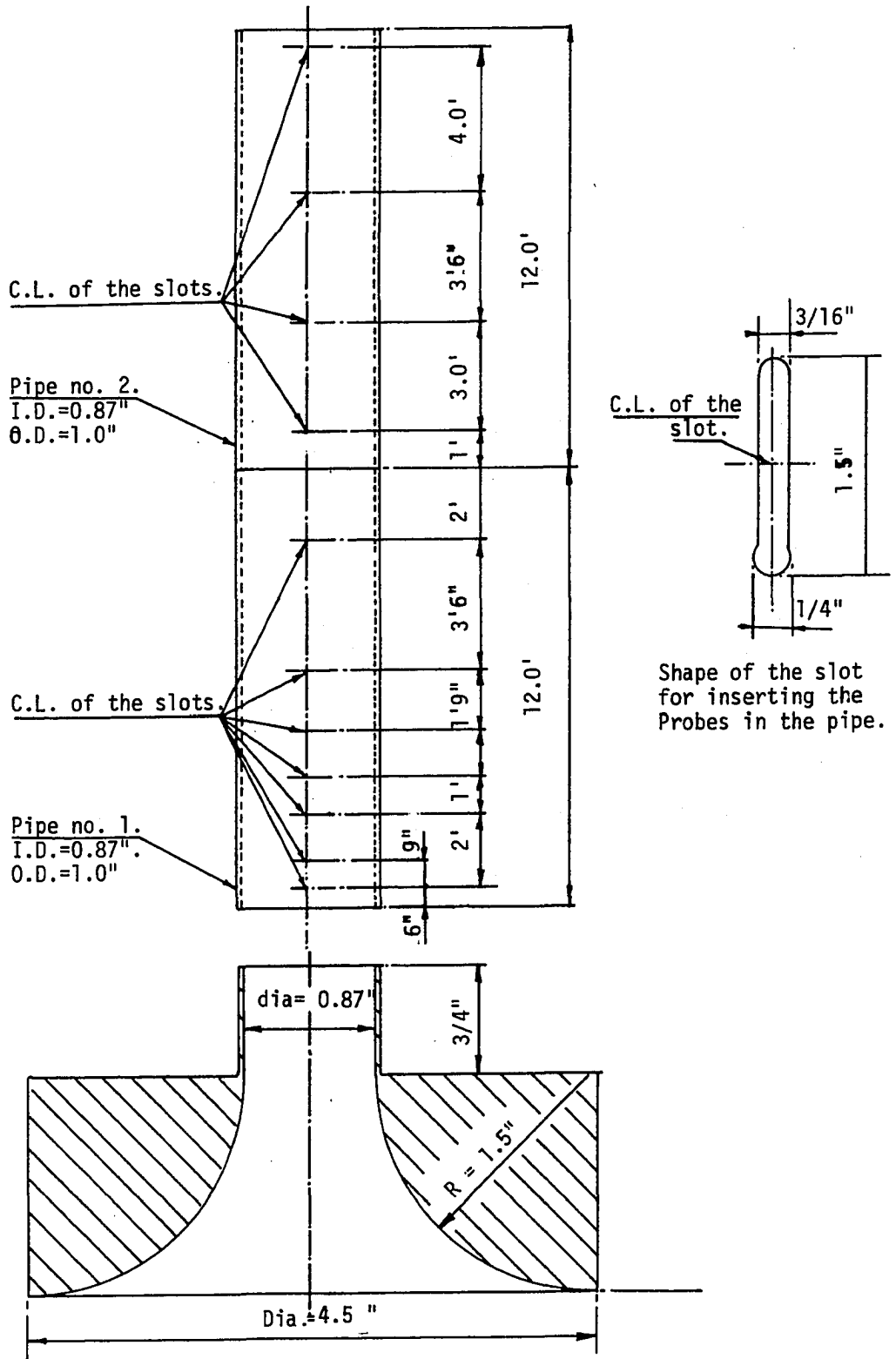


Fig. 3. Dimensions of the Bell Mouth and Test Pipe.

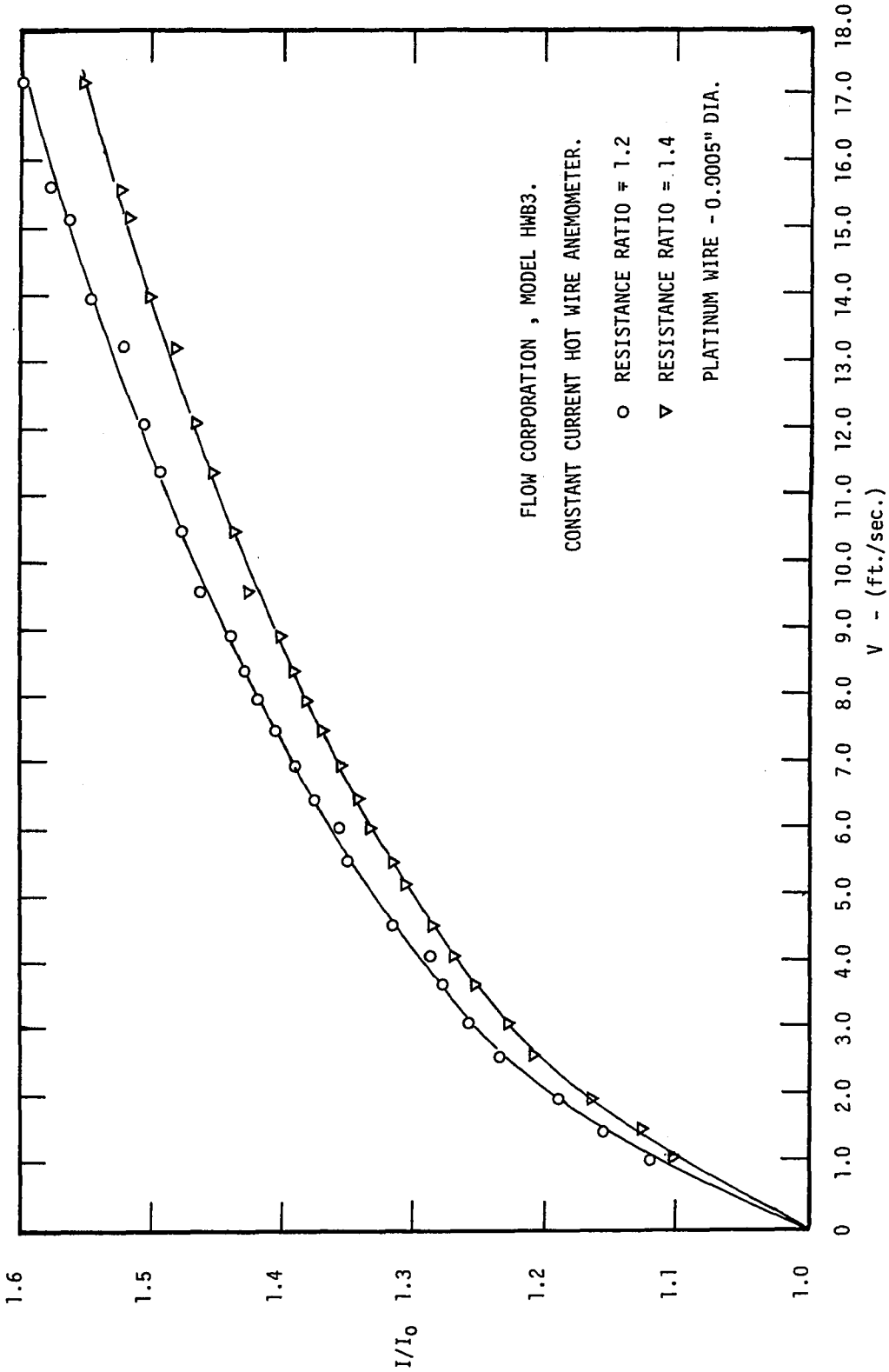


Fig. 4. Variation of  $I/I_0$  with  $V$  for Two Resistance Ratios.

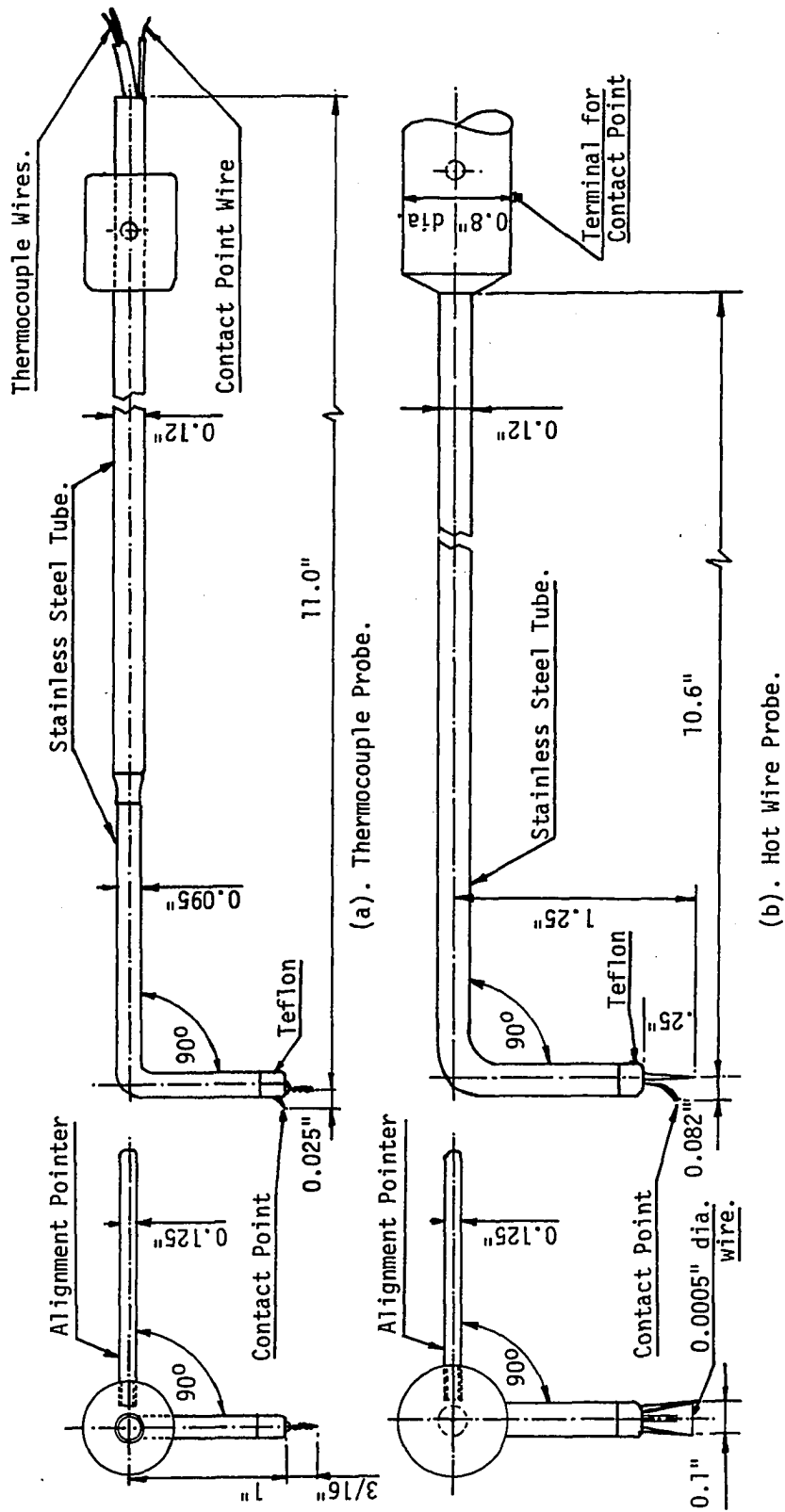


Fig. 5. Hot Wire and Thermocouple Probes.

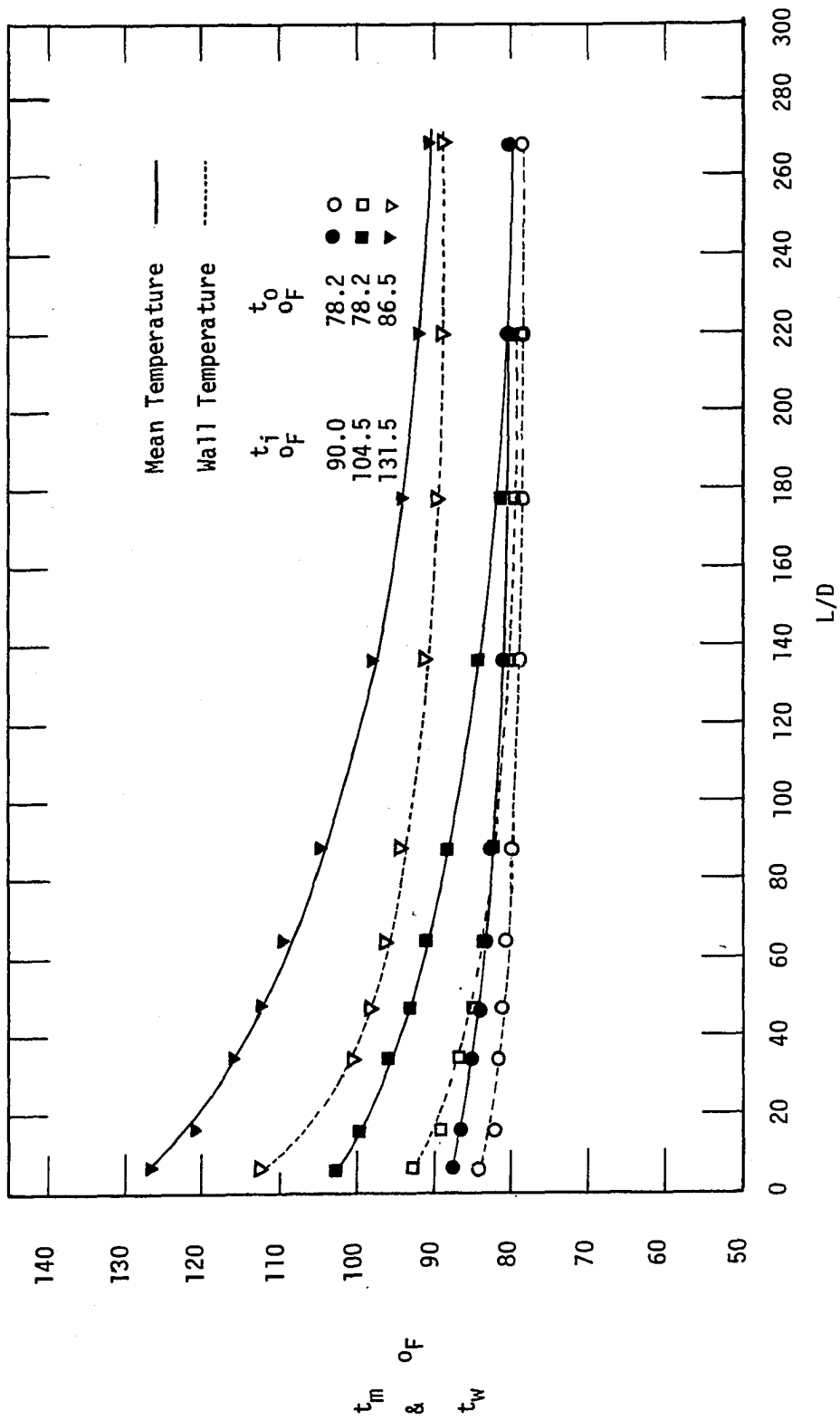


Fig. 6. Axial Variation of Mean and Wall Temperatures for  $N_{Rej} \approx 1500$ .

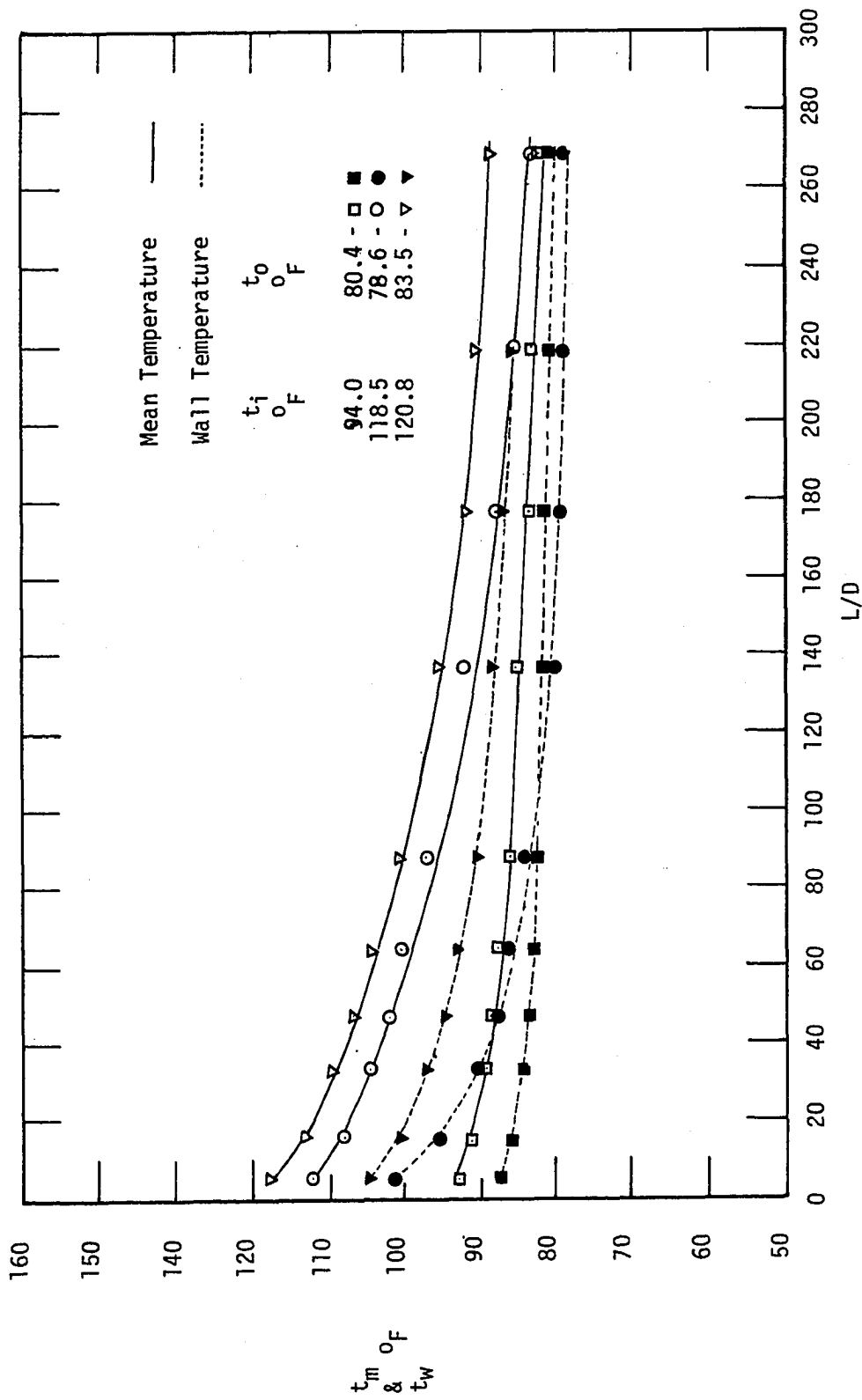


Fig. 7. Axial Variation of Mean and Wall Temperatures for  $N_{Rei} \approx 2000$ .

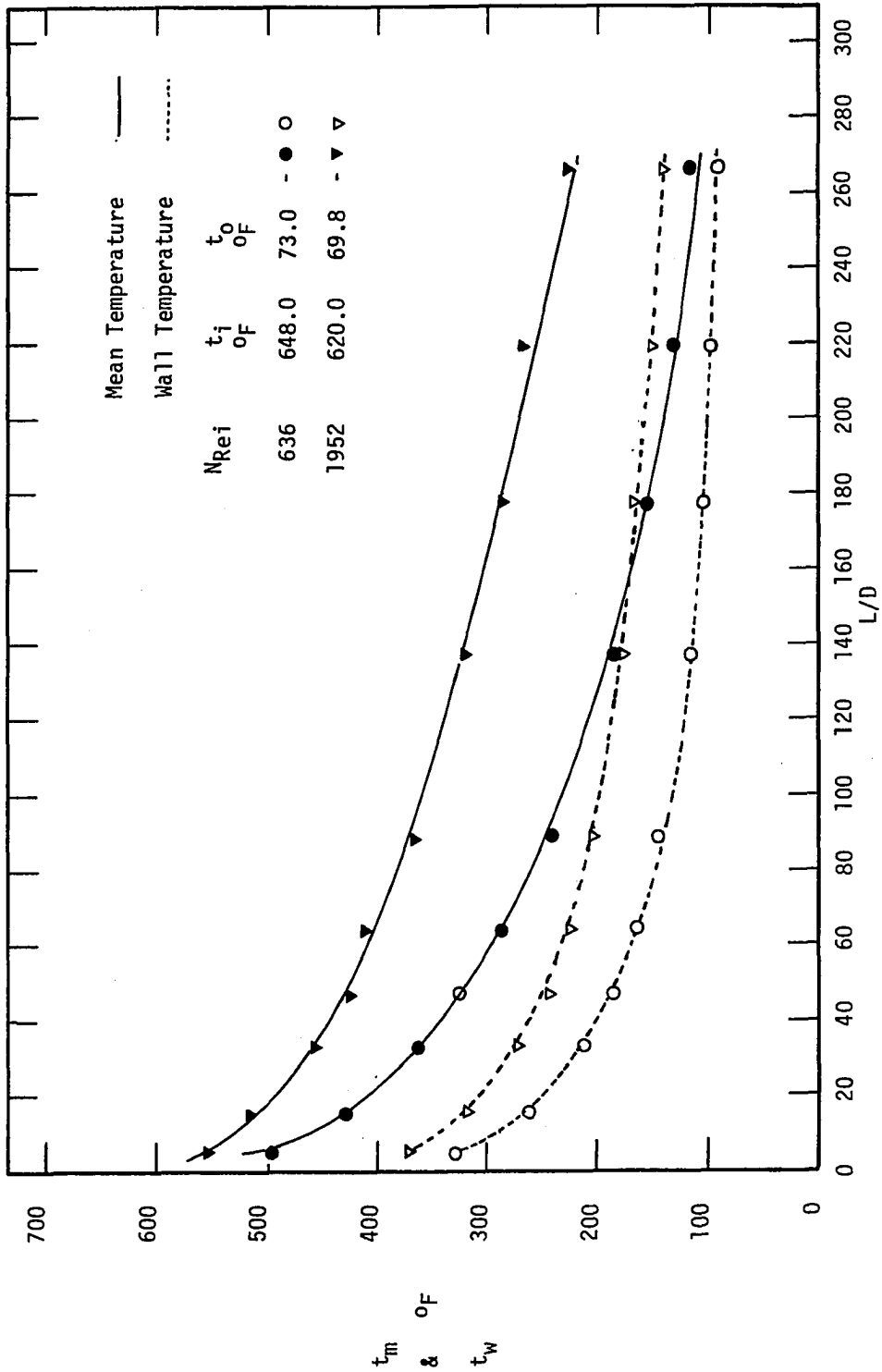


Fig.8. Axial Variation of Mean and Wall Temperatures at High Inlet Temperatures ( $t_i > 600^{\circ}F$ ).

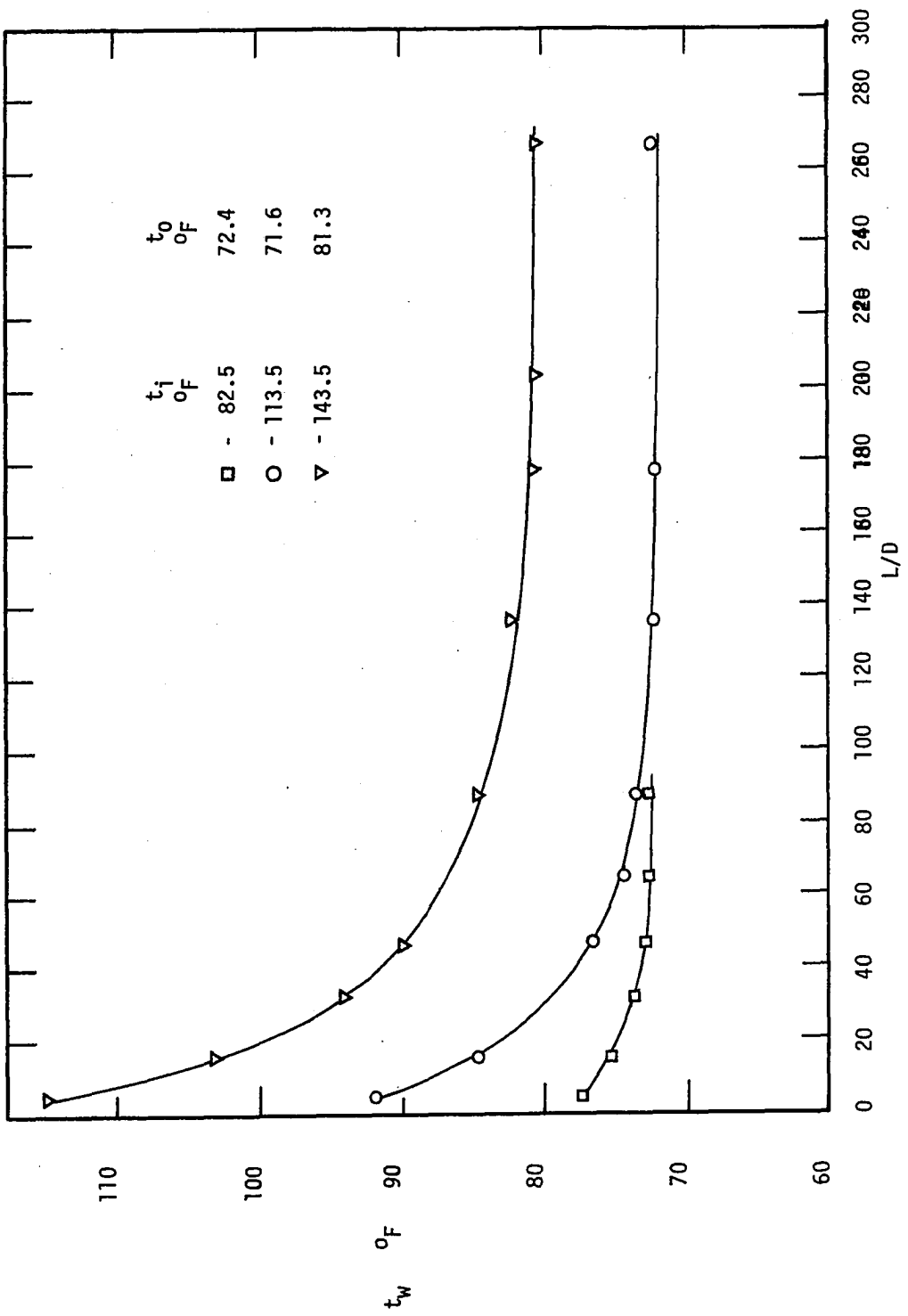


Fig. 9. Axial Variation of Wall Temperature for  $N_{Re} \approx 600$ .

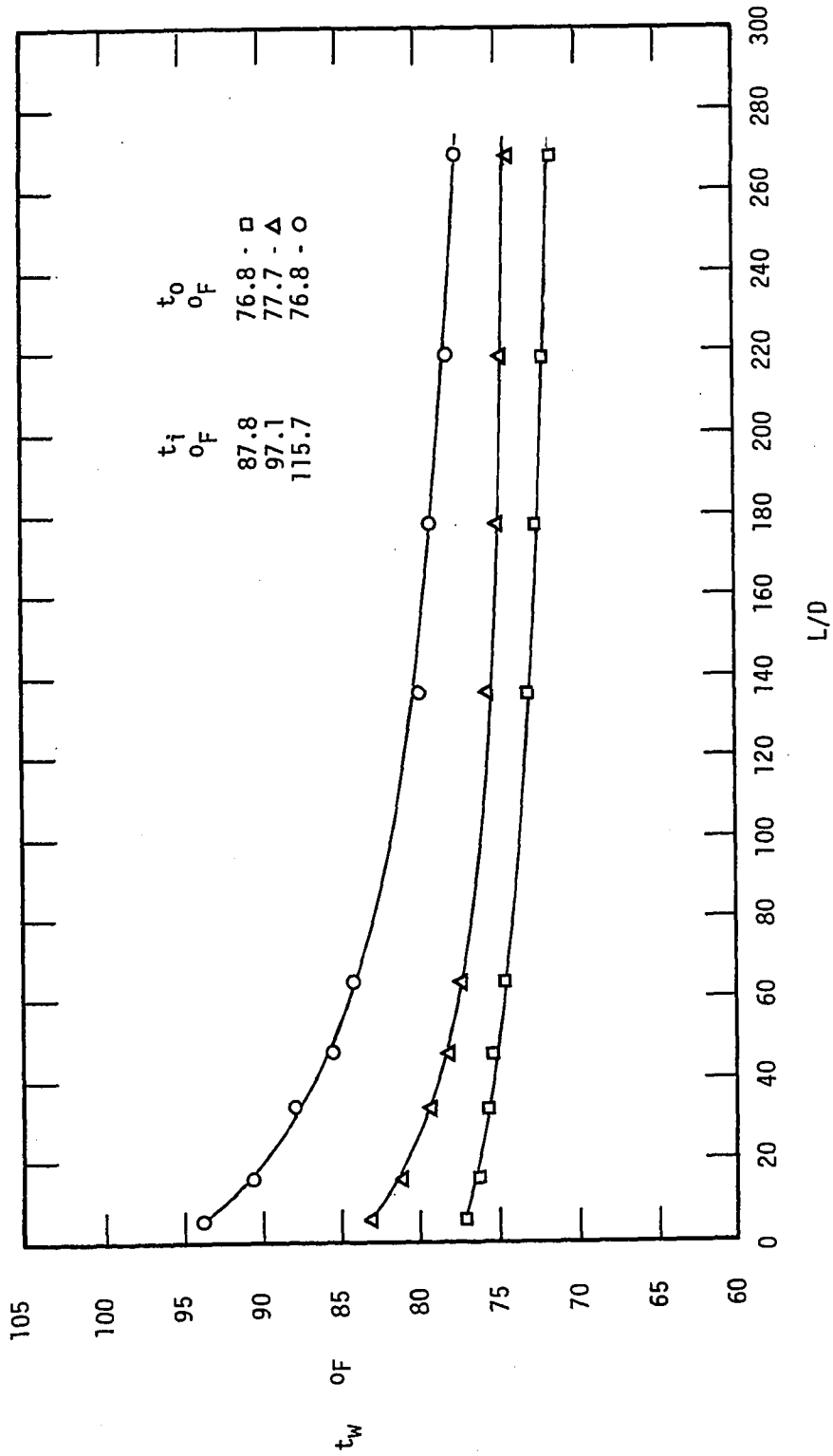


Fig.10. Axial Variation of Wall Temperature for  $N_{Re} \approx 3000$ .

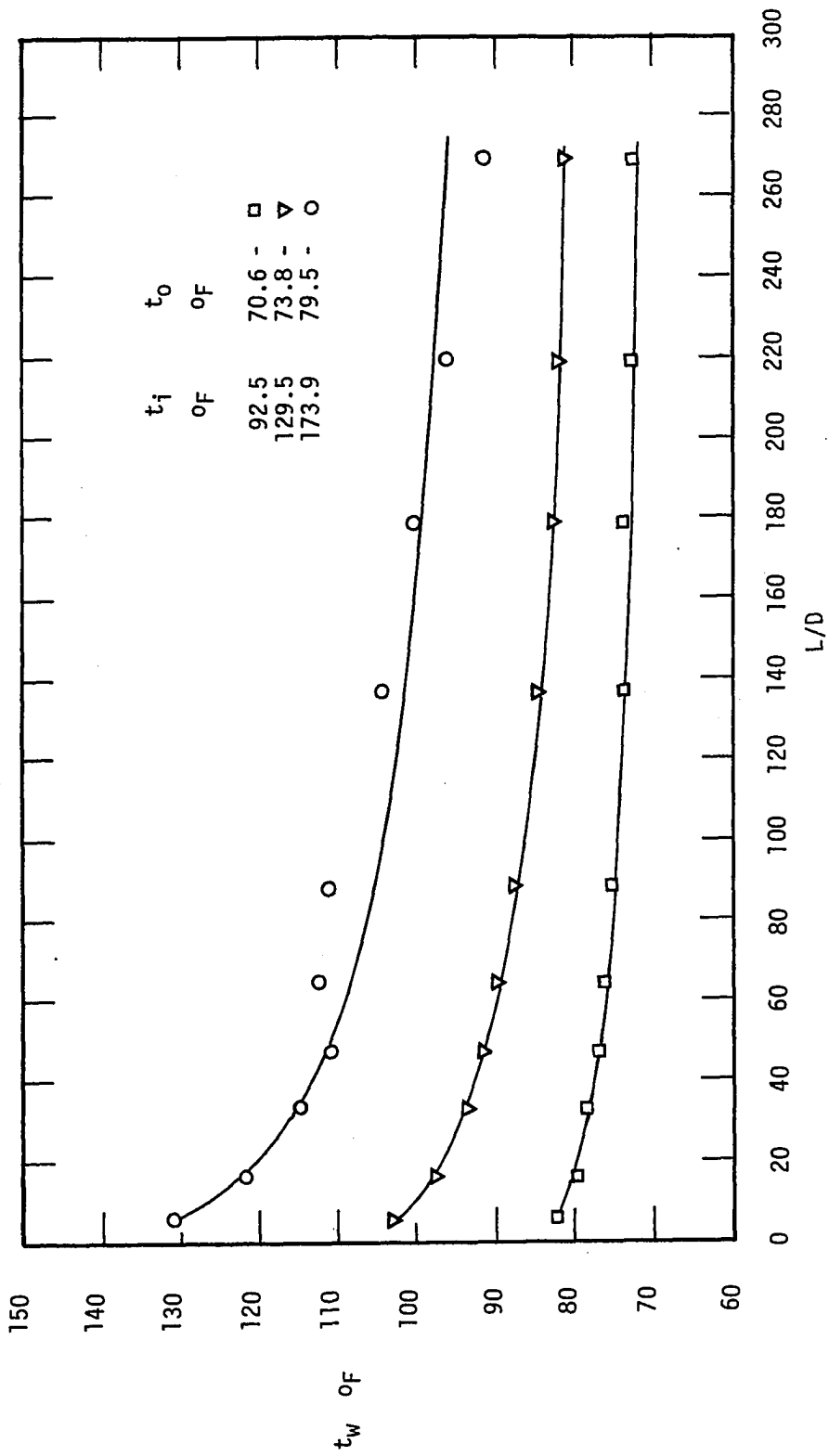


Fig. 11. Axial Variation of Wall Temperature for  $N_{Rej} \approx 4000$ .

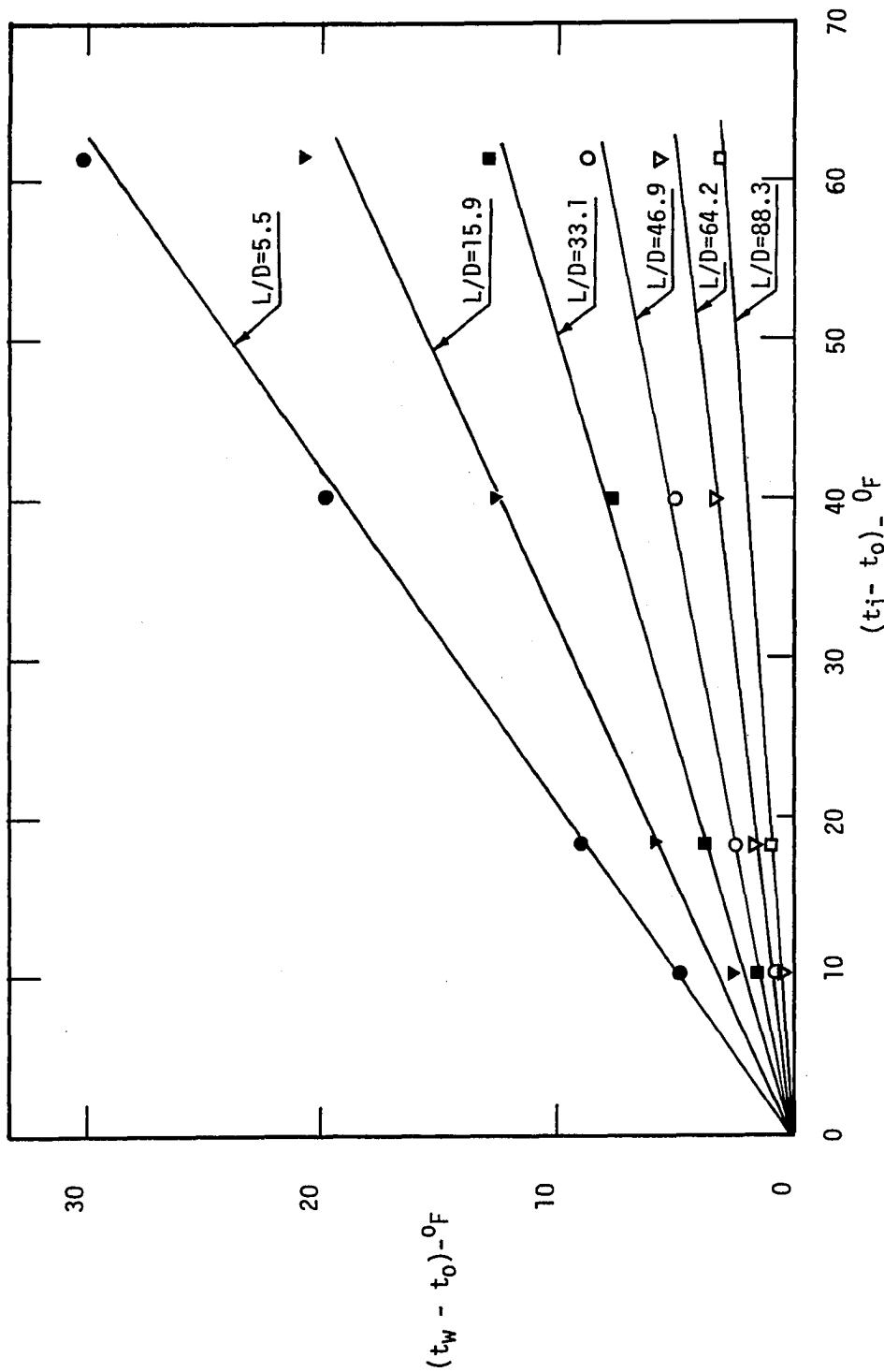


Fig. 12. Variation of  $(t_w - t_0)$  with  $(t_i - t_0)$  for  $N_{Rej} \approx 600$ .

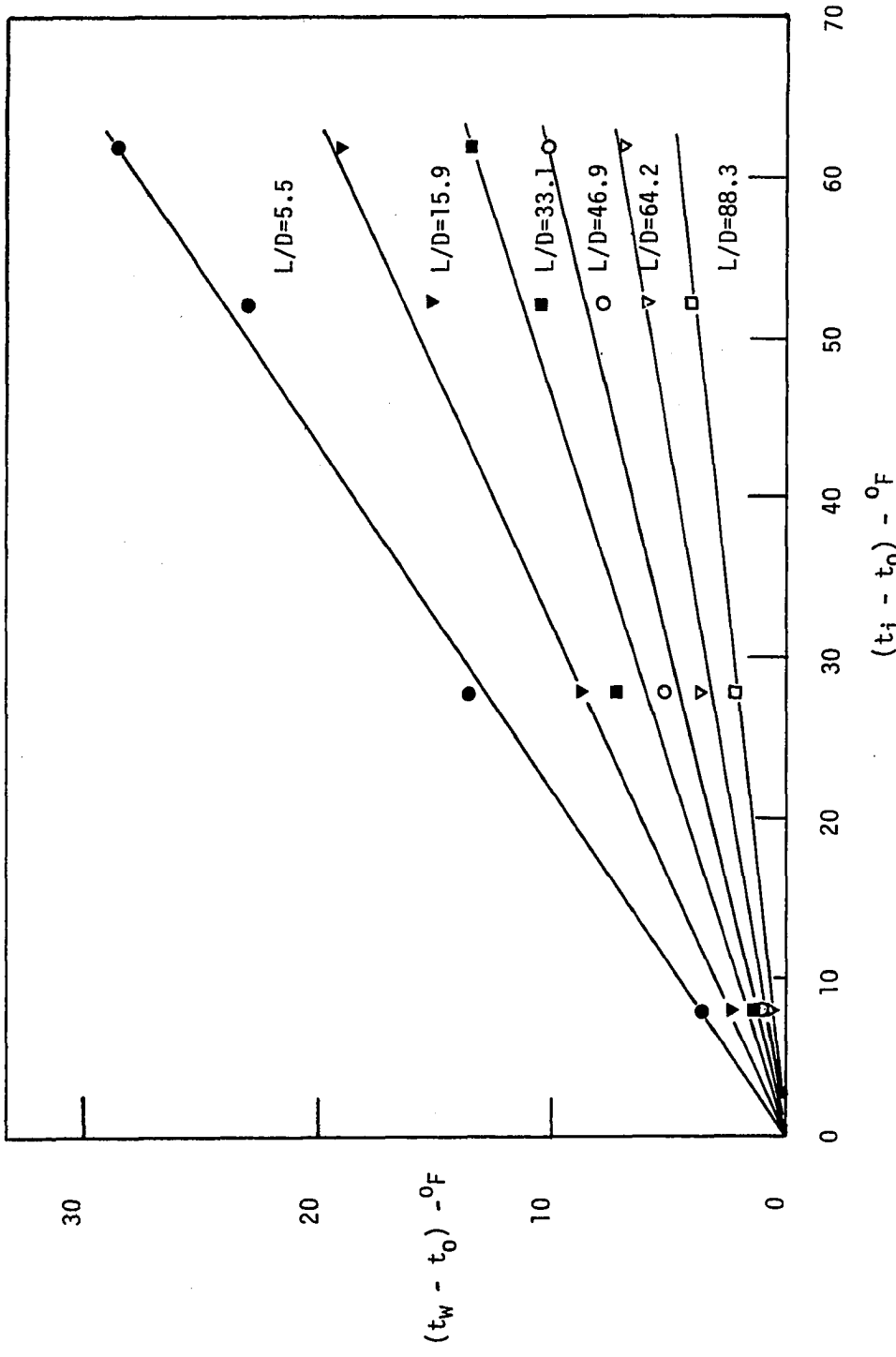


Fig. 13. Variation of  $(t_w - t_o)$  with  $(t_i - t_o)$  for  $N_{Rei} = 1000$ .

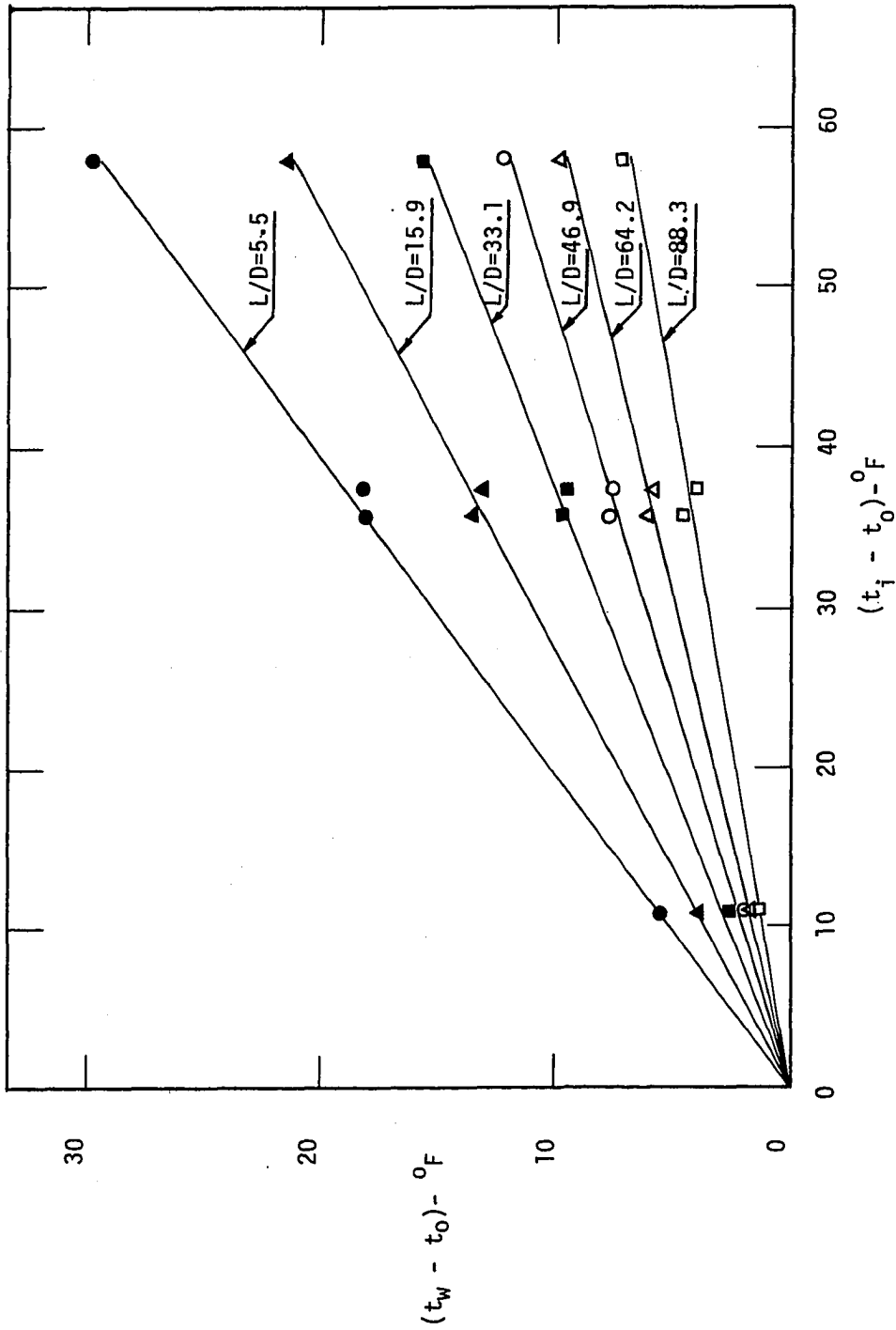


Fig. 14. Variation of  $(t_w - t_0)$  with  $(t_i - t_0)$  for  $NRe_j \approx 1500$ .

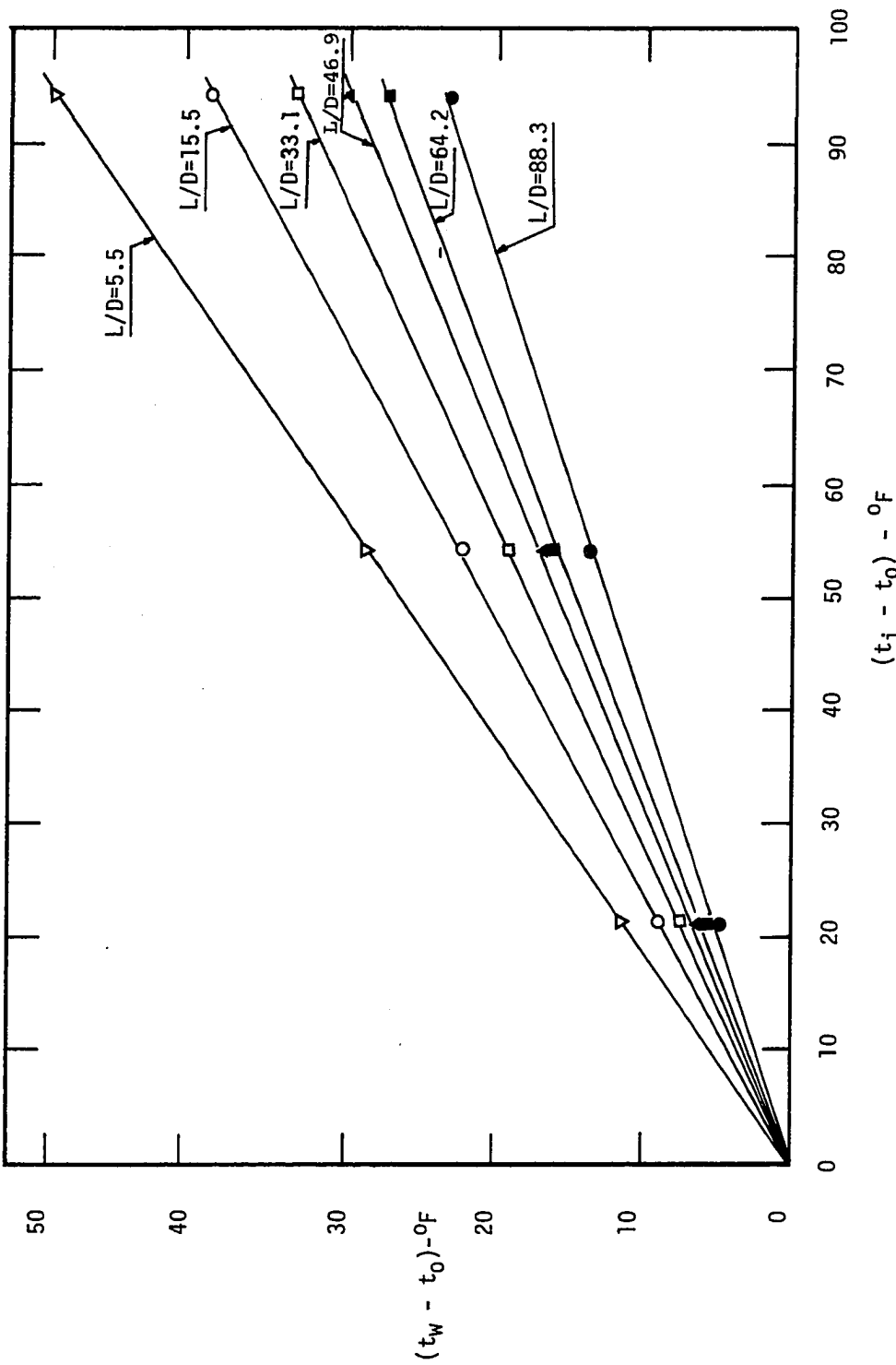


Fig. 15. Variation of  $(t_w - t_0)$  with  $(t_i - t_0)$  for  $N_{Rej} \approx 4000$ .

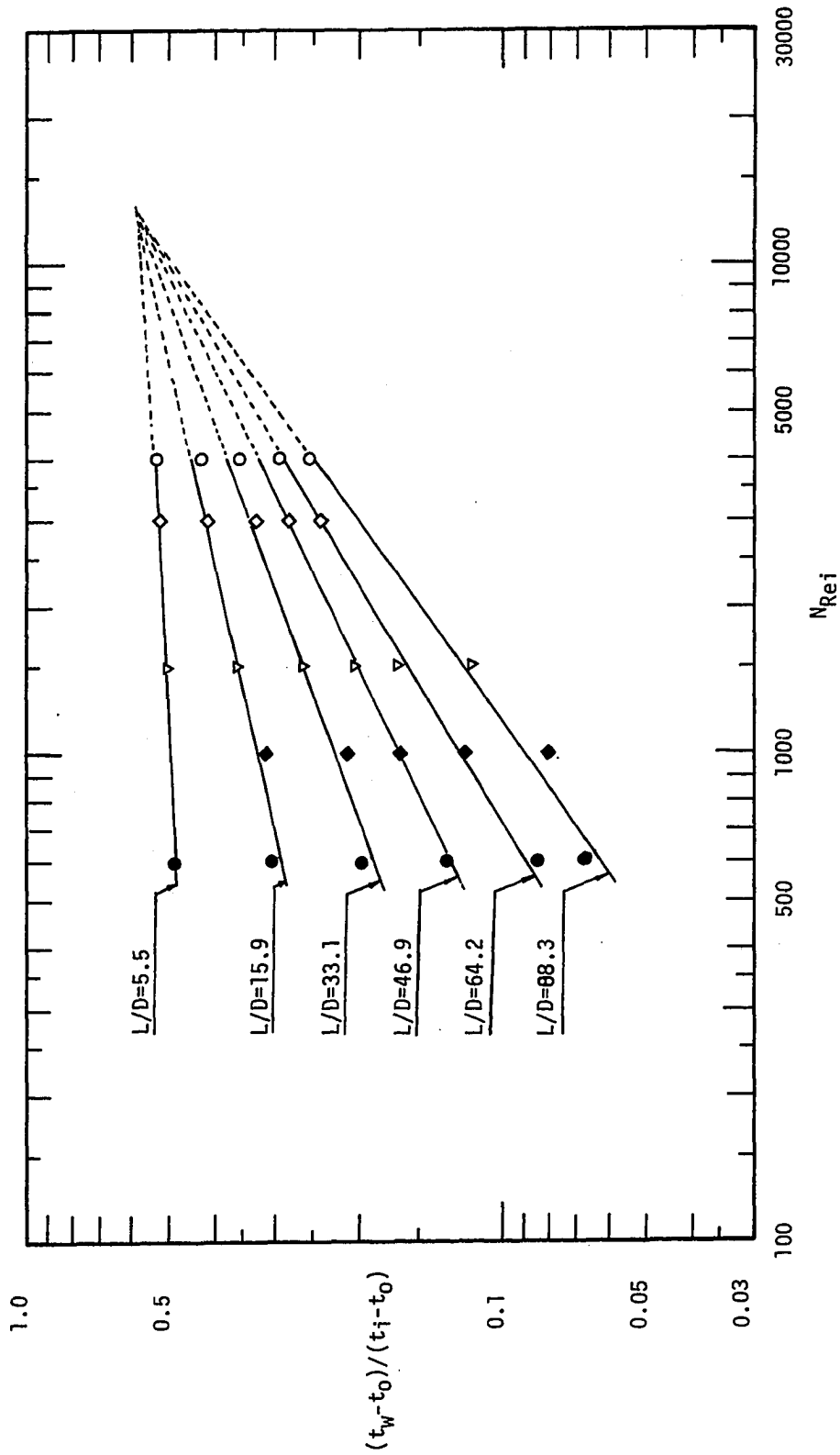


Fig.16. Variation of the Slope  $m$ , ( $m = (t_w - t_0) / (t_i - t_0)$ ) with  $N_{Rei}$  at Low Inlet Temperatures ( $t_i \leq 200^\circ F$ ).

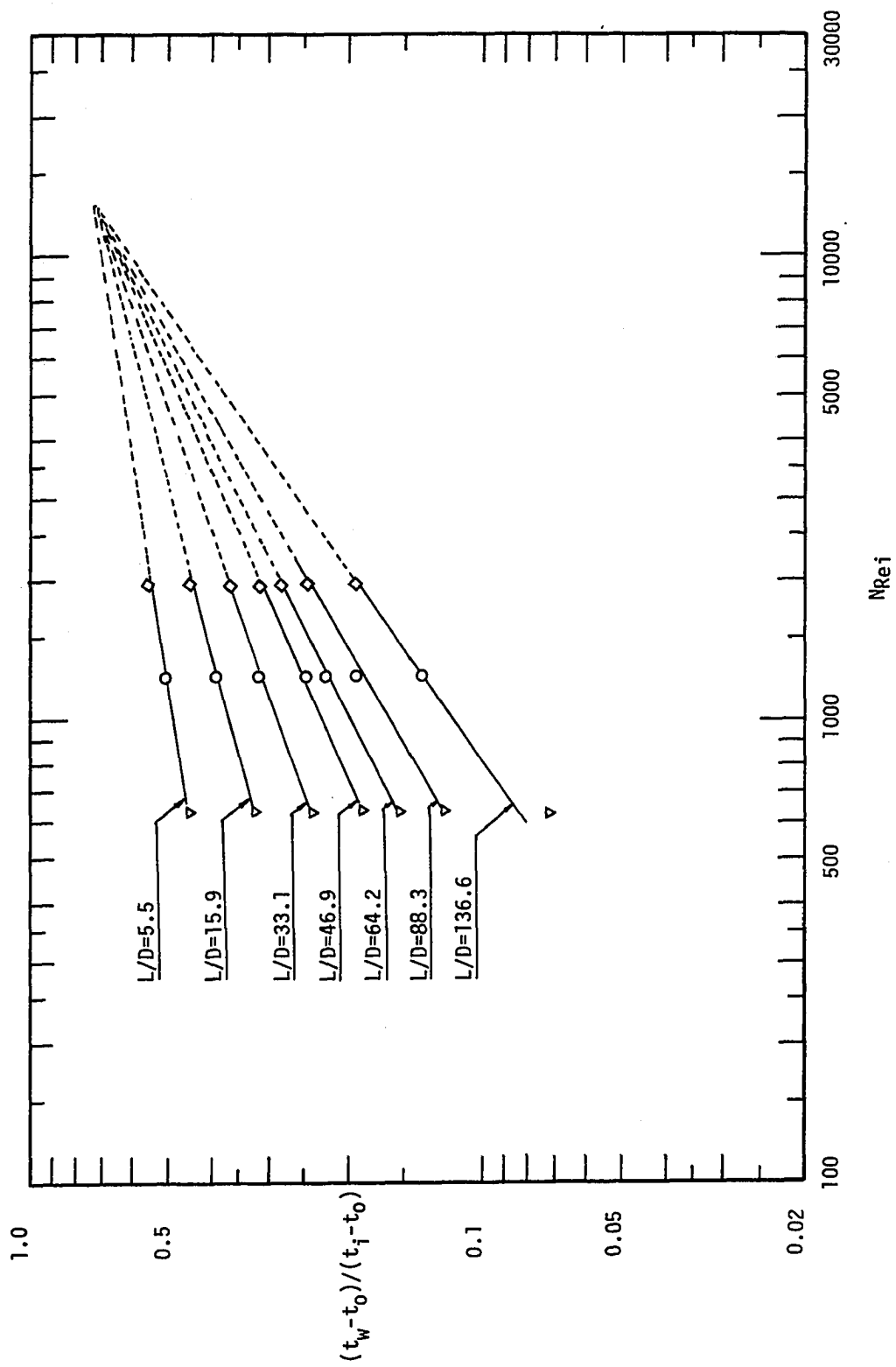


Fig. 17. Variation of the Slope  $m$ ,  $(m = (t_w - t_0) / (t_i - t_0))$  with  $N_{Rei}$  at High Inlet Temperatures ( $t_i \geq 600^\circ F$ ).

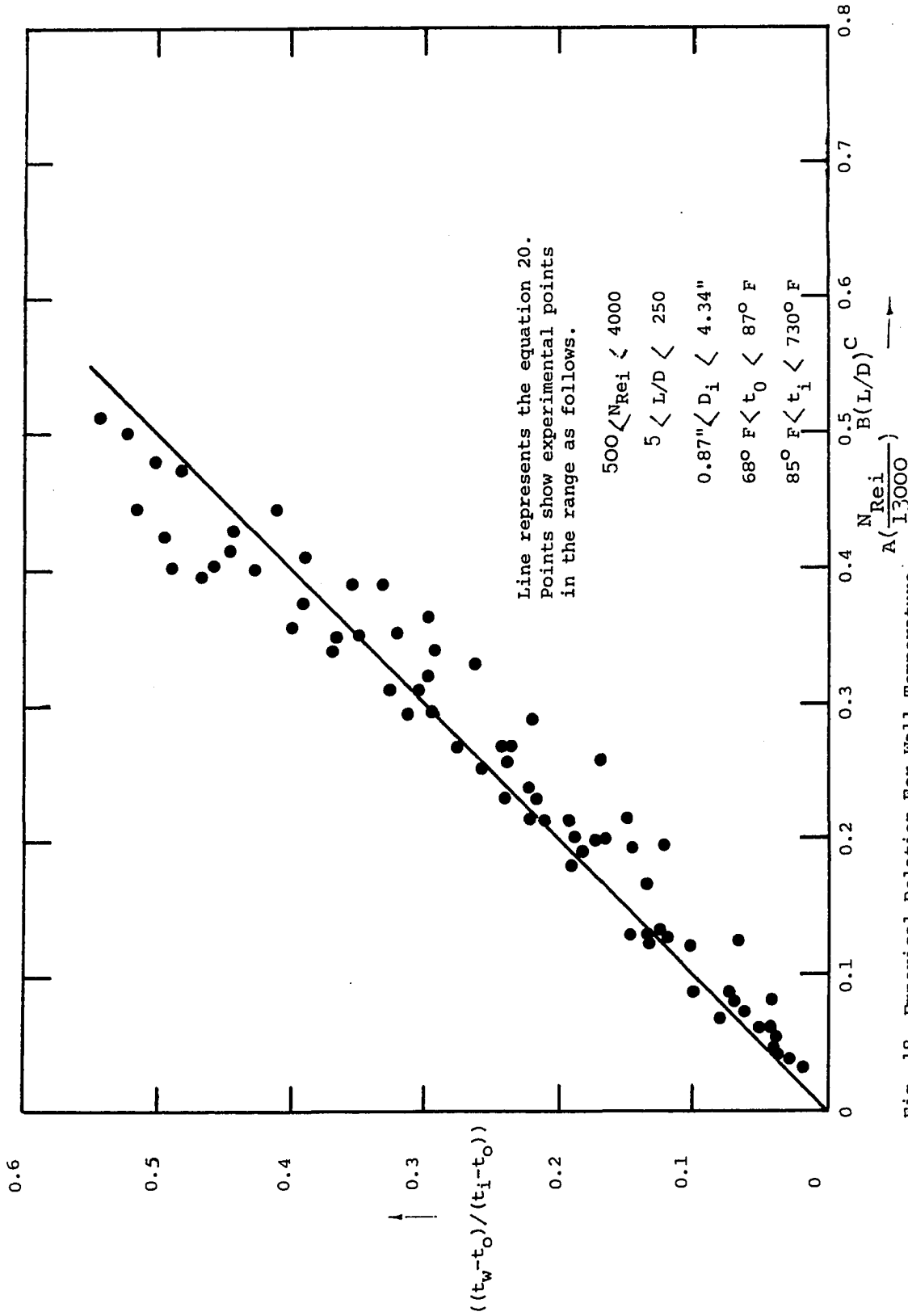


Fig. 18. Empirical Relation For Wall Temperature.

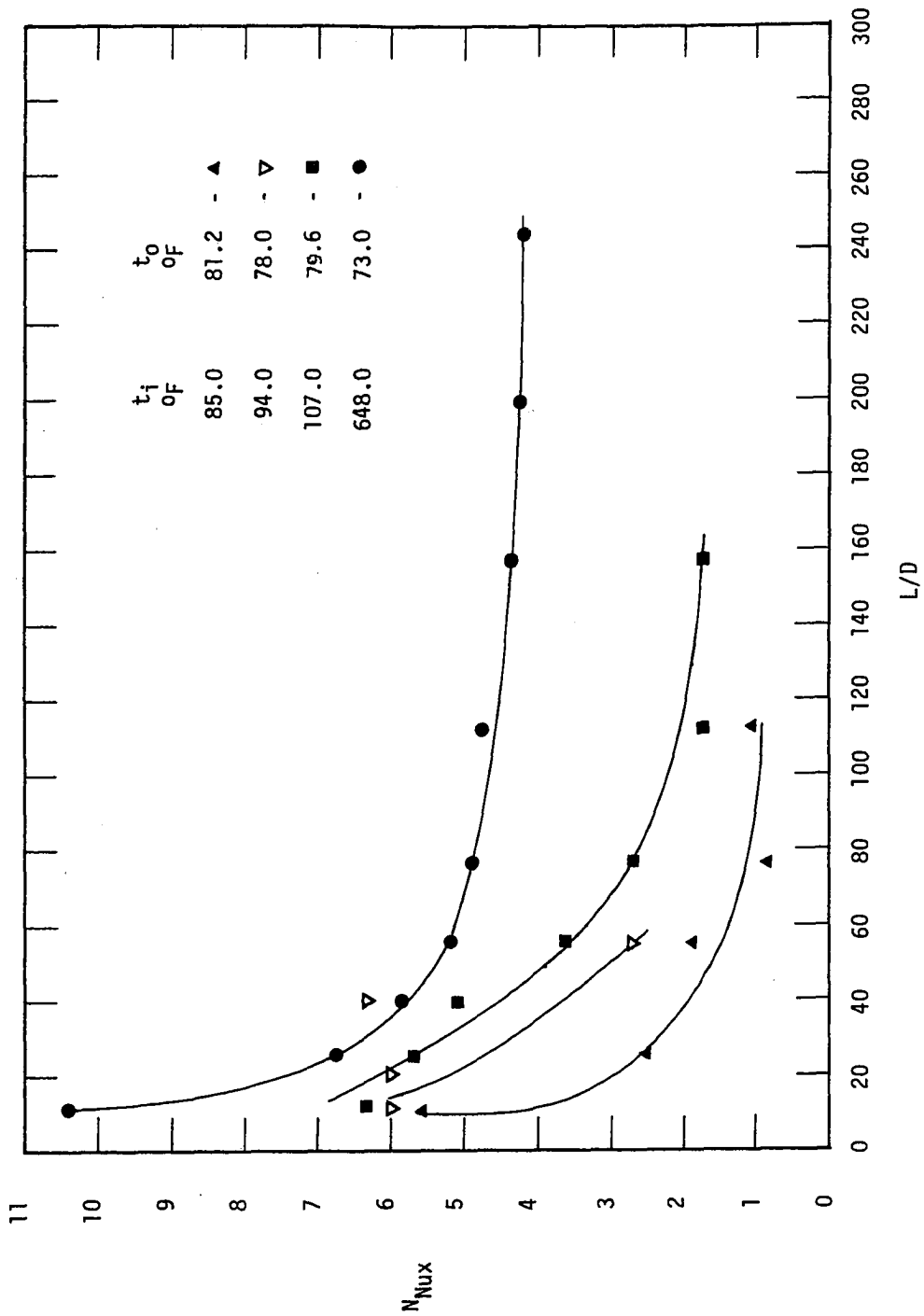


Fig. 19. Axial Variation of Local Nusselt Number for  $N_{Rei} \approx 600$ .

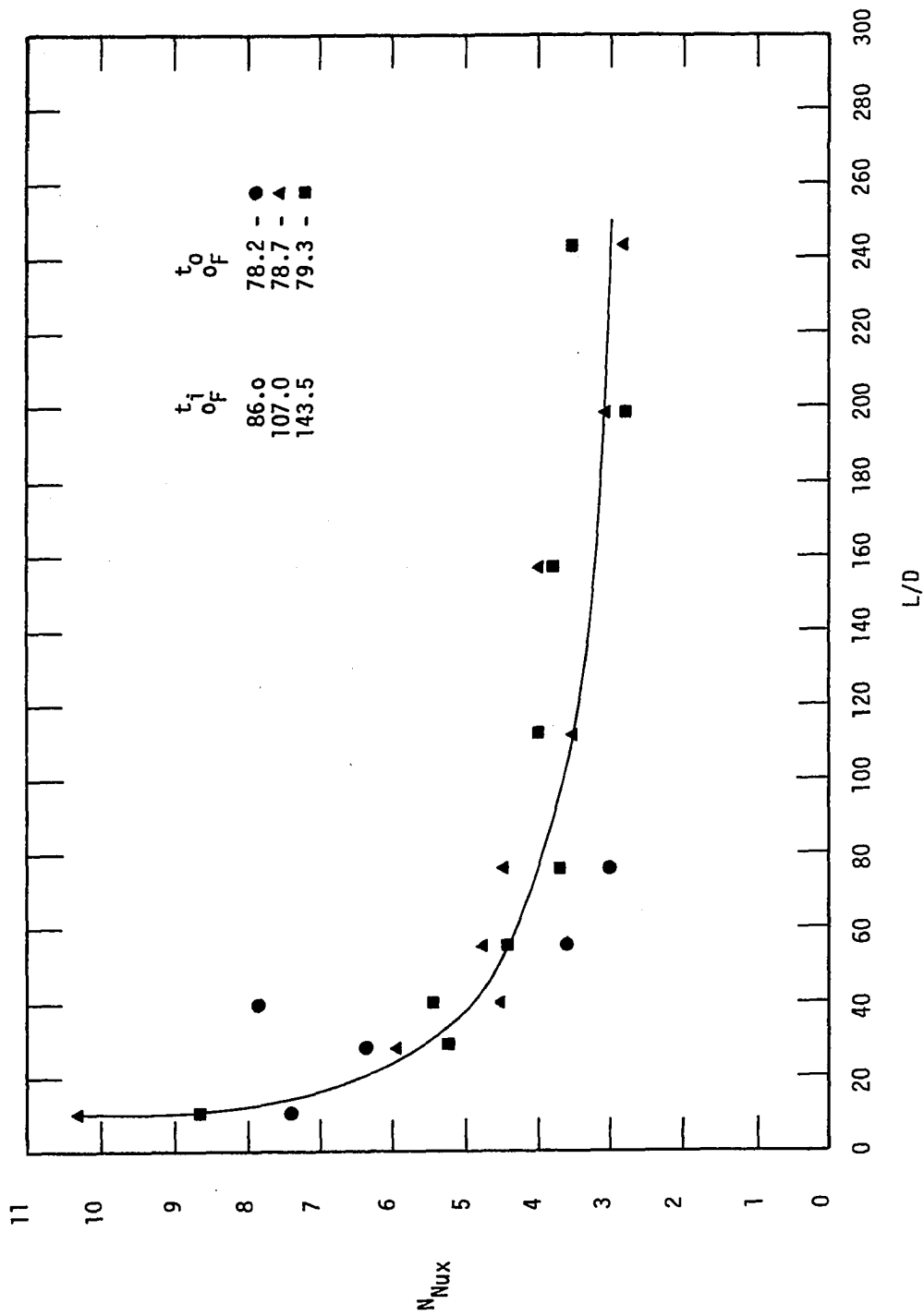


Fig. 20. Axial Variation of Local Nusselt Number for  $N_{Rej} \approx 1000$ .

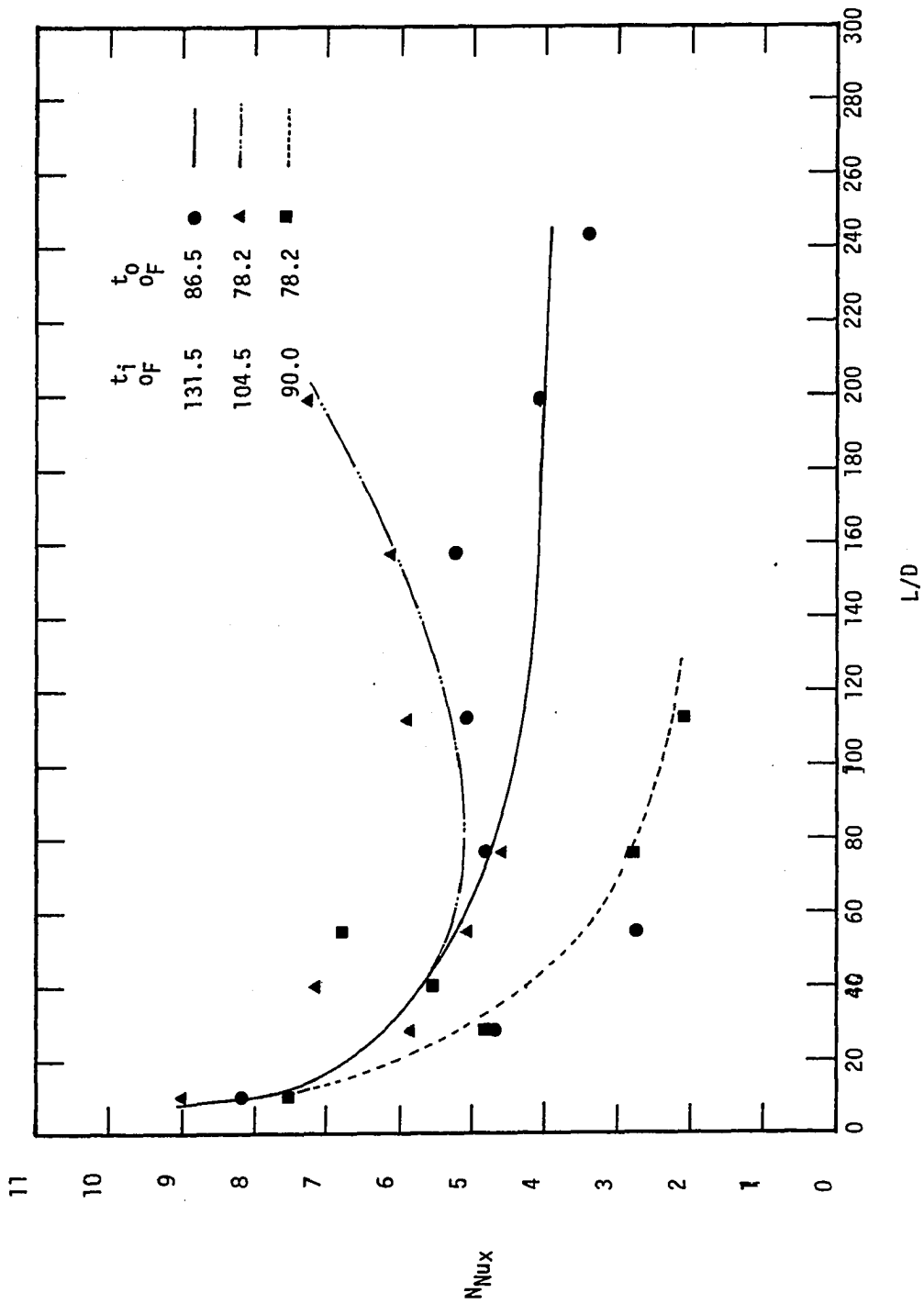


Fig. 21. Axial Variation of Local Nusselt Number for  $N_{Rej} \approx 1500$ .

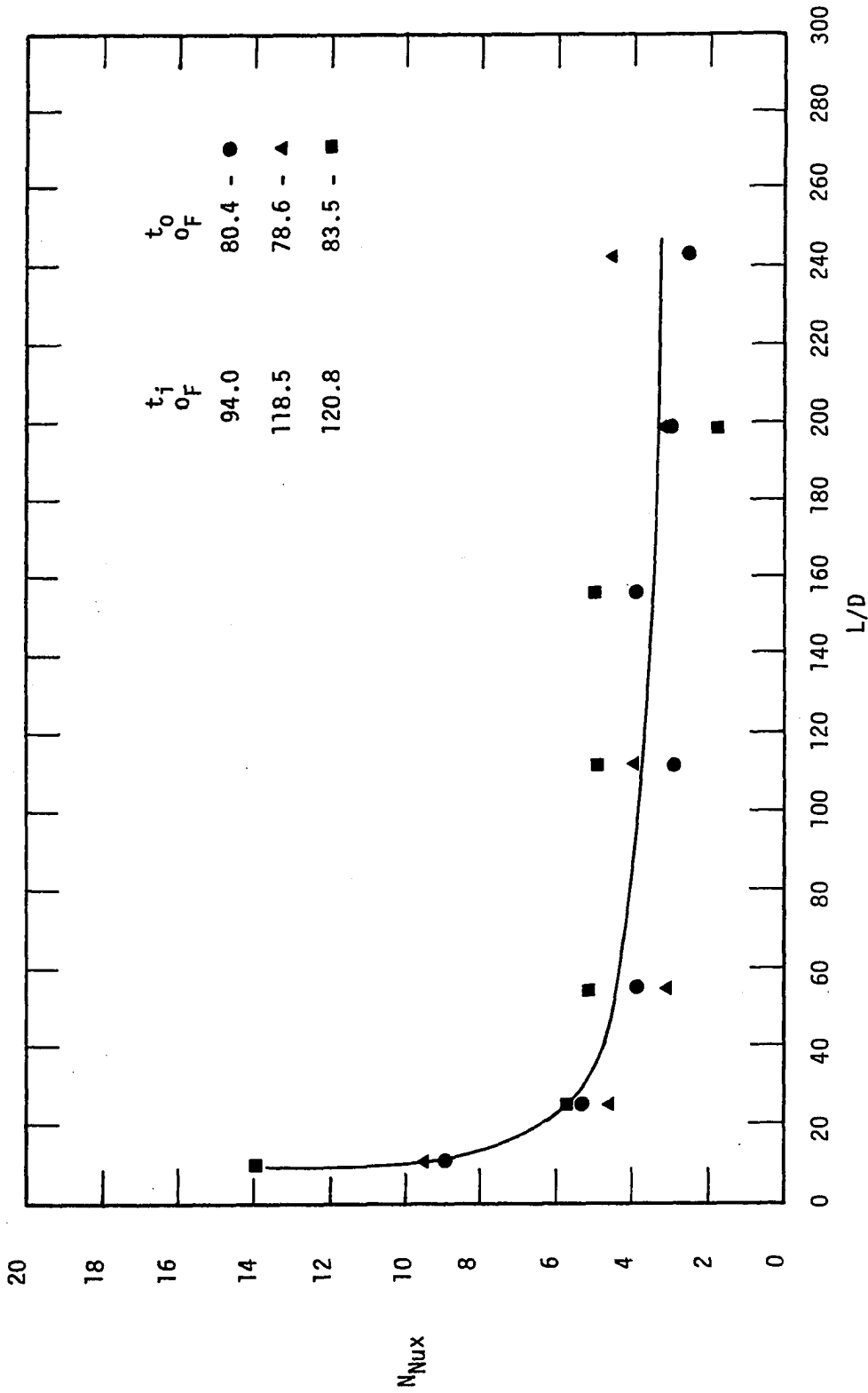


Fig. 22. Axial Variation of Local Nusselt Number for  $Re_j \approx 2000$ .

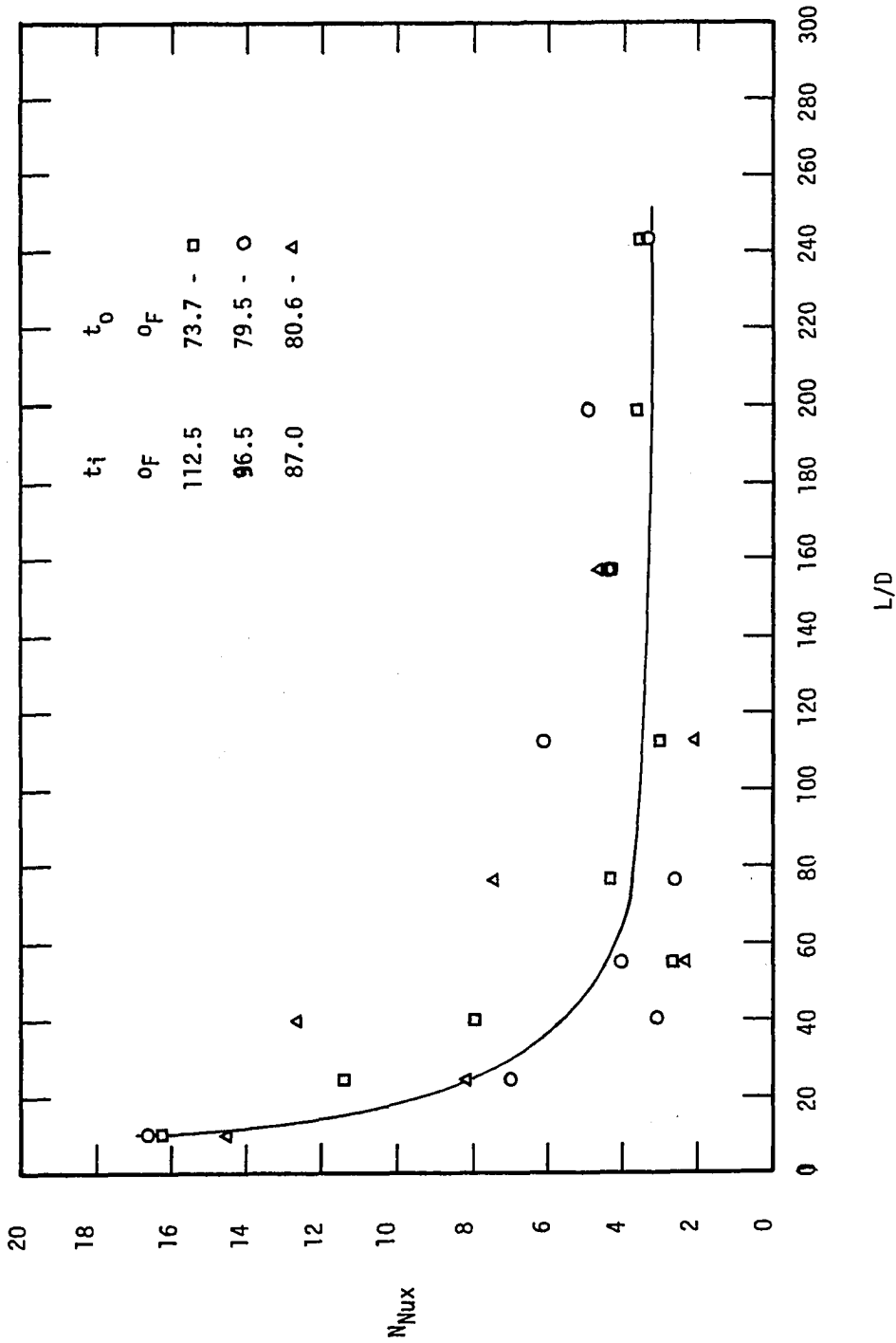


Fig. 23. Axial Variation of Local Nusselt Number for  $N_{Rej} \approx 3000$ .

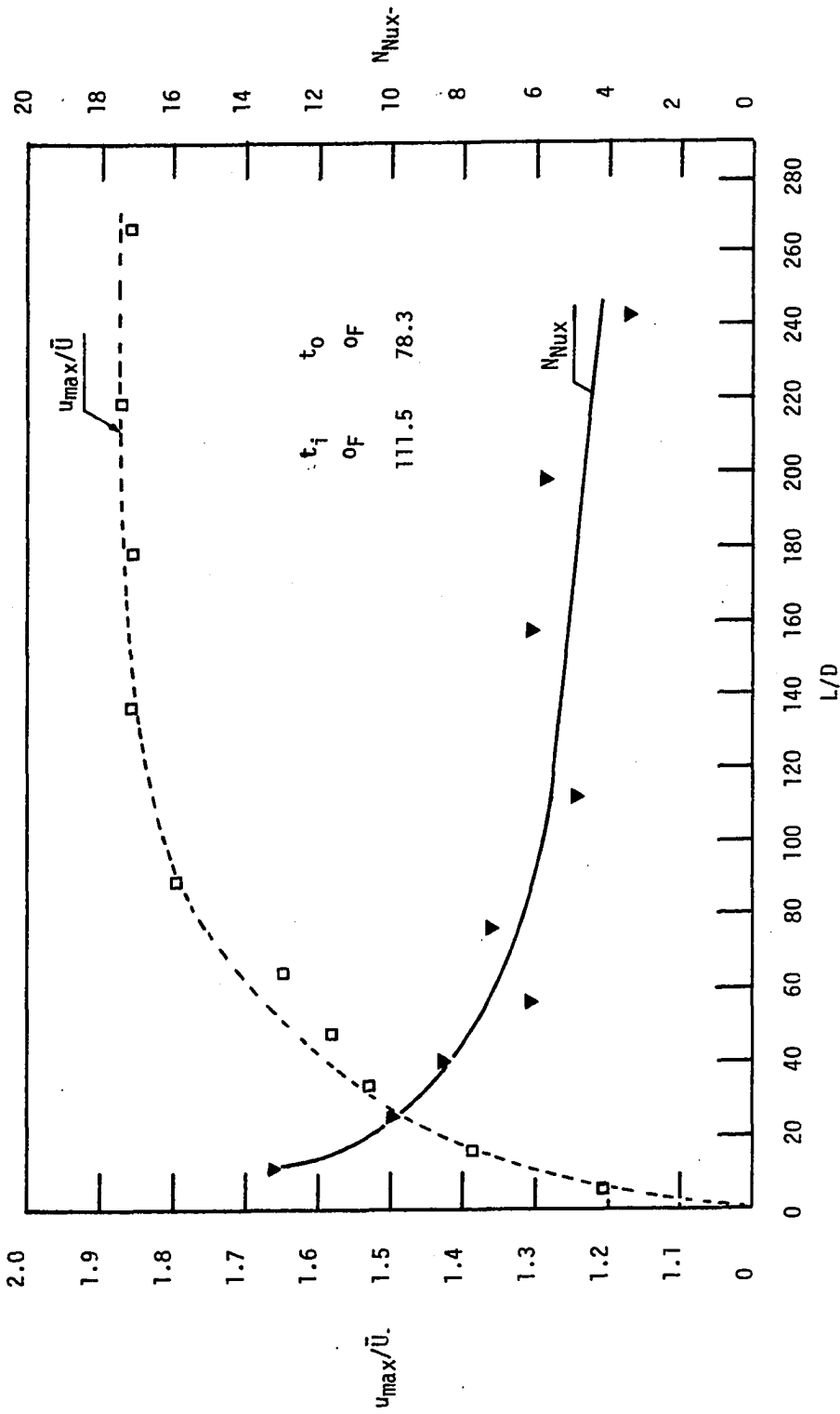


Fig. 24. Variation of  $u_{max}/\bar{u}$  and Local Nusselt Number with  $L/D$  for Non-Isothermal Flow at  $N_{Rej} = 3886$ .

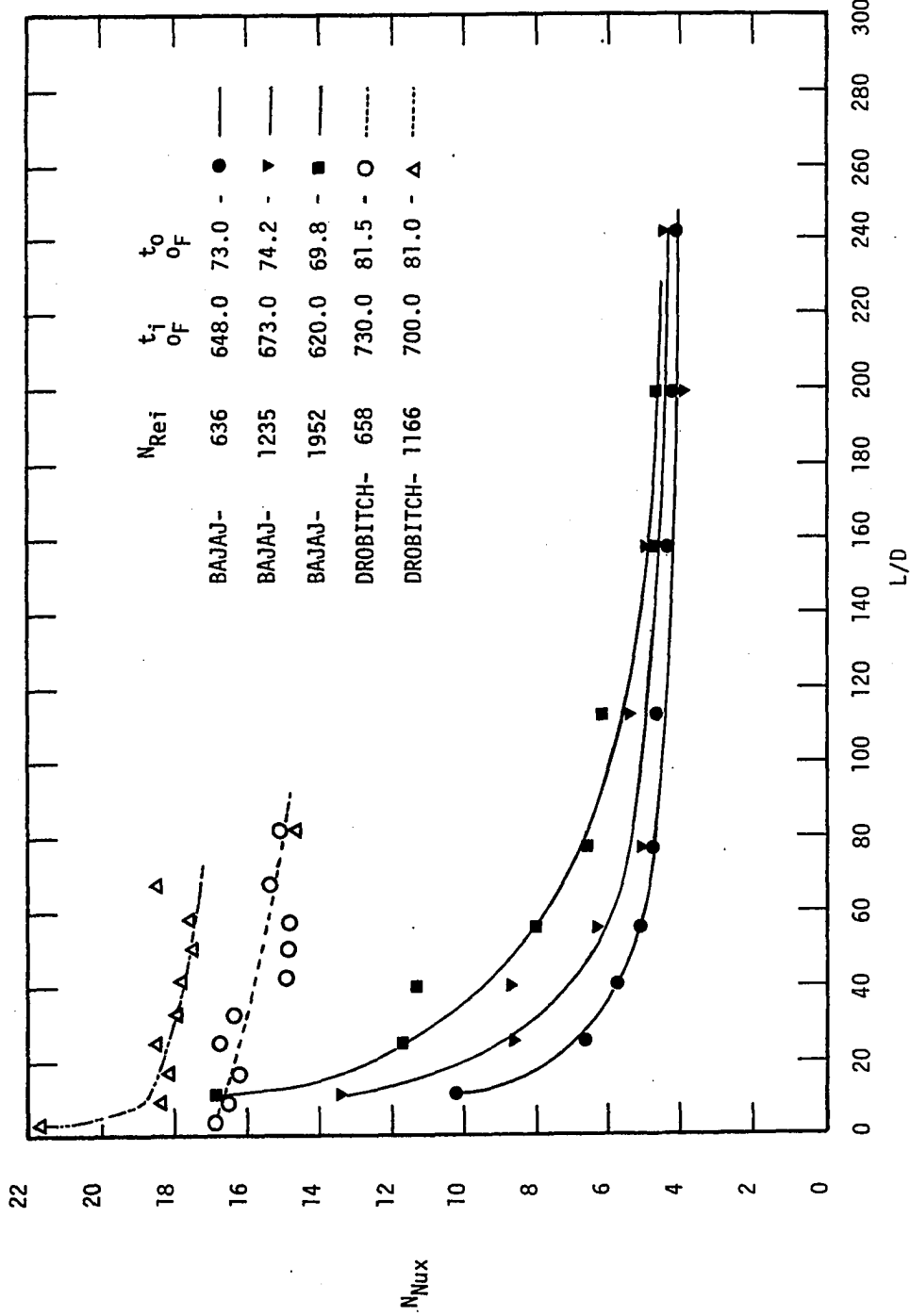


Fig. 25. Axial Variation of Local Nusselt Number for  $N_{Rei} \approx 2000$ , at High Temperatures ( $t_i \geq 600$  °F).

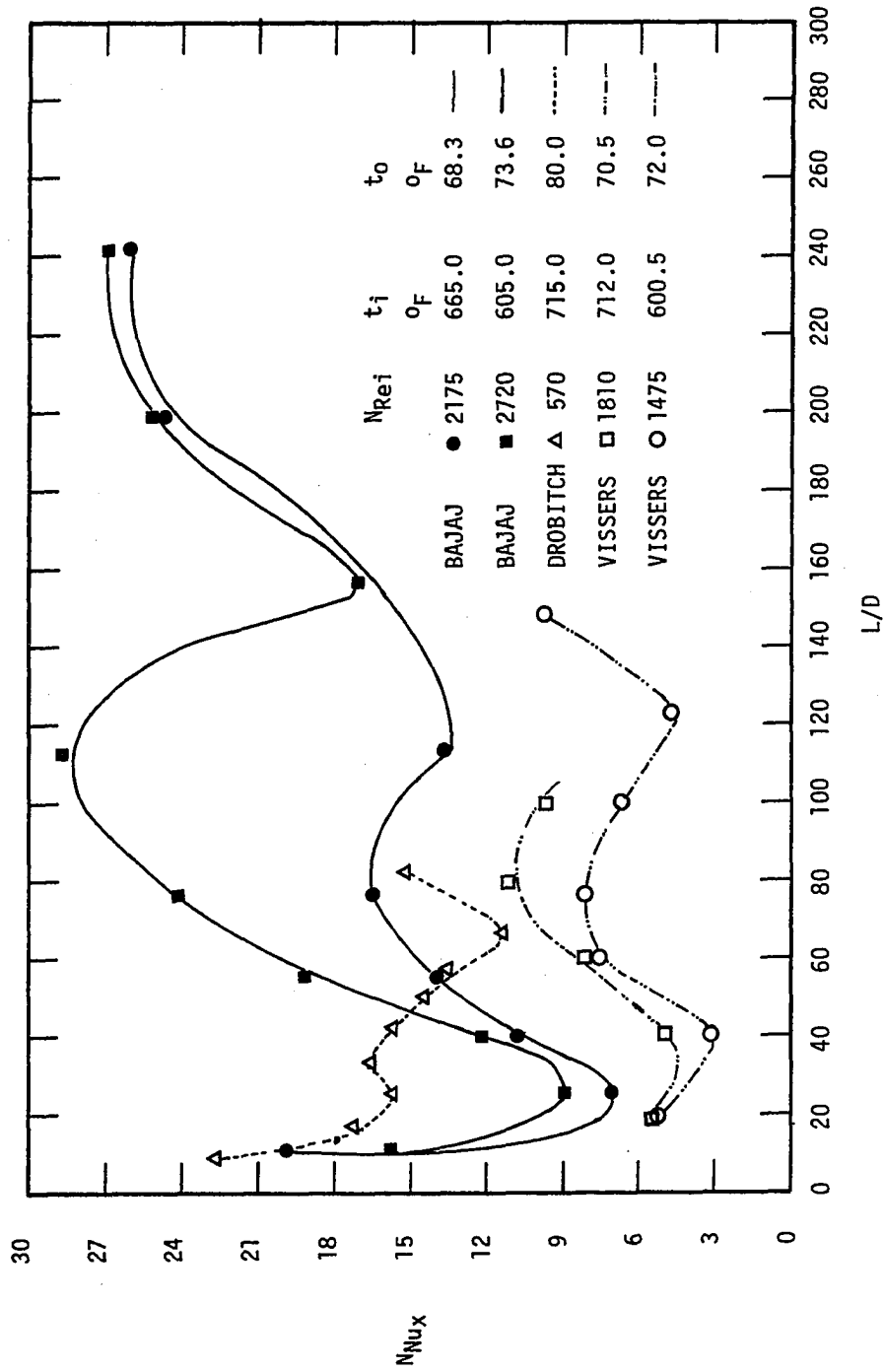


Fig. 26. Axial Variation of Local Nusselt Number at high Inlet Temperatures [ $t_i \geq 600$  °F ] for Bajaj, Viissers, & Drobitch.



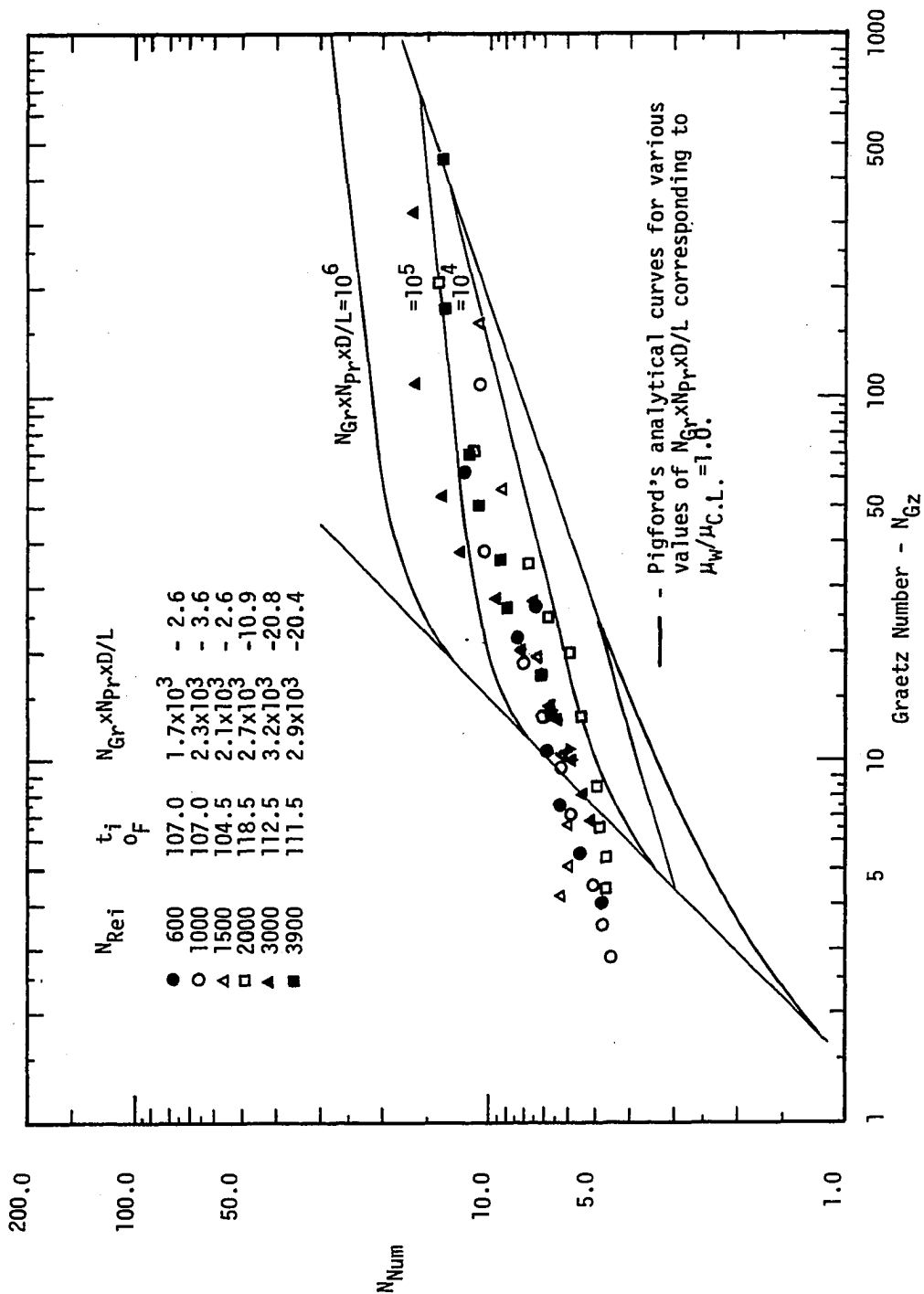


Fig. 28. Variation of Mean Nusselt Number with Graetz Number.

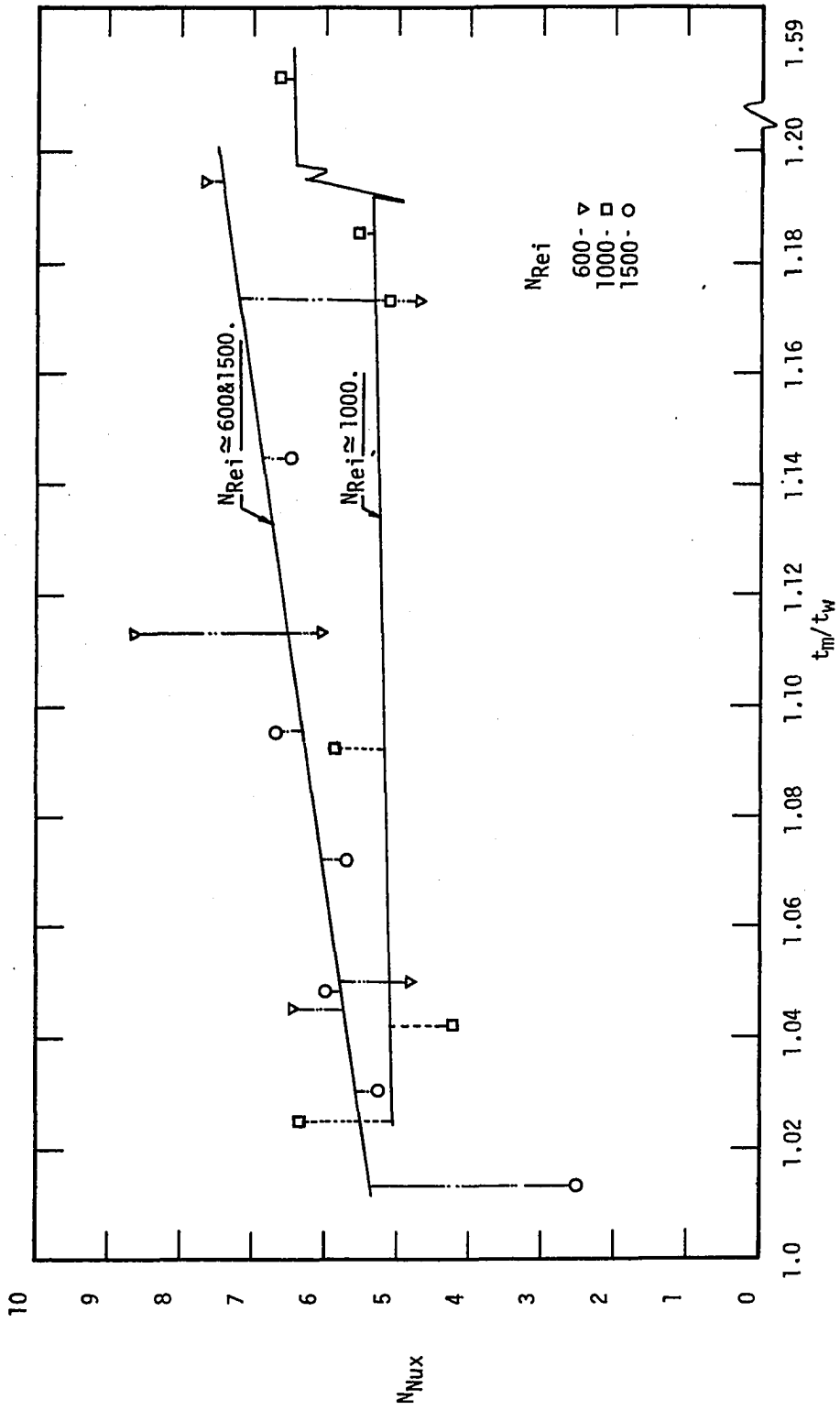


Fig. 29. Variation of Local Nusselt Number with  $t_m/t_w$  for  $N_{Rei} \approx 600, 1000, \& 1500$  at  $L/D = 24.5$

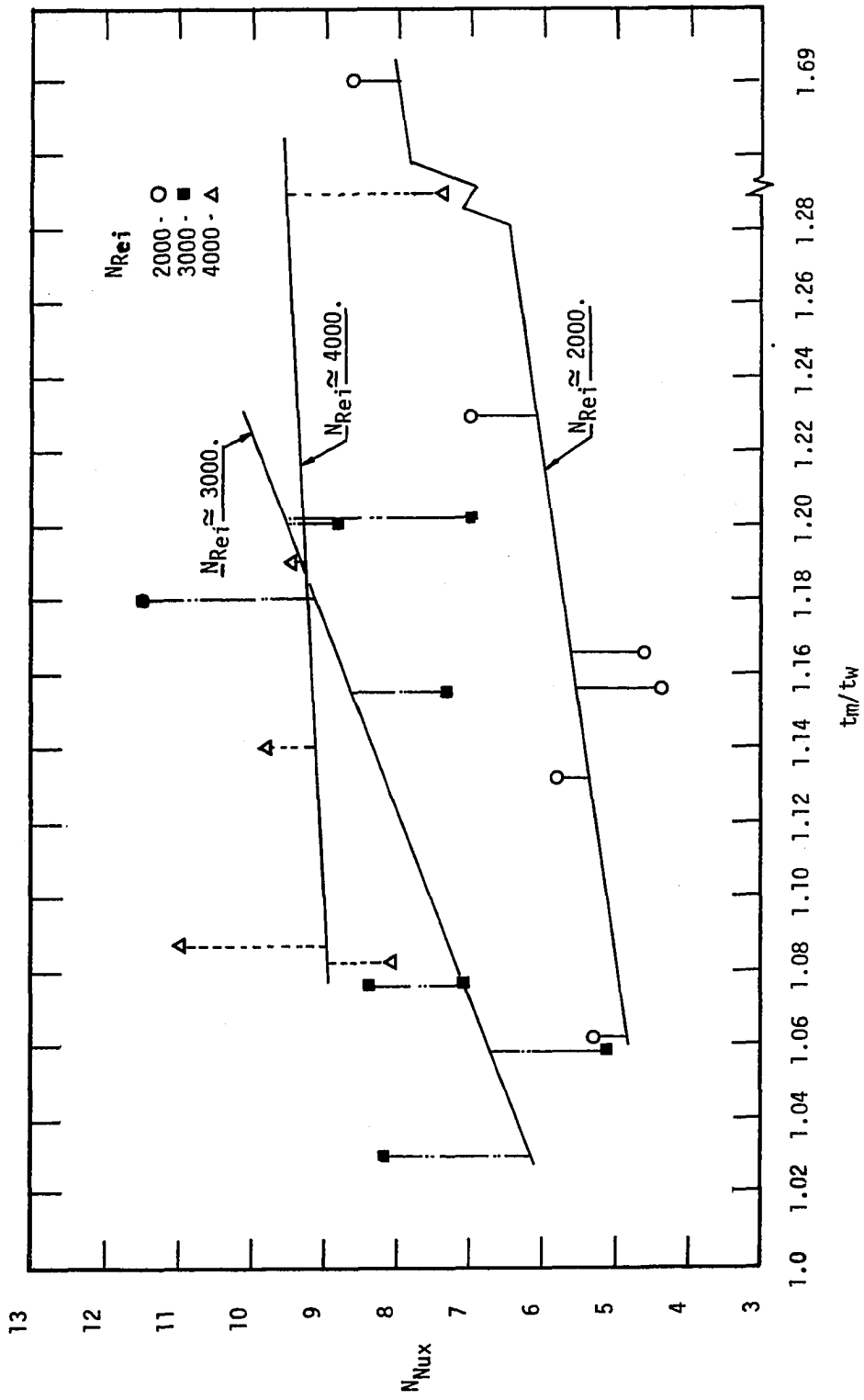


Fig. 30. Variation of Local Nusselt Number with  $t_m/t_w$  for  $N_{Rei} \approx 2000, 3000, 4000$  at  $L/D = 24.5$

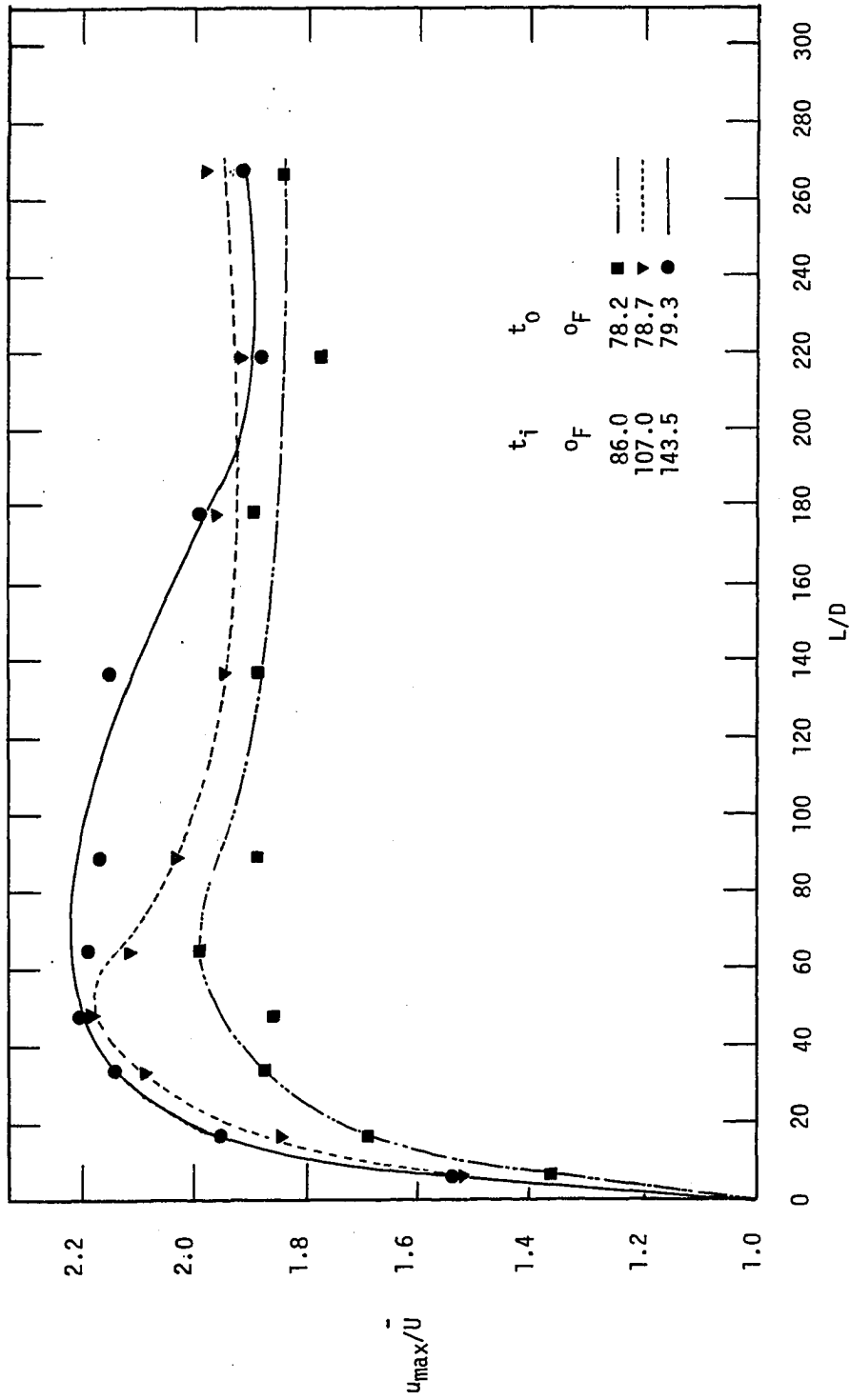


Fig. 31. Variation of  $u_{\max}/\bar{u}$  with  $L/D$  for Non-Isothermal Flow at  $N_{Rej} \approx 1000$ .

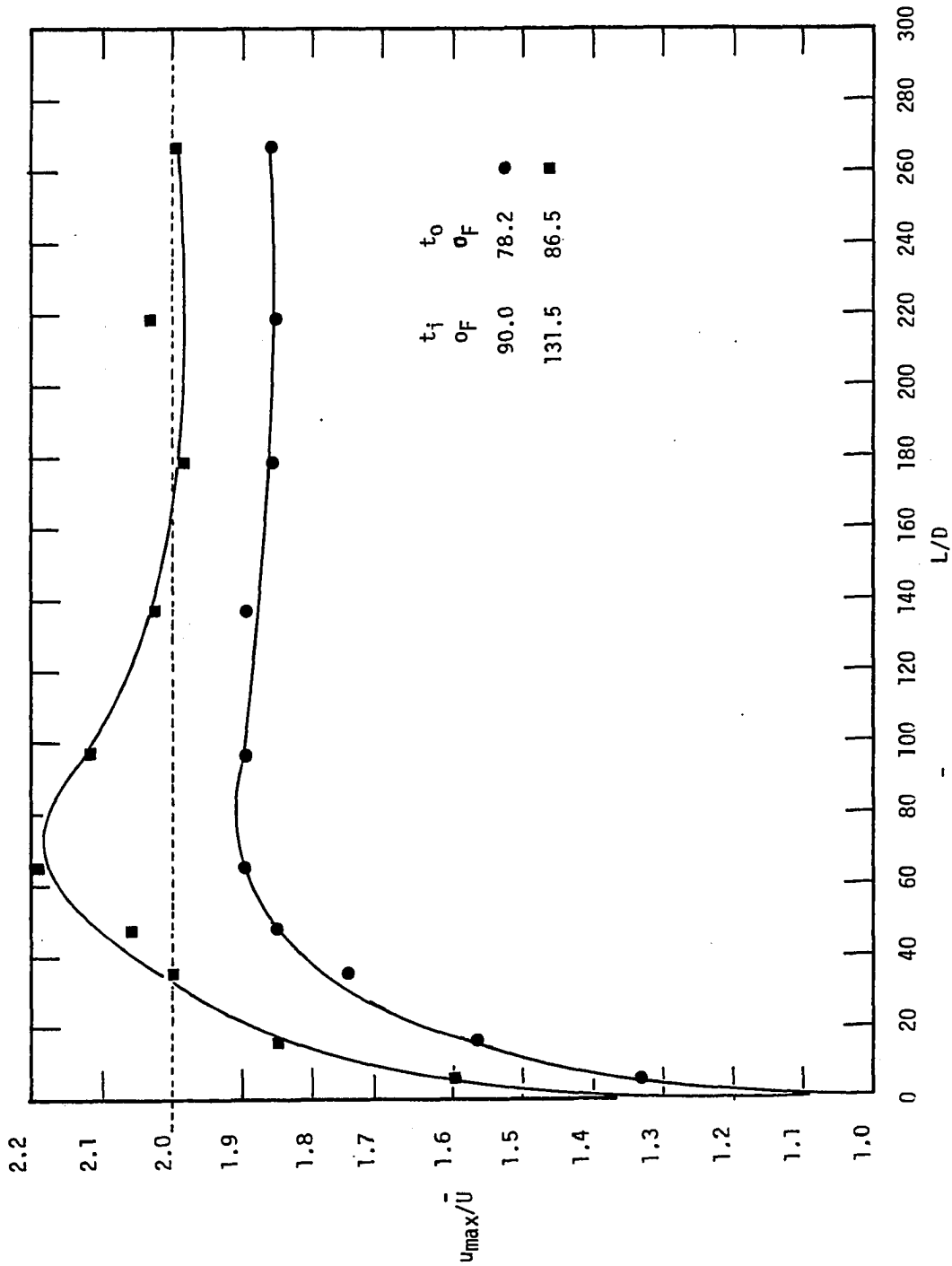


Fig. 32. Variation of  $u_{max}/\bar{U}$  with  $L/D$  for Non-Isothermal Flow at  $N_{Rej} \approx 1500$ .

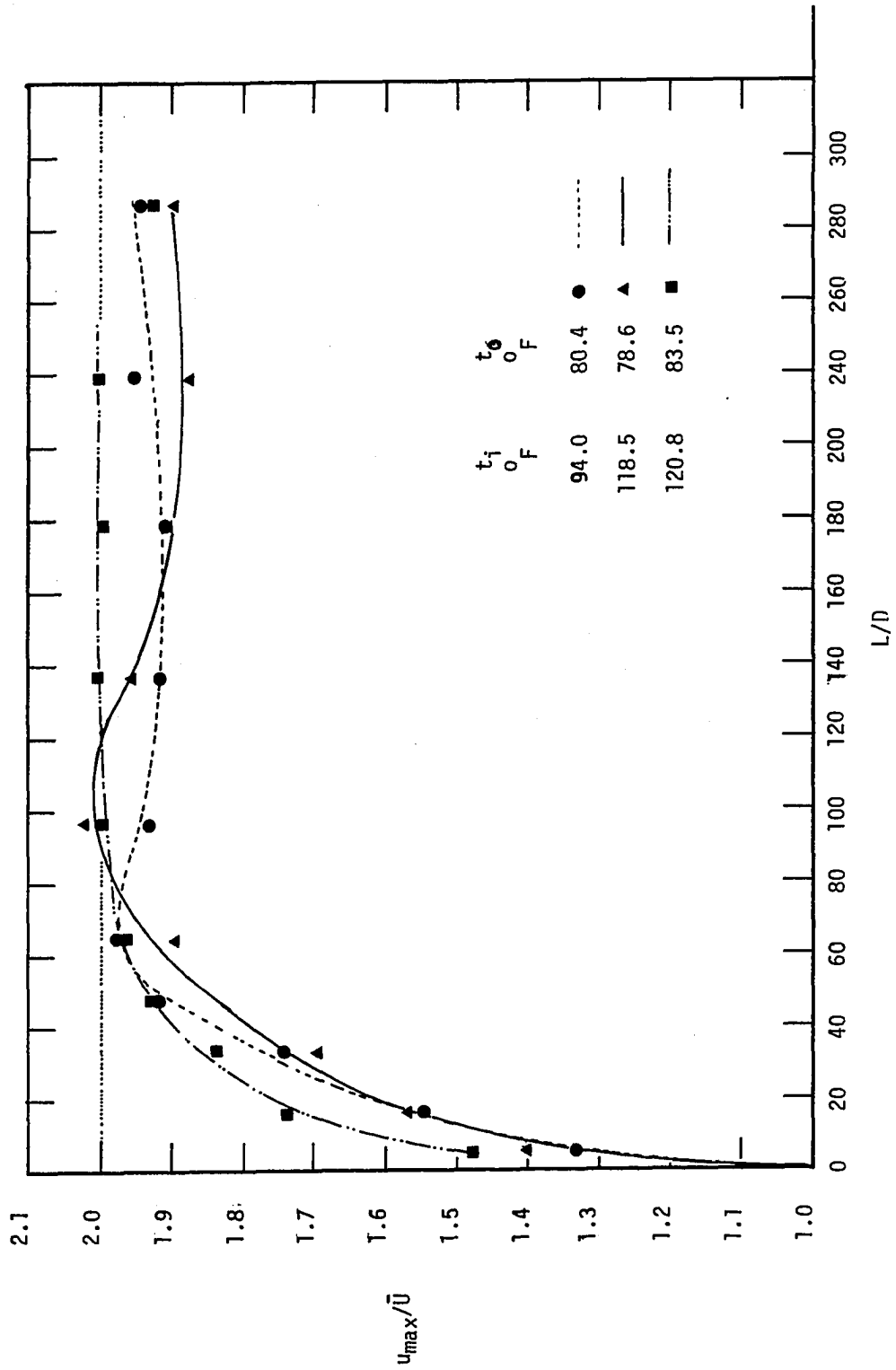


Fig. 33. Variation of  $u_{\max}/\bar{u}$  with  $L/D$  for Non-Isothermal Flow at  $N_{Re1} \approx 2000$ .

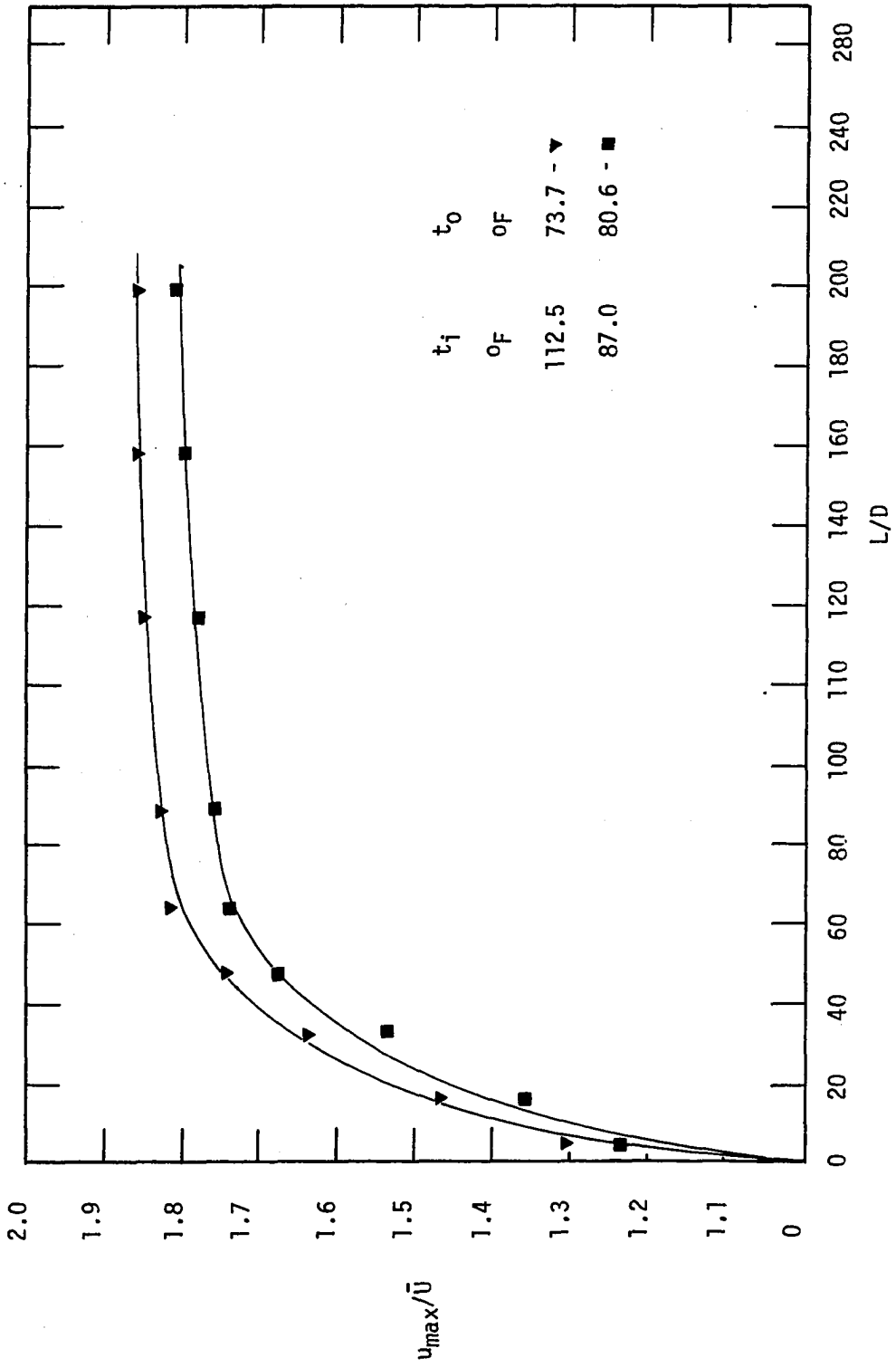


Fig. 34. Variation of  $u_{\max}/\bar{u}$  with  $L/D$  for Non-Isothermal Flow at  $N_{Rej} \approx 3000$ .

## CHAPTER 5

### DISCUSSION

#### 5.1 AXIAL VARIATION OF TEMPERATURE

From the mean air and wall surface temperature curves shown in figures 6 to 11 inclusive it was observed that the rate of temperature drop decreased with an increase in  $N_{Rei}$  for the same  $(t_i - t_o)$  and increased with an increase of  $(t_i - t_o)$  for the same  $N_{Rei}$ . As the  $L/D$  ratio became larger the air of course became cooler and the difference between  $t_m$  and  $t_w$  decreased. At large  $L/D$  ratios  $t_m$  was approximately equal to  $t_w$ . The accurate calculation of heat transfer for these small differences between  $t_i$  and  $t_o$  is difficult, also isothermal or near isothermal conditions are reached at lower  $L/D$  ratios for smaller rates of flow. From figures 12 to 15 inclusive it was observed that  $(t_w - t_o)$  was directly proportional to  $(t_i - t_o)$  for a given  $N_{Rei}$  and  $L/D$ .  $(t_w - t_o)$  is a function of  $(t_i - t_o)$ ,  $L/D$  &  $N_{Rei}$  as shown in figures 16 & 17.

The observed  $t_w$  for different values of  $t_i$ ,  $t_o$ ,  $L/D$  and  $N_{Rei}$  has been found to follow an empirical relation of the form ( See figure 18 ).

$$\frac{t_w - t_o}{t_i - t_o} = A \left( \frac{N_{Rei}}{13000} \right)^B (L/D)^C \quad \text{--- (20)}$$

where A, B and C are empirical constants.

The above equation was solved for  $t_w$ , using the method of least squares to obtain the numerical values of the constants A, B and C. With the help of the above equation, wall temperature  $t_w$ , at a particular L/D can be predicted if  $t_i$ ,  $t_o$  and  $N_{Rei}$  are known.

It was observed that the constants A, B and C attain different values depending upon the inlet temperature and Reynolds number to give the best possible fit.. Suitable values of A, B and C were selected to give the least spread in the calculated values of  $t_w$  when compared to the experimental values of  $t_w$ .

The deviations of the predicted values of  $t_w$  from the experimental values, along with the various values of A, B and C, are given below.

$$A = 0.60 \quad (\text{For } t_i < 200^\circ\text{F})$$

$$A = 0.69 \quad (\text{For } t_i > 600^\circ\text{F})$$

$$B = 0.07$$

$$C = 0.47$$

The above values apply to:

$$N_{Rei} < 4000$$

$$68^\circ\text{F} < t_o < 87^\circ\text{F}$$

$$L/D < 250$$

The deviations of the  $t_w$  measured experimentally from the value obtained from the empirical relation were within  $\pm 8\%$ . The majority of values fell within  $\pm 4\%$ .

Equation (20) was found to hold for the experimental results of Drobitch (6). He had conducted the experiments under similar boundary conditions as the present investigation, in a 4.34" diameter pipe at high inlet temperatures ( $t_1 > 600^\circ \text{F}$ ). The values of A and B were found to be nearly the same as in the present investigation and C was found to be a function of the diameter of the pipe. It could be expressed as  $C = 0.49 (D)^{0.25}$  where D is in inches.

The deviation between experimental values and calculated values of  $t_w$  using this data were within  $\pm 7\%$ .

Combining the results of the present investigation with those of Drobitch, we can express 'A' as a function of inlet temperature, 'B' as a constant and 'C' as a function of diameter giving :

$$A = \frac{T_i}{585} + 0.5$$

$$B = 0.07$$

$$C = 0.49 (D)^{0.25}$$

From the above sets of values of A, B and C it is obvious that the inlet temperature and the diameter of the pipe play an important role in the heat transfer results.

## 5.2 HEAT TRANSFER CHARACTERISTICS

Figures 19 to 26 inclusive show the variation of local Nusselt number  $N_{Nux}$  vs. L/D ratio for various  $N_{Rei}$  and  $t_i$ . The graphs of  $N_{Nux}$  vs. L/D ratio for  $N_{Rei}$  less than 2000 show that  $N_{Nux}$  decreased in a non-linear fashion with increasing L/D ratio. For the particular case of  $N_{Rei}=1500$  and  $t_i=104^\circ\text{F}$  the above trend was not followed. It was seen that for  $L/D > 60$  the  $N_{Nux}$  values increased with increasing L/D ratios. The experimental data obtained at  $N_{Rei} \approx 3000$  is scattered. This may be due to the onset of turbulence in the flow. Figure 25 shows the results of the present investigation for high inlet temperatures  $t_i > 600^\circ\text{F}$ . The values of  $N_{Nux}$  were found to be lower at the same L/D ratio, and the rate of decrease of  $N_{Nux}$  with L/D were found to be higher, when compared to the results of Drobitch (6) for nearly the same entrance conditions. Fig. 26 shows that the changes of  $N_{Nux}$  were not consistent with increasing values of L/D ratio. While taking the temperature readings for the tests shown in figure 26, fluctuations of large magnitude were observed in the potentiometer pointer. The behaviour of the experimental results for these two sets of readings could be due to variation in the magnitude and frequency of the velocity fluctuations or a fluctuation in the flow rate. Drobitch (6) and Vissers (29) obtained similar graphs for a temperature range of  $600-700^\circ\text{F}$ , but the fluctuations appeared at lower values of  $N_{Rei}$ .

Local Nusselt number variation with  $t_m/t_w$  shown in figures 29 & 30 confirm the observations reported by Zellnik and Churchill (31). They had also observed the increase of  $N_{Nux}$  with  $t_m/t_w$  while studying the local convective heat transfer coefficient at high inlet temperatures for a constant wall temperature case, where the gas was being cooled. Attempts were not made to correlate the data as was done by the above authors because of an insufficient number of data points. The different  $t_m/t_w$  for the same Reynolds number represents different inlet temperatures. The scatter of the points in all cases except for  $N_{Rei} \approx 3000$  was within  $\pm 20\%$ . The slopes of the curves are different for different local Reynolds numbers.

The experimental results of the present investigation were compared with the analytical results given by Kays (16), Pigford (23), Hausen (7), and are discussed below.

Figure 27 shows local Nusselt number ( $N_{Nux}$ ) vs. Graetz number ( $N_{Gz}$ ). The conditions applying to curves 1, 2, 3 & 4 are as follows :

- a. Curve 1 was derived analytically by Kays (16) using the velocity profile development given by Langhaar for laminar flow. Constant wall temperature was selected as the boundary condition. The air in the pipe was being heated and the heating began at the pipe entrance. Experiments were also performed by Kays under the conditions specified for curve 1. The test pipe diameters were less than  $\frac{1}{4}$ " , with air flowing vertically upwards. The results agreed with curve 1.
- b. Curve 2 was also derived analytically by Kays using the same laminar velocity profile development. The boundary condition

was now constant heat flux at the wall and the air was heated beginning at the entrance.

c. Curve 3 gives the experimental results obtained by Bajaj in a vertical pipe when the air was being cooled. The boundary condition was the wall temperature defined by equation (20). The velocity & temperature profiles were both flat at the test pipe entrance.

d. Curve 4 shows the experimental results obtained by Drobitch (6). The test conditions were the same as used by Bajaj except the pipe diameter was 4.34" rather than 0.87" as used by Bajaj.

Kays experimental and analytical results under the conditions of curve 1 showed excellent agreement. It could be concluded therefore that the natural convection effects were negligible in the pipe diameters less than  $\frac{1}{4}$ ". Curve 3 showed good agreement with curves 1 and 2 except at the higher Graetz numbers. The higher mean temperatures at the entrance of the test pipe would cause natural convection which in turn would increase the local Nusselt number. Because of the larger pipe diameter used for curve 4 natural convection effects would be again greater resulting in higher local Nusselt numbers. It would appear that Grashoff number could be used to indicate the extent of the natural convection and hence the increase in local Nusselt number.

In figure 28, the variation of mean Nusselt number with Graetz number for data from the present investigation and also from Pigford (23) for  $(\mu_w/\mu_{C.L.} = 1.0)$  is shown.

Pigford analytically considered the heat transfer with superimposed natural and forced convection to a fluid flowing in a laminar motion through a vertical tube. He calculated the variation of arithmetic average Nusselt number with the Graetz number for several selected values of Grashof-Prandtl product ( $N_{Gr}$ ,  $N_{Pr}$ ,  $D/L$ ) and of the ratio of fluid viscosity at the wall to that at the average bulk fluid temperature. The graph corresponding to  $\mu_w/\mu_{C.L.} = 1.0$  was selected for comparison. Of the values of  $\mu_w/\mu_{C.L.}$  which Pigford selected the value of 1.0 came closest to the experimental values in the present work. The numerical values of  $N_{Gr}$  for the various runs are given in the appendix. It may be noted from Pigford's data that the mean Nusselt number definitely increases with the Grashof modulus ( $N_{Gr}$ ,  $N_{Pr}$ ,  $D/L$ ). Considering the results of the present investigation alone, shown in figure 28, it may be concluded that the Reynolds number does not seem to play an important role, as a majority of the points are scattered within 30%. The values of the mean Nusselt number are higher for the same Grashof modulus and Graetz number than the values given by Pigford. Pigford calculated the mean Nusselt number based on the average of the differences between wall and mixed fluid temperatures at the entrance and exit of the pipe. The mean Nusselt number for the present investigation was calculated using local Nusselt numbers as explained in appendix A. For

the work of Drobitch (6) again Reynolds number does not seem to affect the mean Nusselt number.

Vissers (29) who had done the experiments on a 1.74" diameter pipe under similar boundary conditions as the present investigation found that his experimental data agreed well with the correlation given by Hausen (7) shown on page 5 . The mean Nusselt number variation with  $(N_{Re}, N_{Pr.})/L/D$  for the present investigation did not agree with Hausen's correlation. Hausen used constant wall temperature and a parabolic velocity distribution to obtain equation (1). He neglected free convection effects.

The equation suggested by Drobitch (6) correlating  $N_{Num}$  with  $N_{Rei}$  also does not satisfy the present data. The mean Nusselt numbers are consistently higher in the larger diameter pipe.

As Hanratty, Rosen and Kabel (13) point out, the expressions for calculating the heat transfer coefficient suggested by various authors depend upon an assumed model for the flow field in which the field is not turbulent. The disagreement of the present data with any derived equation probably arises from the inadequacy of the flow model assumed in their various analytical solutions. One such inadequacy would be a failure to consider different levels of turbulence across the pipe.

As pointed out by Gross and Vanness (10) the temperature profile at any given cross section will depend

upon the boundary conditions, whether the fluid is being heated or cooled and on the fluid properties. Thus the local heat transfer coefficient will be affected by the above mentioned variables.

### 5.3 VELOCITY RATIO $u_{\max}/\bar{U}$

Figures 24 & 31 to 34 inclusive show that this velocity ratio is over 2.0 for some of the runs where  $N_{Rei} \approx 2000$ . For lower flow rates and larger temperature differences a ratio of more than 2.2 is obtained. This is caused by buoyancy forces which elongate the profile. For the same temperature difference ( $t_i - t_o$ ) and smaller flow rates, the buoyancy forces predominate and a higher peak in the velocity profile is obtained. As the mass flow is increased the relative effect of buoyancy forces decreases which can be noticed in figures 24, 33 and 34 for  $N_{Rei} \approx 3886, 2000$  and  $3000$ . For these, the buoyancy forces play a smaller role in the velocity development since the inertia forces dominate. The maximum value of the velocity ratio decreases with increasing Reynolds numbers and decreasing temperature differences ( $t_i - t_o$ ) for  $N_{Rei} < 2000$ . When the Reynolds number becomes large ( $N_{Rei} > 2000$ ) the temperature differences flatten the profile thus decreasing the velocity ratio. For smaller temperature differences the flow becomes turbulent and the velocity ratio never reaches 2.0. From the same

figures, it may be noted that the velocity ratios reach a maximum at an  $L/D$  which nearly coincides with the settling length for isothermal flow. Following the point of maximum  $u_{\max}/\bar{U}$ , steady cooling reduces the value of this velocity ratio. It tends to approach a value which would be expected for turbulent flow. This thermally induced turbulence has been referred to as non-laminar flow. Due to continuous cooling the flow becomes isothermal, the velocity then increases, reaching the usual parabolic value of 2.0 if the  $L/D$  ratio is sufficiently large.

#### 5.4 TYPE OF FLOW

Isothermal flow is generally considered to be laminar when the Reynolds number is below 2300. The hot wire indicated no turbulence for flows as high as  $N_{Re} \approx 3000$ , but for  $N_{Re} > 3000$ , it showed that turbulence was initiated and increased as Reynolds number increased. Depending upon the entrance conditions, turbulence may set in much earlier or may not occur even up to  $N_{Re} \approx 4000$ .

For non-isothermal flow, the hot wire anemometer indicated turbulence for  $N_{Re} > 1000$ . Vissers (29), Drobitch (6) and Gulati (8) had observed turbulence for Reynolds numbers as low as 500. Hanratty indicated in his investigation using water, that turbulence may well be present at lower Reynolds numbers and he found the flow to be completely turbulent at a  $N_{Re} \approx 50$ . The difference

in the Reynolds number at which turbulence was noticed between this investigation and other investigations could be due to the fact that the pipe diameter was much smaller for this investigation, also there were more screens for control of turbulence ahead of the entrance to the test pipe.

The oscilloscope connected to the hot wire anemometer indicated fluctuations in the hot wire output. These fluctuations could be due to a variation of velocity or temperature. The fluctuations in the hot wire anemometer readings increased:

- a. With increasing mean temperature.
- b. With increasing distance from the centre of the pipe

All these observations confirm the results of Vissers (29) and Drobitch (6).

## 5.5 ERROR ANALYSIS

Although every effort was made to maintain constant boundary conditions and constant flow conditions, small fluctuations did in fact occur. Some of these fluctuations are listed below.

- a. The air flow rate had a maximum variation of  $\pm 3\%$  in some of the tests.
- b. The ambient temperature (room temperature) was

permitted to vary  $\pm 2^\circ$  during a test. The test was discontinued if the variation exceeded this value.

c. The presence of the thermocouple probe in the pipe had a small effect on mean and wall temperatures.

d. Small natural drafts in the room would vary slightly, depending on time of the day, outdoor conditions etc.

e. It was noted that the inlet air temperature fluctuated  $\pm 1$  degrees during some of the tests.

The Nusselt number has been calculated as

$$N_{Nux} = \text{Constant} \times \frac{(t_{m1} - t_{m2})}{\left( \frac{t_{m1} + t_{m2}}{2} - \frac{t_{w1} + t_{w2}}{2} \right)}$$

Taking representative values of temperatures which are not necessarily the expected accuracies.

$$t_{m1} = 126.5 \pm 0.5$$

$$t_{m2} = 120.3 \pm 0.5$$

$$t_{w1} = 106.7 \pm 0.5$$

$$t_{w2} = 102.6 \pm 0.5$$

$$\text{Nominal value of } N_{Nux} = \text{Constant} \times \left( \frac{126.6 - 120.3}{\left( \frac{246.9 - 209.3}{2} \right)} \right)$$

$$= \text{Constant} \times 0.335$$

$$\text{Max. value of } N_{Nux} = \text{Constant} \times 0.399$$

$$\text{Min. value of } N_{Nux} = \text{Constant} \times 0.275$$

The deviation from the Nominal value  $+ 19.7\%$  &  $- 17.9\%$ .

The above sample calculation shows that the maximum deviation in the nominal value of the local Nusselt number could be  $\pm 20\%$ .

## CHAPTER 6

### CONCLUSIONS

From the study of heat transfer characteristics, velocity profile development and the wall temperature, the following conclusions were made.

1. Wall temperature  $t_w$  was a function of  $t_i$ ,  $t_o$ ,  $L$ ,  $D$  &  $N_{Rei}$  and was found to follow an empirical relation of the form

$$\frac{t_w - t_o}{t_i - t_o} = A \left( \frac{N_{Rei}}{13000} \right)^B (L/D)^C$$

where

$$A = \frac{T_i}{585} + 0.5$$

$$B = 0.07$$

$$C = 0.49 (D)^{0.25}$$

This equation applies to a round pipe of negligible thermal conductivity. It is valid for both high and low entering temperatures and for various pipe diameters.

Pipes tested had diameters which fell between 0.87" and 4.34", and  $t_i$  fell between 85.0 & 730.0° F.

2. In the type of flow investigated in this work, the buoyancy forces had the effect of elongating the velocity profile. The relative effect of these buoyancy forces on velocity profile shape decreased with increasing Reynolds number.

3. For non-isothermal flow, four distinct regions were apparent. These were :

a. Entrance region; from entrance to maximum  $u_{\max}/\bar{U}$ . Comparable to  $L/D$  for entrance region in isothermal flow.

b. Cooling region; where the velocity ratio decreased continuously due to cooling.

c. Isothermal developing region; the effect of temperature difference became negligible and the velocity profile developed isothermally.

d. Fully developed laminar isothermal flow; this will continue if no disturbances are encountered.

These observations confirm Vissers (29) conclusions who had also observed similar distinct regions.

4. The flow was of a turbulent nature for  $N_{Rei} \gg 1000$ , even when the temperature of the air flowing in the pipe was only a few degrees above the ambient air temperature.

5. The local Nusselt numbers agreed well with the values given by Kays. The values near the pipe entrance were slightly higher than the values given by Kays probably due to natural convection effects. As the pipe diameter was increased the Grashoff number was larger and so was the local Nusselt number as indicated by the results of Drobitch.

The local Nusselt number was found to increase with  $t_m/t_w$ . Data could not be correlated because of the limitation and scatter of the data points.

6. The mean Nusselt numbers were compared with the results of Pigford (23) and were found to be slightly higher as shown in figure 28.

## BIBLIOGRAPHY

1. Brown, C.K. and Gauvin, W.H., "Combined Free and Forced convection" I-Heat Transfer in Aiding Flow II- Heat Transfer in opposing Flow. The Canadian Journal of Chemical Engineering, pp 306-318 (December 1965).
2. Brown, W.G., VDI- Forschungsh. 480, 26, 32 pp (1960).
3. Deissler, R.G., "Analytical Investigation of Fully Developed Laminar Flow in Tubes with Fluid Properties Variable Along the Radius". NACA Technical Note, No.2410 (July 1951).
4. Deissler, R.G., "Analytical Investigation of Turbulent Flow in Tubes with Heat Transfer with Variable Fluid Properties for Prandtl Number of 1" NACA Technical Note, No.2242, (December 1950).
5. Deissler, R.G., and Presler, A.F., "Analysis of Developing Laminar Flow and Heat Transfer in a Tube for a Gas with Variable Properties".
6. Drobitch, A.J., "Non-isothermal Flow of Air in a Vertical Tube", An Experimental Study with the Hot-wire Anemometer, M.A.Sc., Thesis, University of Windsor, Ontario, (1965).
7. Grober, H., Erk, S., Grigull, U., "Fundamentals of Heat Transfer" McGraw Hill Book Company Inc. (1961).
8. Gulati, U.S., "Non-isothermal Flow of Air in a Vertical pipe at Low Velocities, M.A.Sc., Thesis, Assumption University of Windsor, Windsor, Ontario (1963).

9. Goresh, J.W., "Heat Transfer in Cylindrical Pipes with Fully Established Turbulent Flow and Exposed to a Uniform Temperature Environment", Journal of Heat Transfer, pp 305-313 (August 1966).
10. Gross, F.G., Vanness, H.C., "A Study of Laminar Flow Heat Transfer in Tubes A.I.Ch.E., Journal p 172 June, 1957.
11. Hallman, T.M., "Combined Forced and Free Laminar Heat Transfer in Vertical Tubes with uniform Internal Heat Generation", A.S.M.E., Vol.78, No.8 p.1831 (November 1956).
12. Hallman, T.M., "Experimental Study of Combined Forced and Free Laminar Convection in a Vertical Tube", NASA, TN-D-1104, (1961).
13. Hanratty, T.J., and Rosen, E.M., and Kabel, R.L., "Effect of Heat Transfer on Flow Field at Low Reynolds Numbers in Vertical Tubes" Ind. Eng. Chem., Vol.50, p 815 (May 1958).
14. Hsu, S.T. Engineering Heat Transfer, D. Van Nostrand Company, Inc. Princeton, New Jersey.
15. Jackson, T.W., Harrison, W.B., and Boteler, W.C., "Combined Free and Forced Convection in a Constant Temperature Vertical Tube" A.S.M.E. page 739, (April 1958).
16. Kays, W.M., "Numerical Solutions for Laminar Flow Heat Transfer in Circular Tubes", ASME Vol.77 p 1265 (November 1955).

17. Keevil, C.S., and McAdams, W.H., "How Heat Transmission Affects Fluid Friction in Pipes", Chem. Met. Eng., Vol. 36, p. 464, (1929).
18. Knudsen, J.G., and Katz, D.L., "Fluid Dynamics and Heat Transfer", McGraw Hill Book Co., Inc., N.Y., (1959).
19. Lawrence, W.T., and Chato, J.C., "Heat Transfer on Developing Laminar Flow Inside Vertical Tubes" ASME, Paper No. 65-WA/HT-11
20. Martinelli, R.C., and Boelter, L.M.K., "The Analytical Prediction of Superposed Free and Forced Viscous Convection in a Vertical Pipe", Univ. Calif. (Berkeley) Publs. Eng., 5.23, (1942).
21. McAdams, W.H., "Heat Transmission", McGraw-Hill Series in Chemical Engineering, N.Y., (1954).
22. McMordie, R.K., Emery, A.F., "A Numerical Solution for Laminar-Flow Heat Transfer in Circular Tubes with Axial Conduction and Developing Thermal and Velocity Fields" ASME, Paper No. 66-WA/HT-7.
23. Pigford, R.L., "Non-isothermal Flow and heat Transfer Inside Vertical Tubes", Chem. Eng., Prog., Sym. Series, Vol. 51, No. 17, p 79, (1953).
24. Scheele, G.F., Rosen, E.M., and Hanratty, T.J., "Effect of Natural Convection on Transition to Turbulence in a Vertical Pipe", Can. Jour. Chem. Engg., Vol. 38, p 67 (1960).

25. Seider, E.N., and Tate, G.E., "Heat Transfer and Pressure Drop of Liquid in Tubes", Ind. Eng. Chem., Vol. 28, p. 1429 (1936).
26. "Selected Topics Hot-wire Anemometer Theory", Flow Corp. Bulletin 25, Cambridge, Mass.
27. Test, F.L., "Laminar Flow Heat Transfer and Fluid Flow for Liquids with Temperature-Dependent Viscosity", Journal of Heat Transfer, November 1968, p. 385.
28. Urichson, D.L., and Schmitz, R.A., "Laminar Flow Heat Transfer in the Entrance Region of Circular Tubes" Int. J. Heat and Mass Transfer Vol. 8, pp. 253-258.
29. Vissers, J.I., "Isothermal and Non-isothermal Flow of Air in a Vertical Tube", M.A.Sc., Thesis University of Windsor, Windsor, Ontario, Canada (1965).
30. Yamagata, K., "A Contribution to the Theory of Non-Isothermal Laminar Flow of Fluids Inside a Straight Tube of Circular Cross-section", Memoirs of the Faculty of Engineering, Kyushu Imperial University, Japan, Vol. 8, No. 6, p. 365-449, (1940).
31. Zellnik, H.E., and Churchill, S.W., "Convective Heat Transfer from High Temperature Air Inside a Tube", A.I.ChE., p. 37 (March 1958).
32. Kreith., "Principles of Heat Transfer" International Text Book Company.

## APPENDIX A

### EVALUATION OF DIMENSIONLESS PARAMETERS

The dimensionless parameters used in this study were: (1) Grashof number- $N_{Gr}$ ; (2) Nusselt number- $N_{Nu}$  (3) Reynolds number- $N_{Re}$ ; (4) Prandtl number- $N_{Pr}$ ; and (5) Graetz number- $N_{Gz}$

The fact that all physical properties in dimensionless groups must be evaluated at a certain temperature creates a problem in heat transfer calculations. There is no definite rule for the selection of a particular temperature to use in determining the properties. The choice for a reference temperature depends upon the conditions under which the empirical equation is derived. The most commonly used are (1) centre line temperature- $t_c$ ; (2) mean temperature- $t_m$ ; (3) bulk mean temperature- $t_b$ ; and (4) arithmetic mean temperature- $t_a$ .

Figure A shows a typical pipe section

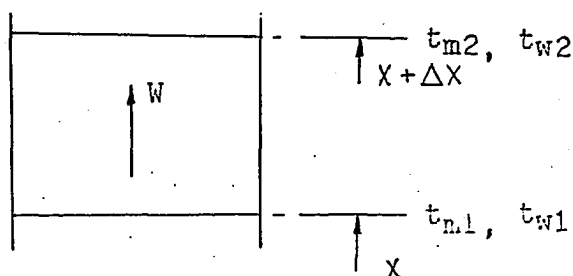


Figure A

$t_{m1}$  and  $t_{w1}$  are the mean and wall temperature at X,  
 $t_{m2}$  and  $t_{w2}$  are the mean and wall temperature at  $X + \Delta X$

and  $W$  is the weight flow (in lbs/hr.)

a. The centre line temperature is the local temperature of the fluid at the centre line of the pipe.

b. The mean temperature over a cross-section area of pipe is determined from the temperature profile across the diameter:

$$\begin{aligned}
 t_m &= \frac{1}{\pi R^2} \int_0^R t \cdot 2\pi r dr \\
 &= \frac{2}{R^2} \int_0^R t r dr
 \end{aligned}$$

c. The bulk mean temperature of a given fluid mass is obtained by thoroughly mixing in a cup the fluid passing through a cross sectional area of the pipe per unit time and is defined as:

$$\begin{aligned}
 t_b &= \frac{\int_0^R \rho C_p t_r u_r 2\pi r dr}{\rho C_p \int_0^R u_r 2\pi r dr} \\
 &= \frac{\int_0^R t_r u_r r dr}{\int_0^R u_r r dr}
 \end{aligned}$$

The mean temperature agreed well with the bulk mean and so this was used as the base for determining properties.

d. The arithmetic mean temperature is defined as

$$t_{am} = \frac{t_b + t_w}{2}$$

After having defined the temperatures usually encountered for defining the properties the various non-dimensional parameters are defined as follows:

a. Nusselt number:

The important parameter in heat transfer studies is the heat transfer coefficient or Nusselt number.

The local Nusselt number is given by

$$N_{Nux} = \frac{h_x D}{K_x}$$

where the film coefficient,  $h_x$  is given by

$$h_x = q_x / (A_s \Delta t)$$

The  $\Delta t$  in this equation was taken as the difference between the mean fluid temperature and wall temperature.

The heat transferred from the fluid can be evaluated by means of the following equation

$$q_x = W C_p \Delta t_m$$

The Nusselt number was considered local when it was the average Nusselt number between two adjacent stations.

It is therefore given by

$$N_{Nu_{x+\frac{\Delta x}{2}}} = \frac{hD}{K} = \frac{WC_p (t_{m1} - t_{m2}) D}{A_s \cdot \Delta T \cdot K}$$

where  $C_p$  and  $K$  are the specific heat and conductivity respectively evaluated at  $(t_{m1} + t_{m2})/2$  and  $\Delta T$  in the denominator is defined as

$$\Delta T = \frac{(t_{m1} + t_{m2})}{2} - \frac{(t_{w1} + t_{w2})}{2}$$

The average or mean Nusselt number over a length  $L$  was determined by the following equation.

$$N_{Num} = \frac{1}{L} \int_0^L N_{Nu(x+\frac{\Delta x}{2})} \cdot \Delta x$$

#### b. GRASHOF NUMBER

The Grashof number at the position  $X$  was defined as

$$N_{Grx} = \frac{D^3 \rho^2 \beta \Delta T}{\mu^2}$$

where  $\beta = \frac{1}{T^{\circ}} \left( \frac{1}{^{\circ}R} \right)$

$$\Delta T = (t_{m1} - t_o) \quad (^{\circ}R \text{ or } ^{\circ}F)$$

and  $\rho$  and  $\mu$  are properties of the air evaluated at  $t_{m1}$ .

#### c. REYNOLDS NUMBER

The Reynolds number at any position  $X$  was defined as

$$N_{Rex} = \frac{\rho_x \cdot D \cdot \bar{U}_x}{\mu_x}$$

where  $\rho_x$ ,  $\mu_x$  &  $\bar{U}_x$  are determined at  $t_{mx}$ .

#### d. PRANDTL NUMBER

The prandtl number was defined as

$$N_{Pr} = \frac{C_p U}{K}$$

It was assumed to be constant at 0.71 (for air)

e. GRAETZ NUMBER

The Graetz number at the position X was defined as

$$N_{Gzx} = \frac{W C_p}{K X}$$

X is the length of the pipe from the entrance to the position X where Graetz number is to be evaluated;  $C_p$  and P are to be evaluated at  $t_{m1}$ .

For the plot of local Nusselt number vs. Graetz number, Graetz number was evaluated at  $(X + \frac{\Delta X}{2})$ . For the plot of mean Nusselt number vs. Graetz number, Graetz number was evaluated at  $(X + \Delta X)$ .

## APPENDIX - B

Table B-1. Variation of Temperature and Dimensionless parameters with L/D Ratio.

Run No.1 Barometric Pressure - 29.40" Hg.  
 Ambient Air Temperature - 81.2 °F.  
 Inlet Air Temperature (C.L.) - 85.0 °F.  
 Weight Flow - 1.59 lbs/hr.

L/D	$t_m$ °F	$t_w$ °F	$N_{Re}$	$N_{Nu}$	$N_{Gz}$	$N_{Gr} \cdot L$ x 10
0	85.0		615			
5.5	84.2	83.1	617	15.4		0.22
15.9	83.7	82.6	618	5.6	32.6	0.17
33.1	83.3	82.1	619	2.5	14.3	0.14
46.9	83.0	81.8	619	1.9	8.7	0.12
64.2	82.8	81.7	620	0.9	6.3	0.11
88.3	82.6	81.5	620	1.1	4.6	0.09
136.6	81.2	81.2	622	0.8	3.1	
178.0	81.2	81.2	622		2.2	
219.3	81.2	81.2	622			

Table B-2. Variation of Temperature and Dimensionless parameters with L/D Ratio.

Run No.2      Barometric Pressure                    - 29.57" Hg.  
 Ambient Air Temperature                    - 78.0 °F.  
 Inlet Air Temperature (C.L.) - 94.0 °F.  
 Weight Flow                                    - 1.61 lbs/hr.

L/D	$t_m$ °F	$t_w$ °F	$N_{Re}$	$N_{Nux}$	$N_{Gz}$	$N_{Gr}^{-4}$ x 10
0	94.0		594			
5.5	91.4	86.6	599	11.95		0.98
15.9	88.6	83.6	604	6.0	32.7	0.79
33.1	84.8	81.7	611	6.0	14.4	0.51
46.9	82.7	80.3	615	6.3	8.8	0.35
64.2	81.6	79.9	617	2.7	6.3	0.26
88.3	79.5	79.4	618	5.3	4.7	0.09
136.6	79.0	78.7	620	5.85	3.2	
178.0	78.3	78.3	621	5.5	2.3	
219.3	78.0	78.0	621			

Table B-3. Variation of Temperature and Dimensionless parameters with L/D Ratio.

Run No.3 Barometric Pressure - 29.46" Hg.  
 Ambient Air Temperature - 79.6 °F.  
 Inlet Air Temperature (C.L.) - 107.0 °F.  
 Weight Flow - 1.62 lbs/hr.

L/D	$t_m$ °F	$t_w$ °F	$N_{Re}$	$N_{Nux}$	$N_{Gz}$	$N_{Gr}$ x 10 <sup>-4</sup>
0	107.0		575			
5.5	101.8	94.8	582	11.96	62.5	1.32
15.9	97.4	89.6	590	6.3	32.5	1.04
33.1	91.7	86.6	602	5.7	22.0	0.66
46.9	88.8	84.6	607	5.1	14.3	0.46
64.2	86.7	82.8	611	3.6	10.6	0.30
88.3	84.8	82.0	614	2.6	8.8	0.13
136.6	83.0	80.6	618	1.7	7.5	0.05
178.0	81.6	79.6	620	1.7	6.4	
					5.5	
					4.7	
					4.0	
					3.2	
					2.6	
					2.3	
					2.0	

Table B-4. Variation of Temperature and Dimensionless parameters with L/D Ratio.

Run NO.4 Barometric Pressure - 29.47" Hg.  
 Ambient Air Temperature - 79.3 °F.  
 Inlet Air Temperature (C.L.) -143.5 °F.  
 Weight Flow - 3.02 lbs/hr.

L/D	$t_m$ °F	$t_w$ °F	NRe	$N_{Nux}$	$N_{Gz}$	$N_{Gr}$ -4 x 10	$u_{max}/\bar{U}$
0	143.5		1014				
5.5	128.9	110.4	1031	19.35		2.91	1.53
15.9	120.3	100.7	1059	8.7	58.7	2.52	1.95
33.1	112.2	95.4	1080	5.25	26.0	2.09	2.14
46.9	106.3	91.3	1096	5.50	16.0	1.84	2.21
64.2	101.2	88.2	1110	4.4	11.6	1.53	2.19
88.3	96.1	85.6	1128	3.7	8.5	1.21	2.17
136.6	88.5	82.4	1157	4.0	5.8	0.70	2.09
178.0	84.3	79.0	1171	3.8	4.2	0.52	1.98
219.3	81.9	78.4	1179	2.8	3.3	0.34	1.88
267.0	79.8	77.9	1187	3.5	2.7	0.17	1.92

Table B-5. Variation of Temperature and Dimensionless parameters with L/D Ratio.

Run No.5 Barometric Pressure - 29.50" Hg.  
 Ambient Air Temperature - 78.7 °F.  
 Inlet Air Temperature (C.L.) - 108.0 °F.  
 Weight Air Temperature - 2.83 lbs/hr.

L/D	$t_m$ °F	$t_w$ °F	$N_{Re}$	$N_{Nux}$	$N_{Gz}$	$N_{Gr}$ x 10 <sup>-4</sup>	$u_{max}/\bar{U}$
0	108.0		1022				
5.5	104.8	93.2	1028	10.7	108.8	1.77	1.53
15.9	98.8	88.6	1044	10.3	56.6	1.40	1.85
33.1	94.1	86.7	1061	5.9	38.3	1.1	2.08
46.9	91.7	84.6	1070	4.6	24.9	0.94	2.19
64.2	89.0	83.1	1079	4.8	18.5	0.72	2.11
88.3	86.2	81.8	1088	4.5	15.3	0.55	2.03
136.6	83.4	80.2	1098	3.5	13.1	0.33	1.94
178.0	80.8	79.3	1105	4.0	11.1	0.15	1.96
219.3	80.0	79.3	1107	3.0	9.6	0.11	1.92
267.0	80.0	79.3	1107	2.7	8.1		1.98

Table B-6. Variation of Temperature and Dimensionless Parameters with L/D Ratio.

Run No.6 Barometric Pressure - 29.40" Hg.  
 Ambient Air Temperature - 78.2° F.  
 Inlet Air Temperature (C.L) - 86.0° F.  
 Weight Flow - 2.58 lbs/hr.

L/D	$t_m$ °F	$t_w$ °F	$N_{Re}$	$N_{Nux}$	$N_{Gz}$	$N_{Gr}$ $\times 10^{-4}$	$u_{max}/\bar{U}$
0	86.0		987	11.28			
5.5	85.3	83.1	989	7.42	52.8	0.55	1.37
15.9	84.3	81.9	989	6.33	23.1	0.47	1.69
33.1	83.0	81.3	995	7.82	14.2	0.38	1.88
46.9	82.1	80.8	995	3.64	10.2	0.30	1.86
64.2	81.7	80.5	999	3.0	7.5	0.28	1.99
88.3	81.3	80.4	1000				1.89
136.6	78.5	78.5	1008				1.90
178.0	78.4	78.4	1009				1.89
219.3	78.4	78.4	1009				1.77
267.0	78.4	78.2	1009				1.84

Table B-7. Variation of Temperature and Dimensionless parameters with L/D Ratio.

Run No.7 Barometric Pressure - 29.25" Hg.  
 Ambient Air Temperature - 78.2 °F.  
 Inlet Air Temperature (C.L.)- 90.0 °F.  
 Weight Flow - 3.89 lbs/hr.

L/D	$t_m$ °F	$t_w$ °F	$N_{Re}$	$N_{Nu}$	$N_{Gz}$	$N_{Gr} \cdot L$ x 10.	$u_{max}/\bar{U}$
0	90.0		1513				
5.5	87.8	83.9	1523	19.2		0.79	1.33
15.9	86.6	81.9	1528	7.5	79.3	0.70	1.56
33.1	85.2	81.6	1535	4.8	39.8	0.60	1.75
46.9	84.2	80.9	1540	5.5	21.3	0.43	1.86
64.2	83.4	80.3	1541	6.9	15.4	0.41	1.89
88.3	82.8	79.5	1545	2.8	11.2	0.34	1.90
136.6	81.4	78.7	1552	2.0	7.6	0.17	1.90
178.0	80.6	78.2	1556	2.8	5.5	0.10	1.86
219.3	80.6	78.2	1556			0.10	1.85
267.	80.6	78.2					1.86

Table B-8. Variation of Temperature and Dimensionless parameters with L/D Ratio.

Run No.8 Barometric Pressure - 29.65" Hg.  
 Ambient Air Temperature - 78.2 °F.  
 Inlet Air Temperature (C.L.) -104.5 °F.  
 Weight Flow - 4.16 lbs/hr.

L/D	$t_m$ °F	$t_w$ °F	$N_{Re}$	$N_{Nux}$	$N_{Gz}$	$N_{Gr}$ x 10 <sup>-4</sup>
0	104.5		1509			
5.5	102.5	92.9	1515	10.6	160.3	1.66
15.9	99.3	88.7	1540	8.5	83.4	1.49
33.1	95.8	86.4	1552	6.0	56.2	1.26
46.9	92.8	84.7	1566	7.2	36.6	1.06
64.2	90.5	83.5	1575	5.1	27.2	0.90
88.3	88.0	82.2	1586	4.6	22.5	0.72
136.6	83.6	80.6	1567	5.9	19.2	0.45
178.0	81.4	79.3	1617	6.1	16.3	0.28
219.3	79.8	78.9	1625	7.3	14.1	0.08
					11.9	
					10.3	
					8.1	
					6.7	
					5.8	
					5.2	
					4.6	
					4.2	

Table B-9. Variation of Temperature and Dimensionless parameters with L/D Ratio.

Run No.9      Barometric Pressure                      - 29.37" Hg.  
                   Ambient Air Temperature                - 86.5 °F.  
                   Inlet Air Temperature (C.L.) -131.5 °F.  
                   Weight Flow                                        - 4.29 lbs/hr.

L/D	$t_m$ °F	$t_w$ °F	$N_{Re}$	$N_{Nux}$	$N_{Gz}$	$N_{Gr} \frac{-L}{x 10}$	$u_{max}/\bar{U}$
0	131.5		1470				
5.5	126.6	106.7	1486	12.		2.41	1.59
15.9	120.3	102.6	1515	8.2	83.5	2.11	1.85
33.1	115.3	98.2	1534	4.7	36.8	1.84	1.99
46.9	112.6	97.5	1544	4.0	22.6	1.67	2.06
64.2	109.3	95.7	1557	2.7	16.4	1.47	2.19
88.3	104.5	93.6	1575	4.8	12.0	1.18	2.11
136.6	97.4	91.0	1607	5.1	8.2	0.77	2.02
178.0	93.6	89.4	1628	5.1	6.0	0.52	1.98
219.3	91.6	88.8	1639	4.1	4.7	0.37	2.03
267.0	90.4	88.8	1646	3.4	3.8	0.28	2.00

Table B-10. Variation of Temperature and Dimensionless parameters with L/D Ratio.

Run No.10. Barometric Pressure - 29.81" Hg.  
 Ambient Air Temperature - 83.5 °F.  
 Inlet Air Temperature (C.L.) -120.8 °F.  
 Weight Flow - 5.41 lbs/hr.

L/D	$t_m$ °F	$t_w$ °F	$N_{Re}$	$N_{Nux}$	$N_{Gz}$	$N_{Gr}^{-4}$ x 10	$u_{max}/\bar{U}$
0	120.8		2043				
5.5	117.4	105.0	2056	16.9		2.20	1.48
15.9	112.6	100.1	2080	13.9	106.4	1.93	1.74
33.1	109.5	97.1	2096	5.8	46.8	1.75	1.84
46.9	106.8	94.9	2110	5.1	28.8	1.59	1.93
64.2	104.2	92.8	2124	5.1	20.8	1.35	1.97
88.3	100.5	91.0	2143	5.7	15.2	1.12	1.99
136.6	95.1	87.6	2181	5.0	10.4	0.89	2.00
178.0	91.7	86.0	2207	5.0	7.4	0.64	1.99
219.3	90.6	85.2	2215	1.9	5.9	0.57	2.00
267.0	88.6	83.7	2229		4.9	0.42	1.93

Table B-11. Variation of Temperature and Dimensionless parameters with L/D Ratio.

Run No.11 Barometric Pressure - 29.85" Hg.  
 Ambient Air Temperature - 78.6 °F.  
 Inlet Air Temperature (C.L.) -118.5 °F.  
 Weight Flow - 5.35 lbs/hr.

L/D	$t_m$ °F	$t_w$ °F	$N_{Re}$	$N_{Nux}$	$N_{Gz}$	$N_{Gr}$ x 10 <sup>-4</sup>	$u_{max}/\bar{U}$
0	118.5		2022	22.9			
5.5	111.7	97.0	2053	9.5	203.8	2.10	1.4
15.9	107.8	92.3	2073	4.6	105.9	1.88	1.57
33.1	104.7	90.0	2088	5.0	71.5	1.69	1.69
46.9	102.2	88.0	2101	3.0	46.5	1.55	1.92
64.2	100.3	86.6	2111	4.5	34.5	1.42	1.89
88.3	97.1	84.9	2133	4.0	28.6	1.22	2.02
136.6	92.0	83.3	2170	5.0	24.5	1.11	1.95
178.0	87.5	79.2	2202	3.3	20.7	0.74	1.9
219.3	85.1	79.2	2217	4.4	17.9	0.56	1.87
267.0	83.1	79.2	2230		15.1	0.41	1.90

Table B-12. Variation of Temperature and Dimensionless parameters with L/D Ratio.

Run No.12      Barometric Pressure                    - 29.51" Hg.  
                          Ambient Air Temperature                - 80.4 °F.  
                          Inlet Air Temperature (C.L.)        - 94.0 °F.  
                          Weight Flow                                        - 5.22 lbs/hr.

L/D	$t_m$ °F	$t_w$ °F	NRe	NNux	NGz	NGr <sub>-4</sub> x 10	$u_{max}/\bar{U}$
0	94.0		1965				
5.5	92.4	87.2	1971	18.65		0.85	1.33
15.9	91.0	85.6	1980	8.9	105.8	0.75	1.55
33.1	89.7	84.6	1989	5.3	46.4	0.66	1.74
46.9	88.7	83.9	1995	5.1	28.4	0.59	1.92
64.2	87.9	83.4	2000	3.8	20.5	0.53	1.98
88.3	86.5	83.0	2008	5.4	15.0	0.43	1.93
136.6	85.2	82.0	2015	2.9	10.2	0.40	1.92
178.0	83.8	81.0	2023	3.9	7.3	0.30	1.9
219.3	83.0	80.9	2028	3.0	5.8	0.24	1.95
267.0	82.4	80.6	2032	2.6	4.7	0.23	1.94

Table B-13. Variation of Temperature and Dimensionless parameters with L/D Ratio.

<u>Run No.13</u>	Barometric Pressure	- 29.80" Hg
	Ambient Air Temperature	- 73.7 °F
	Inlet Air Temperature (C.L.)	-112.5 °F
	Weight Flow	- 8.19 lbs/hr.

L/D	$t_m$ °F	$t_w$ °F	$N_{Re}$	$N_{Nux}$	$N_{Gz}$	$N_{Gr_{-4}}$ x 10	$u_{max}/\bar{U}$
0.0	112.5		2903				
5.5	111.7	95.8	2910	16.3	312.0 162.2	2.49	1.31
15.9	107.2	90.1	2938	11.5	109.5 71.4	2.20	1.46
33.1	101.5	86.4	2980	8.0	53.1 48.0	1.87	1.57
46.9	98.6	84.4	3005	2.6	37.6 31.8	1.70	1.74
64.2	97.4	82.2	3016	4.4	27.5 23.3	1.62	1.82
88.3	94.8	81.6	3044	3.1	20.1 15.9	1.46	1.83
136.6	91.4	78.8	3079	4.4	13.0 11.3	1.39	1.85
178.0	87.6	76.8	3115	3.7	10.1 9.0	1.31	1.86
219.3	85.0	76.6	3148	3.7	8.2 7.4	0.95	1.86
267.0	83.0	76.0			6.8	0.79	1.72

Table B-14. Variation of Temperature and Dimensionless  
parametres with L/D Ratio.

Run No.14      Barometric Pressure            - 29.32" Hg.  
                   Ambient Air Temperature        - 79.5 °F  
                   Inlet Air Temperature (C.L.) - 96.7 °F  
                   Weight Flow                         - 8.08 lbs/hr.

L/D	$t_m$ °F	$t_w$ °F	$N_{Re}$	$N_{Nux}$	$N_{Gz}$	$N_{Gr}$ x 10 <sup>-4</sup>
0	96.5		3014	16.0		
5.5	95.8	88.7	3015	15.85	163.1	1.15
15.9	93.7	86.8	3038	7.0	71.5	1.01
33.1	92.3	85.8	3053	3.0	43.9	0.91
46.9	91.8	84.8	3059	3.6	31.6	0.88
64.2	91.0	83.7	3067	1.6	23.1	0.82
88.3	90.5	83.1	3072	6.1	15.7	0.79
136.6	87.2	81.9	3102	4.4	11.3	0.62
178.0	85.5	80.5	3118	5.0	8.9	0.50
219.3	83.9	79.9	3133	3.4	7.3	0.38
267.0	82.8	79.5	3142			0.29

Table B-15. Variation of temperature and Dimensionless parameters with L/D Ratio.

Run No.15 Barometric Pressure - 29.53" Hg  
 Ambient Air Temperature - 80.6 °F  
 Inlet Air Temperature (C.L.) - 87.0 °F  
 Weight Flow - 7.7 lbs/hr.

L/D	$t_m$ °F	$t_w$ °F	$N_{Re}$	$N_{Nux}$	$N_{Gz}$	$N_{Gr}$ $\times 10^{-4}$	$u_{max}/\bar{U}$
0.0	87.0		2953				
5.5	86.6	83.9	2955	14.6	157.2	0.46	1.23
15.9	85.9	83.2	2961	8.2	68.8	0.40	1.36
33.1	85.2	82.9	2967	12.7	42.2	0.35	1.53
46.9	84.5	82.6	2973	1.3	30.4	0.30	1.67
64.2	84.4	82.5	2973	7.6	21.2	0.29	1.74
88.3	83.9	82.4	2978	2.0	15.0	0.25	1.75
136.6	83.6	81.6	2981	4.6	10.8	0.23	1.78
178.0	82.8	80.6	2988		8.5	0.17	1.80
219.3	82.5	80.6	2991		7.0	0.14	1.81
267.0	82.2	80.6	2993			0.12	

Table B-16. Variation of Temperature and Dimensionless parameters with L/D Ratio.

Run No.16 Barometric Pressure - 29.42" Hg  
 Ambient Air Temperature - 78.3 °F  
 Inlet Air Temperature - 111.5 °F  
 Weight Flow - 10.88 lbs/hr.

L/D	$t_m$ °F	$t_w$ °F	$N_{Re}$	$N_{Nux}$	$N_{Gz}$	$N_{Gr_{-4}}$ x 10 <sup>4</sup>	$u_{max}/\bar{U}$
0.0	111.5		3886				
5.5	110.4	97.4	3897		415.0	2.15	1.21
15.9	108.2	94.4	3919	13.3	215.5		
33.1	105.1	92.6	3948	9.9	145.3	2.03	1.39
46.9	103.1	91.0	3968	8.5	94.6	1.85	1.53
64.2	101.4	89.5	3985	6.2	70.3	1.73	1.58
88.3	98.7	87.9	4015	7.2	58.1	1.59	1.65
136.6	95.5	85.8	4059	4.9	49.7	1.42	1.8
178.0	92.4	84.2	4102	6.2	42.0	1.23	1.86
219.3	90.0	82.8	4136	5.8	36.4	1.04	1.85
267.0	88.4	81.7	4155	3.5	30.7	0.86	1.87
					26.5	0.75	1.87
					20.9		
					17.2		
					15.0		
					13.3		
					11.9		
					10.8		
					9.7		
					8.9		

Table B-17. Variation of Temperature and Dimensionless parameters with L/D Ratio.

Run No.17      Barometric Pressure                      - 29.49" Hg.  
                   Ambient Air Temperature                - 73.0 °F.  
                   Inlet Air Temperature (C.L.) -648.0 °F.  
                   Weight Flow                                        - 5.67 lbs/hr.

L/D	$t_m$ °F	$t_w$ °F	$N_{Re}$	$N_{Nux}$	$N_{Gz}$	$N_{Gr}$ x 10 <sup>-4</sup>
0	648.0		636			
5.5	496.5	328.8	808	31.2	170.8	4.69
15.9	429.9	256.5	913	10.3	80.1	5.04
33.1	363.9	207.7	1039	6.7	55.9	5.32
46.9	323.5	179.9	1130	5.9	36.9	5.42
64.2	285.4	160.9	1231	5.1	28.1	5.45
88.3	244.5	142.0	1360	4.8	23.7	5.38
136.6	185.7	113.8	1592	4.7	20.7	4.84
178.0	154.5	103.2	1729	4.4	17.6	4.13
219.3	133.5	96.4	1836	4.2	15.8	3.45
267.0	116.2	88.1	1886	4.1	13.3	2.60

Table B-18. Variation of Temperature and Dimensionless parameters with L/D Ratio.

Run No.18      Barometric Pressure                    - 29.73" Hg.  
                   Ambient Air Temperature                - 74.2 °F.  
                   Inlet Air Temperature                    -673.0 °F.  
                   Weight Flow                                - 11.66 lbs/hr.

L/D	$t_m$ °F	$t_w$ °F	$N_{Re}$	$N_{Nux}$	$N_{Gz}$	$N_{Gr}$ x 10 <sup>-4</sup>
0	673.0		1235			
5.5	558.2	376.7	1504		297.3	4.37
15.9	508.6	308.4	1628	13.4	156.7	4.59
33.1	456.0	262.7	1786	8.6	107.4	4.86
46.9	416.0	229.0	1928	8.75	71.1	5.07
64.2	383.0	208.5	2057	6.3	53.7	5.21
88.3	349.7	188.1	2198	5.0	45.1	5.30
136.6	288.0	156.6	2515	5.5	39.1	5.43
178.0	251.3	145.9	2748	5.0	33.5	5.38
219.3	227.8	135.9	2922	3.9	29.4	5.28
267.0	200.9	120.8	3157	4.5	25.0	5.09
					21.9	
					17.7	
					15.0	
					13.2	
					12.0	
					10.8	
					9.9	
					9.1	
					8.3	

Table B-19. Variation of Temperature and Dimensionless parameters with L/D Ratio.

Run NO.19      Barometric Pressure                      - 29.28" Hg.  
                     Ambient Air Temperature                      - 69.8 °F.  
                     Inlet Air Temperature (C.L.) -620.0 °F.  
                     Weight Flow    - 16.65 lbs/hr.

L/D	$t_m$ °F	$t_w$ °F	NRe	NNux	NGz	$N_{Gr}^{-4}$ x 10
0	620.0		1952			
5.5	551.2	371.0	2170		422.6	4.48
15.9	508.2	315.2	2327	16.9	224.4	
33.1	459.1	271.0	2537	11.8	155.4	4.69
46.9	424.2	242.9	2710	11.4	101.4	
64.2	411.5	224.1	2768	7.8	76.5	4.95
88.3	365.7	203.5	3027	6.4	64.1	
136.6	317.8	175.5	3346	5.8	55.4	5.15
178.0	290.8	163.6	3562	4.4	47.4	
219.3	267.5	152.3	3765	4.4	41.0	5.17
267.0	228.0	138.2	4154		35.3	
					30.9	5.36
					24.7	
					20.8	5.49
					18.3	
					16.4	5.57
					14.8	
					13.6	5.57
					12.5	
					11.6	5.43

Table B-20. Variation of Temperature and Dimensionless parameters with L/D Ratio.

Run No. 20      Barometric Pressure                      - 29.55" Hg  
                          Ambient Air Temperature                      - 68.3 °F  
                          Inlet Air Temperature                              -665.0 °F  
                          Weight Flow    - 20.07 lbs/hr.

L/D	$t_m$ °F	$t_w$ °F	$N_{Re}$	$N_{Nux}$	$N_{Gz}$	$N_{Gr}$ $\times 10^{-4}$
0	665.0		2175			
5.5	607.2	396.0	2405			4.25
15.9	558.8	331.6	2596	19.9	261.1	4.51
33.1	526.0	290.2	2745	7.2	117.3	4.70
46.9	491.3	271.4	2915	10.9	73.4	4.90
64.2	441.6	260.7	3160	13.9	54.0	5.08
88.3	377.2	243.7	3582	16.8	41.6	5.41
136.6	305.5	203.4	4163	13.6	29.9	5.72
178.0	252.2	181.8	4722	16.9	22.6	5.73
219.3	207.2	172.9	5326	24.7	18.7	5.54
267.0	178.7	157.7	5738	26.2	15.9	5.14

Table B-21. Variation of Temperature and Dimensionless parameters with L/D Ratio.

Run No.21 Barometric Pessure - 29.63" Hg.  
 Ambient Air Temperature - 73.6 °F.  
 Inlet Air Temperature (C.L.) -605.0 °F.  
 Weight Flow - 22.59 lbs/hr.

L/D	$t_m$ °F	$t_w$ °F	$N_{Re}$	$N_{Nux}$	$N_{Gz}$	$N_{Gr}$ x 10 <sup>-4</sup>
0	605.0		2720			
5.5	556.2	373.0	2924	15.9	302.1	4.36
15.9	525.0	318.6	3072	9.0	134.9	4.50
33.1	495.8	302.9	3225	12.2	84.4	4.64
46.9	467.4	299.6	3390	19.1	62.5	4.78
64.2	423.3	295.5	3684	24.4	47.4	5.00
88.3	367.5	277.5	4109	28.9	34.1	5.23
136.6	286.5	235.3	4893	17.2	25.6	5.47
178.0	259.4	213.2	5220	25.4	21.1	5.44
219.3	226.2	188.2	5688	27.0	17.8	5.31
267.0	192.4	159.8	6237			4.98

## Variation of Wall Temperature with L/D Ratio.

Table C-1.

Table C-2.

Table C-1			Table C-2		
Weight Flow - 0.36 lbs/hr.			Weight Flow - 0.37 lbs/hr.		
NRei - 593			NRei - 590		
t <sub>i</sub> (C.L) - 94.0 °F			t <sub>i</sub> (C.L) - 111.5 °F		
L/D	t <sub>w</sub> °F	t <sub>o</sub> °F	L/D	t <sub>w</sub> °F	t <sub>o</sub> °F
0		75.8	0		71.6
5.5	84.9	75.8	5.5	91.9	71.6
15.9	81.7	75.8	15.9	84.5	71.6
33.1	79.5	75.8	33.1	79.4	71.6
46.9	78.3	75.8	46.9	76.6	71.6
64.2	77.5	75.8	64.2	74.8	71.6
88.3	76.8	75.8	88.3	73.5	71.6
136.6	76.1	75.6	136.6	72.2	71.4
178.0	75.8	75.6	178.0	72.0	71.4
219.3	75.8	75.6	219.3	71.9	71.4
267.0	75.8	75.6	267.0	71.9	71.4

## Variation of Wall Temperature with L/D Ratio.

Table C-3.

Table C-4.

Table C-3			Table C-4		
Weight Flow - 0.33 lbs/hr.			Weight Flow - 0.42 lbs/hr.		
N <sub>Rei</sub> - 608			N <sub>Rei</sub> - 624		
t <sub>i</sub> (C.L) - 82.6 °F			t <sub>i</sub> (C.L) - 132.2 °F		
L/D	t <sub>w</sub> °F	t <sub>o</sub> °F	L/D	t <sub>w</sub> °F	t <sub>o</sub> °F
0		72.4	0		70.8
5.5	77.2	72.4	5.5	101.0	70.8
15.9	74.8	72.4	15.9	90.1	70.8
33.1	73.6	72.4	33.1	82.9	70.8
46.9	72.9	72.4	46.9	78.8	70.8
64.2	72.6	72.4	64.2	76.0	70.8
88.3	72.5	72.4	88.3	73.8	70.8
136.6	72.5	72.4	136.6	71.4	70.6
178.0	72.5	72.4	178.0	71.0	70.6
219.3	72.5	72.4	219.3	70.7	70.6
267.0	72.5	72.4	267.0	70.7	70.6

## Variation of Wall Temperature with L/D Ratio.

Table C-5.

Table C-6.

Table C-5			Table C-6		
Weight Flow - 0.404 lbs/hr.			Weight Flow - 0.59 lbs/hr.		
NRei - 620			NRei - 1020		
$t_i$ (C.L) - 143.5 °F			$t_i$ (C.L) - 79.3 °F		
L/D	$t_w$ °F	$t_o$ °F	L/D	$t_w$ °F	$t_o$ °F
0		81.3	0		70.9
5.5	114.6	81.3	5.5	74.5	70.9
15.9	103.0	81.3	15.9	73.2	70.9
33.1	94.0	81.3	33.1	72.3	70.9
46.9	89.9	81.3	46.9	71.9	70.9
64.2	87.0	81.3	64.2	71.6	70.9
88.3	84.7	81.3	88.3	71.5	70.9
136.6	82.3	81.3	136.6	71.1	71.0
178.0	80.6	80.4	178.0	71.3	71.0
219.3	80.5	80.4	219.3	71.3	71.0
267.0	80.4	80.4	267.0	71.3	71.0

## Variation of Wall Temperature with L/D Ratio.

Table C-7.

Table C-8.

Table C-7.			Table C-8.		
Weight Flow - 0.70 lbs/hr.			Weight Flow - 0.685 lbs/hr.		
N <sub>Rei</sub> - 1082			N <sub>Rei</sub> - 1014		
t <sub>i</sub> (C.L) - 121.5 °F			t <sub>i</sub> (C.L) - 143.5 °F		
L/D	t <sub>w</sub> °F	t <sub>o</sub> °F	L/D	t <sub>w</sub> °F	t <sub>o</sub> °F
0		69.5	0		81.6
5.5	92.3	69.5	5.5	110.3	81.6
15.9	84.8	69.5	15.9	100.7	81.6
33.1	82.5	69.5	33.1	95.4	81.6
46.9	77.8	69.5	46.9	91.9	81.6
64.2	75.8	69.5	64.2	88.8	81.6
88.3	74.0	69.5	88.3	86.2	81.6
136.6	72.2	69.6	136.6	83.0	80.1
178.0	71.0	69.6	178.0	80.4	80.1
219.3	70.4	69.6	219.3	80.2	80.1
267.0	70.4	69.6	267.0	79.1	80.1

## Variation of Wall Temperature with L/D Ratio.

Table C-9.

Table C-10.

Table C-9.			Table C-10.		
Weight Flow - 0.64 lbs/hr.			Weight Flow - 0.912 lbs/hr.		
N <sub>Rei</sub> - 1022			N <sub>Rei</sub> - 1415		
t <sub>i</sub> (C.L.) - 107.2 °F			t <sub>i</sub> (C.L.) - 113.5 °F		
L/D	t <sub>w</sub> °F	t <sub>o</sub> °F	L/D	t <sub>w</sub> °F	t <sub>o</sub> °F
0		79.3	0		77.2
5.5	93.2	79.3	5.5	95.4	77.2
15.9	88.6	79.3	15.9	90.6	77.2
33.1	86.7	79.3	33.1	87.0	77.2
46.9	84.6	79.3	46.9	85.1	77.2
64.2	83.1	79.3	64.2	83.5	77.2
88.3	81.8	79.3	88.3	81.9	77.2
136.6	79.8	78.5	136.6	79.6	77.2
178.0	78.5	78.5	178.0	78.8	77.2
			219.3	78.5	77.2
			267.0	78.1	77.2

## Variation of Wall Temperature with L/D Ratio.

Table C-11.

Table C-12.

Table C-11			Table C-12		
Weight Flow - 1.06 lbs/hr.			Weight Flow - 0.96 lbs/hr.		
$N_{Rei}$ - 1513			$N_{Rei}$ - 1515		
$t_i$ (C.L) -126.6 °F			$t_i$ (C.L) - 110.8 °F		
L/D	$t_w$ °F	$t_o$ °F	L/D	$t_w$ °F	$t_o$ °F
0		68.7	0		73.3
5.5	98.5	68.7	5.5	91.5	73.3
15.9	90.2	68.7	15.9	86.4	73.3
33.1	84.0	68.7	33.1	83.0	73.3
46.9	81.0	68.7	46.9	80.9	73.3
64.2	78.7	68.7	64.2	79.2	73.3
88.3	75.9	68.7	88.3	77.4	73.3
136.6	72.9	68.9	136.6	76.9	73.0
178.0	72.3	68.9	178.0	74.5	73.0
219.3	71.4	68.9	219.3	74.5	73.0
267.0	70.4	68.9	219.3	74.4	73.0

## Variation of wall Temperature with L/D ratio.

Table C-13.

Table C-14.

Table C-13.			Table C-14.		
Weight Flow - 0.89 lbs/hr.			Weight Flow - 1.3 lbs/hr.		
$N_{Rei}$ - 1535			$N_{Rei}$ - 1820		
$t_i$ (C.L) - 81.0 °F			$t_i$ (C.L) - 153.4 °F		
L/D	$t_w$ °F	$t_o$ °F	L/D	$t_w$ °F	$t_o$ °F
0		70.7	0		73.4
5.5	75.7	70.7	5.5	115.4	73.4
15.9	74.1	70.7	15.9	105.5	73.4
33.1	73.2	70.7	33.1	97.2	73.4
46.9	72.6	70.7	46.9	92.5	73.4
64.2	72.1	70.7	64.2	88.7	73.4
88.3	71.9	70.7	88.3	85.0	73.4
136.6	71.5	70.1	136.6	81.0	73.4
178.0	71.3	70.1	178.0	78.8	73.4
219.3	71.1	70.1	219.3	78.6	73.4
267.0	71.1	70.1	267.0	77.4	73.4

## Variation of Wall Temperature with L/D Ratio.

Table C-15

Table C-16

Table C-15			Table C-16		
Weight Flow - 1.37 lbs/hr.			Weight Flow - 1.98 lbs/hr.		
N <sub>Rei</sub> - 1965			N <sub>Rei</sub> - 3020		
t <sub>i</sub> (C.L) - 144.6 °F			t <sub>i</sub> (C.L) - 122.5 °F		
L/D	t <sub>w</sub> °F	t <sub>o</sub> °F	L/D	t <sub>w</sub> °F	t <sub>o</sub> °F
0		71.9	0		77.7
5.5	109.1	71.9	5.5	100.6	77.7
15.9	100.1	71.9	15.9	95.6	77.7
33.1	94.1	71.9	33.1	93.0	77.7
46.9	89.6	71.9	46.9	90.2	77.7
64.2	86.9	71.9	64.2	88.6	77.7
88.3	84.1	71.9	88.3	87.0	77.7
136.6	79.6	71.4	136.6	84.4	77.8
178.0	78.3	71.4	178.0	83.6	77.8
219.3	76.8	71.4	219.3	82.2	77.8
267.0	75.2	71.4	267.0	81.0	77.8

## Variation of Wall Temperature with L/D Ratio.

Table C-17

Table C-18

Table C-17			Table C-18		
Weight Flow - 1.88 lbs/hr.			Weight Flow - 1.83 lbs/hr.		
N <sub>Rei</sub> - 3050			N <sub>Rei</sub> - 3100		
t <sub>i</sub> (C.L) = 97.1 °F			t <sub>i</sub> - 86.0 °F		
L/D	t <sub>w</sub> °F	t <sub>o</sub> °F	L/D	t <sub>w</sub> °F	t <sub>o</sub> °F
0		77.6	0		71.3
5.5	88.1	77.6	5.5	78.6	71.3
15.9	86.3	77.6	15.9	76.9	71.3
33.1	84.4	77.6	33.1	76.1	71.3
46.9	83.3	77.6	46.9	75.2	71.3
64.2	82.7	77.6	64.2	74.7	71.3
88.3	81.8	77.6	88.3	74.3	71.3
136.6	80.4	77.9	136.6	73.5	71.4
178.0	79.7	77.9	178.0	73.0	71.4
219.3	79.5	77.9	219.3	72.8	71.4
267.0	79.3	77.9	267.0	72.0	71.4

## Variation of Wall Temperature with L/D Ratio.

Table C-19.

Table C-20.

Table C-19			Table C-20		
Weight Flow - 1.75 lbs/hr.			Weight Flow - 1.92 lbs/hr.		
$N_{Rei}$ - 2975			$N_{Rei}$ - 3010		
$t_i$ (C.L) - 87.8 °F			$t_i$ (C.L) - 115.7 °F		
L/D	$t_w$ °F	$t_o$ °F	L/D	$t_w$ °F	$t_o$ °F
0		76.8	0		79.5
5.5	82.1	76.8	5.5	99.0	79.5
15.9	81.1	76.8	15.9	95.5	79.5
33.1	80.7	76.8	33.1	93.0	79.5
46.9	80.1	76.8	46.9	90.5	79.5
64.2	79.2	76.8	64.2	89.3	79.5
88.3	78.7	76.8	88.3	87.4	79.5
136.6	77.6	75.8	136.6	84.9	79.5
178.0	76.8	75.8	178.0	84.3	79.5
219.3	76.8	75.8	219.3	83.4	79.5
267.0	76.8	75.8	267.0	82.5	79.5

## Variation of Wall Temperature with L/D Ratio.

Table C-21.

Table C-22.

Table C-21			Table C-22		
Weight Flow - 2.38 lbs/hr.			Weight Flow - 2.32 lbs/hr.		
N <sub>Rei</sub> - 4060.			N <sub>Rei</sub> - 4000		
t <sub>i</sub> (C.L) - 92.5 °F			t <sub>i</sub> (C.L) - 91.7 °F		
L/D	t <sub>w</sub> °F	t <sub>o</sub> °F	L/D	t <sub>w</sub> °F	t <sub>o</sub> °F
0		70.6	0		70.4
5.5	82.1	70.6	5.5	81.6	70.4
15.9	79.6	70.6	15.9	79.4	70.4
33.1	78.4	70.6	33.1	77.8	70.4
46.9	77.0	70.6	46.9	76.5	70.4
64.2	76.3	70.6	64.2	75.9	70.4
88.3	75.7	70.6	88.3	75.2	70.4
136.6	74.3	71.0	136.6	73.9	70.1
178.0	73.6	71.0	178.0	73.2	70.1
219.3	73.5	71.0	219.3	73.0	70.1
267.0	72.9	71.0	267.0	72.4	70.1

## Variation of Wall Temperature with L/D Ratio.

Table C-23.

Table C-24.

Table C-23			Table C-24		
Weight Flow - 2.21 lbs/hr.			Weight Flow - 2.93 lbs/hr.		
$N_{Rei}$ - 3940			$N_{Rei}$ - 3880		
$t_i$ (C.L) - 129.5 °F			$t_i$ (C.L) - 173.9 °F		
L/D	$t_w$ °F	$t_o$ °F	L/D	$t_w$ °F	$t_o$ °F
0		73.8	0		82.0
5.5	103.5	73.8	5.5	131.5	82.0
15.9	97.4	73.8	15.9	121.5	82.0
33.1	93.5	73.8	33.1	114.8	82.0
46.9	91.1	73.8	46.9	112.6	82.0
64.2	89.9	73.8	64.2	110.0	82.0
88.3	87.6	73.8	88.3	106.3	82.0
136.6	84.5	73.7	136.6	104.3	81.1
178.0	82.7	73.7	178.0	100.0	81.1
219.3	81.9	73.7	219.3	96.0	81.1
267.0	80.5	73.7	267.0	91.0	81.1

## APPENDIX - D

Variation of Local Nusselt Number  $N_{Nux}$ , with  $t_m/t_w$   
at  $L/D = 24.5$

(The local Nusselt number  $N_{Nux}$ , mean temperature  $t_m$ , and wall temperature  $t_w$ , at  $L/D = 24.5$  were evaluated and interpreted by taking observations at  $L/D = 15.9$  &  $33.1$  respectively.)

$N_{Rei}$	$N_{Rex}$	$N_{Nux}$	$t_i$ OF	$t_m$ OF	$t_w$ OF
<u>Table D-1.</u>					
608	611	5.27	82.6	76.7	74.3
590	612	6.73	111.5	90.4	82.0
620	672	6.5	143.4	113.0	98.8
615	619	2.5	85.0	83.5	82.4
594	608	6.0	94.0	86.7	82.7
575	596	5.7	107.0	94.6	88.1
<u>Table D-2.</u>					
636	996	6.7	648.0	306.9	231.9
1020	1022	4.22	79.3	75.6	72.6
1082	1112	5.11	121.5	98.2	83.7
1014	1070	5.25	143.5	116.3	98.1
1022	1052	5.9	108.0	96.5	87.7
987	992	6.33	86.0	83.7	81.6

Variation of Local Nusselt Number  $N_{Nux}$ , with  $t_m/t_w$   
at  $L/D = 24.5$

( The local Nusselt number  $N_{Nux}$ , mean temperature  $t_m$ , and wall temperature  $t_w$ , at  $L/D = 24.5$  were evaluated and interpreted by taking observations at  $L/D = 15.9$  &  $33.1$  respectively.

$N_{Rei}$	$N_{Rex}$	$N_{Nux}$	$t_i$ OF	$t_m$ OF	$t_w$ OF
<u>Table D-3.</u>					
1415	1445	8.65	113.5	98.9	88.8
1535	1537	6.43	81.0	77.3	73.9
1513	1550	7.68	126.6	104.0	87.1
1470	1524	4.7	131.5	117.8	100.4
1509	1546	6.0	104.5	97.5	87.5
1513	1531	4.8	90.0	85.9	81.8
<u>Table D-4.</u>					
1900	1941	4.38	115.5	99.2	85.8
1955	2005	7.0	144.6	119.5	97.1
1965	1985	5.3	94.0	90.4	85.1
2043	2088	5.8	120.8	111.1	98.6
2022	2080	4.6	118.5	106.3	91.2

Variation of Local Nusselt Number  $N_{Nux}$  with  $t_m/t_w$

at  $L/D = 24.5$

(The local Nusselt number  $N_{Nux}$ , mean temperature  $t_m$ , and wall temperature  $t_w$ , at  $L/D = 24.5$  were evaluated and interpreted by taking observations at  $L/D = 15.9$  &  $33.1$  respectively.)

$N_{Rei}$	$N_{Rex}$	$N_{Nux}$	$t_i$ $^{\circ}F$	$t_m$ $^{\circ}F$	$t_w$
<u>Table D-5.</u>					
3175	3238	8.85	135.5	118.0	98.1
3100	3128	8.39	97.2	90.7	84.2
2975	2978	5.12	87.8	85.1	80.9
2772	2840	6.94	142.1	123.1	100.9
3020	3040	7.29	122.5	109.0	94.3
2903	2959	11.5	112.5	104.4	88.3
3014	3045	7.0	96.5	93.0	86.3
2953	2964	8.2	87.0	85.6	83.1
<u>Table D-6.</u>					
3940	3970	9.48	129.5	113.7	95.4
3880	3930	7.32	173.9	150.6	116.7
4060	4070	10.94	93.7	85.9	79.0
3998	4005	7.61	89.7	83.3	76.9
3886	3933	9.9	111.5	106.7	93.5

## APPENDIX E

## ANALYSIS AND EFFECT OF TEMPERATURE ERRORS

For computing the true temperature of a gas from the reading of a thermocouple, placed in a gas stream and in sight of surrounding walls that may be at various temperatures, a heat balance is used and is given by:

$$q_{gr} + q_c = q_r + q_k$$

where  $q_{gr}$  is the rate of heat flow between gas and the thermocouple by the mechanism of gas radiation,  $q_c$  is the rate of heat flow between gas and thermocouple by convection,  $q_r$  is the sum of various terms representing the radiant heat interchange between the thermocouple and the various surfaces that it sees, and  $q_k$  is the heat conducted from the thermocouple to the walls confining the gas stream. In the case of a gas stream having a true temperature  $T_g$  and flowing through a duct of diameter large compared with that of the thermocouple at temperature  $T_t$ , the inner surfaces of the wall having constant temperature  $T_w$ , a heat balance on the thermocouple gives the equation:

$$q_{gr} + h_c A_t (T_g - T_t) = 0.171 (\epsilon_t A_t) \left[ \left( \frac{T_t}{100} \right)^4 - \left( \frac{T_w}{100} \right)^4 \right] + q_k \dots (21)$$

where  $h_c$  is the convective heat transfer coefficient,  $\epsilon_t$  is the emissivity of the surface and  $A_t$  is the surface area of the thermocouple.

Equation (21) may also be written as:

$$q_{gr} + h_c A_t (t_g - t_t) = h_r A_t (t_t - t_w) + q_k \dots (22)$$

where  $h_r$  is the radiation heat transfer coefficient. For the present investigation  $q_{gr}$  and  $q_k$  are negligible compared with  $q_c$  and  $q_r$ . Equation (22) simplifies to:

$$t_g - t_t = (t_t - t_w) (h_r/h_c) \quad \dots \quad (23)$$

For the thermocouples used  $h_r$  and  $h_c$  can be assumed to have the values equal to 4 (Ref.21) and 25 (Ref.32) respectively.

Figure B shows a typical pipe section

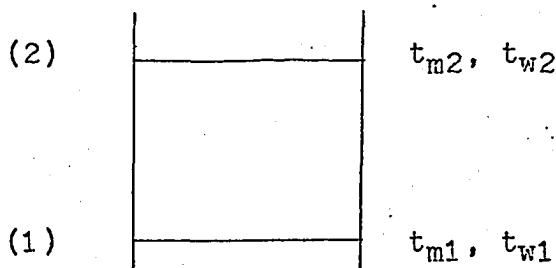


Fig B.

$t_{m1}$  &  $t_{w1}$  are the mean and wall temperatures at (1),  $t_{m2}$  &  $t_{w2}$  are the mean and wall temperatures at (2). We assume that  $t_{m1}$  and  $t_{m2}$  need correction whereas  $t_{w1}$  and  $t_{w2}$  are correct.

The effect on the local Nusselt number due to the temperature correction is given below:

FOR LOW TEMPERATURE:

Typical values of  $t_{m1}$ ,  $t_{w1}$ ,  $t_{m2}$  and  $t_{w2}$  are

$$t_{m1} = 120.3^{\circ}\text{F}$$

$$t_{w1} = 100.7^{\circ}\text{F}$$

$$t_{m2} = 112.2^{\circ}\text{F}$$

$$t_{w2} = 95.4^{\circ}\text{F}$$

corrected values of  $t_{m1}$  and  $t_{m2}$  are:

$$\begin{aligned} t_{m1c} &= 120.3 + (120.3 - 100.7) \times 4/25 \\ &= 123.4^{\circ}\text{F} \end{aligned}$$

$$t_{m2c} = 112.2 + (112.2 - 95.4) \times 4/25$$

$$= 114.9^{\circ} \text{ F}$$

$$N_{Nux} = \text{Constant} \times \frac{(t_{m1} - t_{m2})}{\left( \frac{t_{m1} + t_{m2}}{2} - \frac{t_{w1} + t_{w2}}{2} \right)}$$

$$N_{Nux} \text{ (Before correction)}$$

$$= \text{Constant} \times \frac{120.3 - 112.2}{\frac{232.5}{2} - \frac{196.1}{2}}$$

$$= \text{Constant} \times 0.445$$

$$N_{Nux} \text{ (After Correction)}$$

$$= \text{Constant} \times \frac{123.4 - 114.9}{\frac{238.3}{2} - \frac{196.1}{2}}$$

$$= \text{Constant} \times 0.403$$

In the above example with the temperatures as chosen the correct value of the local Nusselt number is 9.5% lower than the value calculated without temperature correction.

FOR HIGH TEMPERATURE:

Typical values of  $t_{m1}$ ,  $t_{w1}$ ,  $t_{m2}$  and  $t_{w2}$  are:

$$t_{m1} = 456.0^{\circ} \text{ F} \qquad t_{w1} = 262.7^{\circ} \text{ F}$$

$$t_{m2} = 416.0^{\circ} \text{ F} \qquad t_{w2} = 229.0^{\circ} \text{ F}$$

Corrected values of  $t_{m1}$  and  $t_{m2}$  are:

$$t_{m1c} = 456.0 + (456.0 - 262.7) \times 4/25$$

$$= 486.9^{\circ} \text{ F}$$

$$\begin{aligned}
 t_{m2c} &= 416.0 + (416.0 - 229.0) \times 4/25 \\
 &= 446.0^\circ \text{ F}
 \end{aligned}$$

$N_{Nux}$  (Before correction)

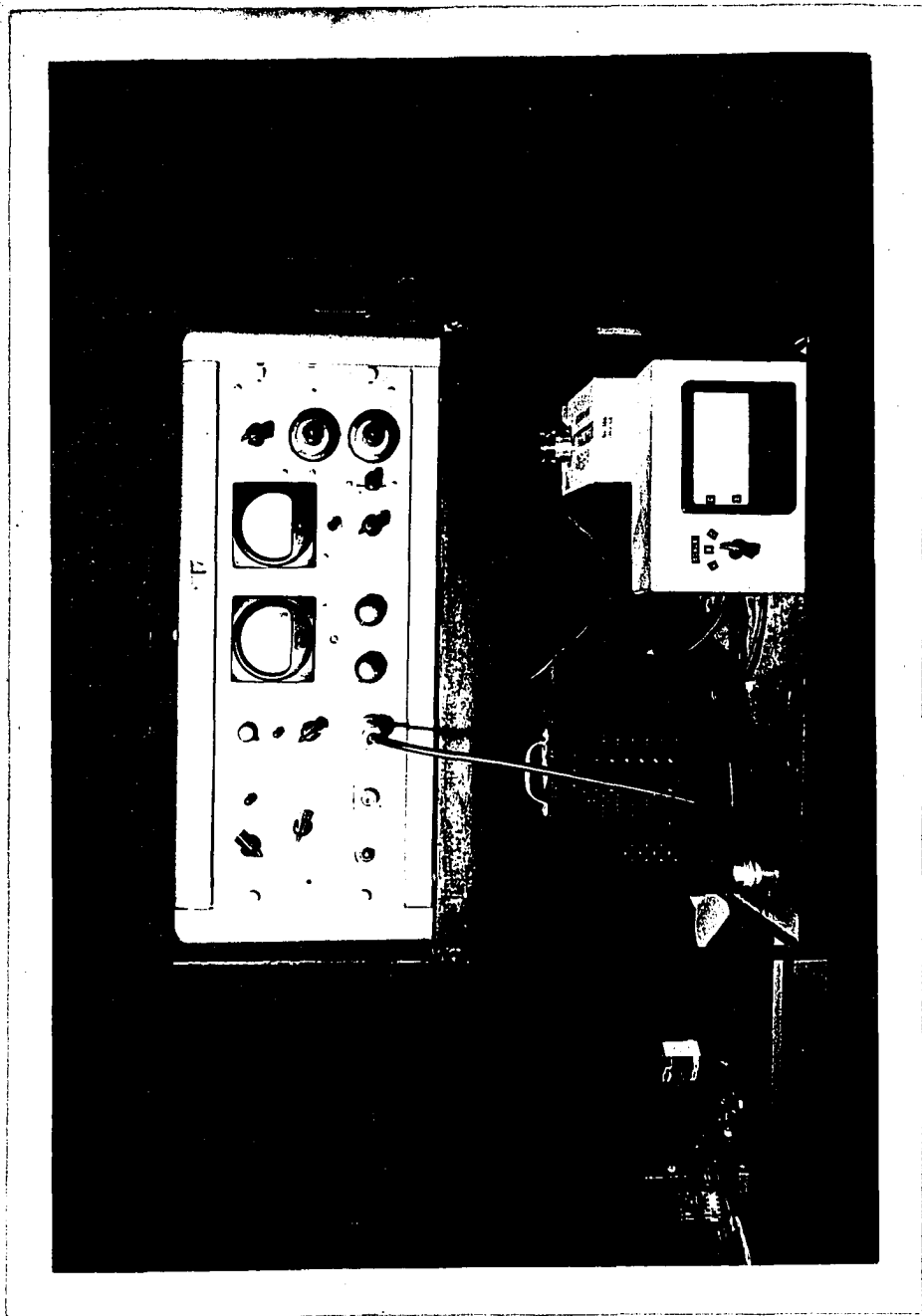
$$\begin{aligned}
 &= \text{Constant} \times \frac{456.0 - 416.0}{\frac{872.0}{2} - \frac{491.7}{2}} \\
 &= \text{Constant} \times 0.21
 \end{aligned}$$

$N_{Nux}$  (After correction)

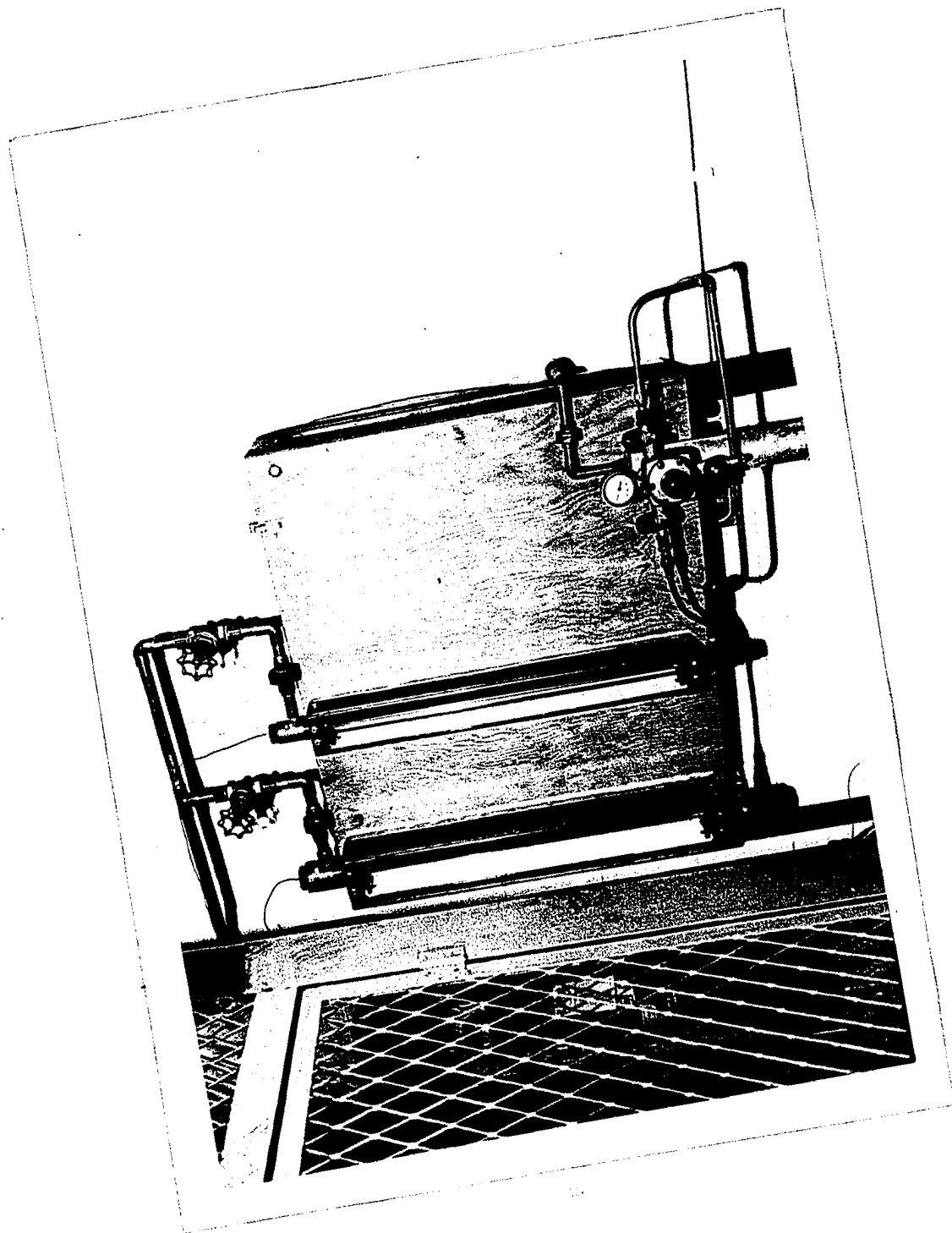
$$\begin{aligned}
 &= \text{Constant} \times \frac{486.9 - 446.0}{\frac{932.9}{2} - \frac{491.7}{2}} \\
 &= \text{Constant} \times 0.185
 \end{aligned}$$

In the above example with the temperatures as chosen the correct value of the local Nusselt number is 12% lower than the value calculated without temperature correction.

The local Nusselt numbers as given in graphs and tables could be as high as 15% above the correct value. As the L/D ratio increases, the percentage error will decrease becoming small at high L/D.

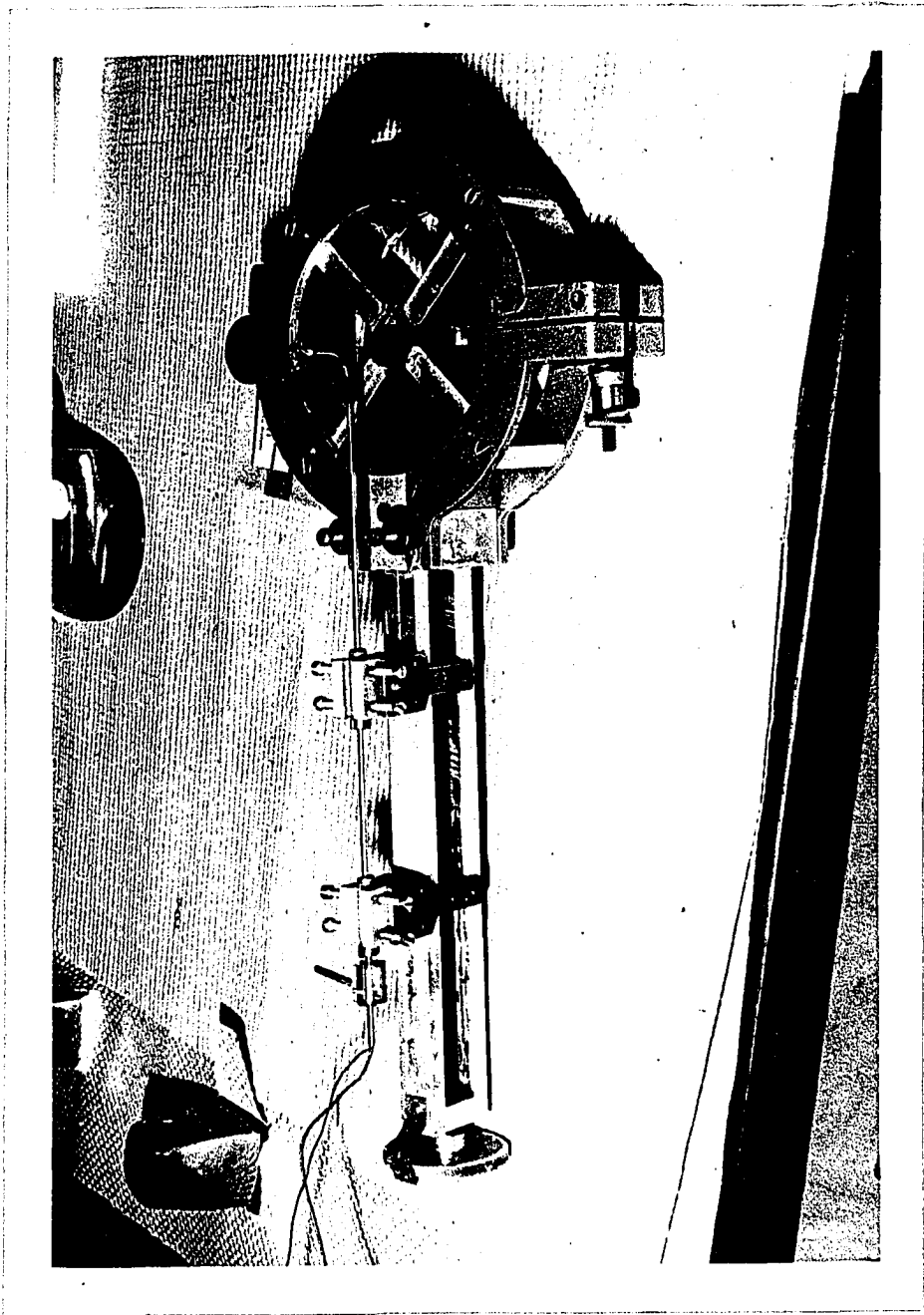


F-1. HOT WIRE ANEMOMETER.

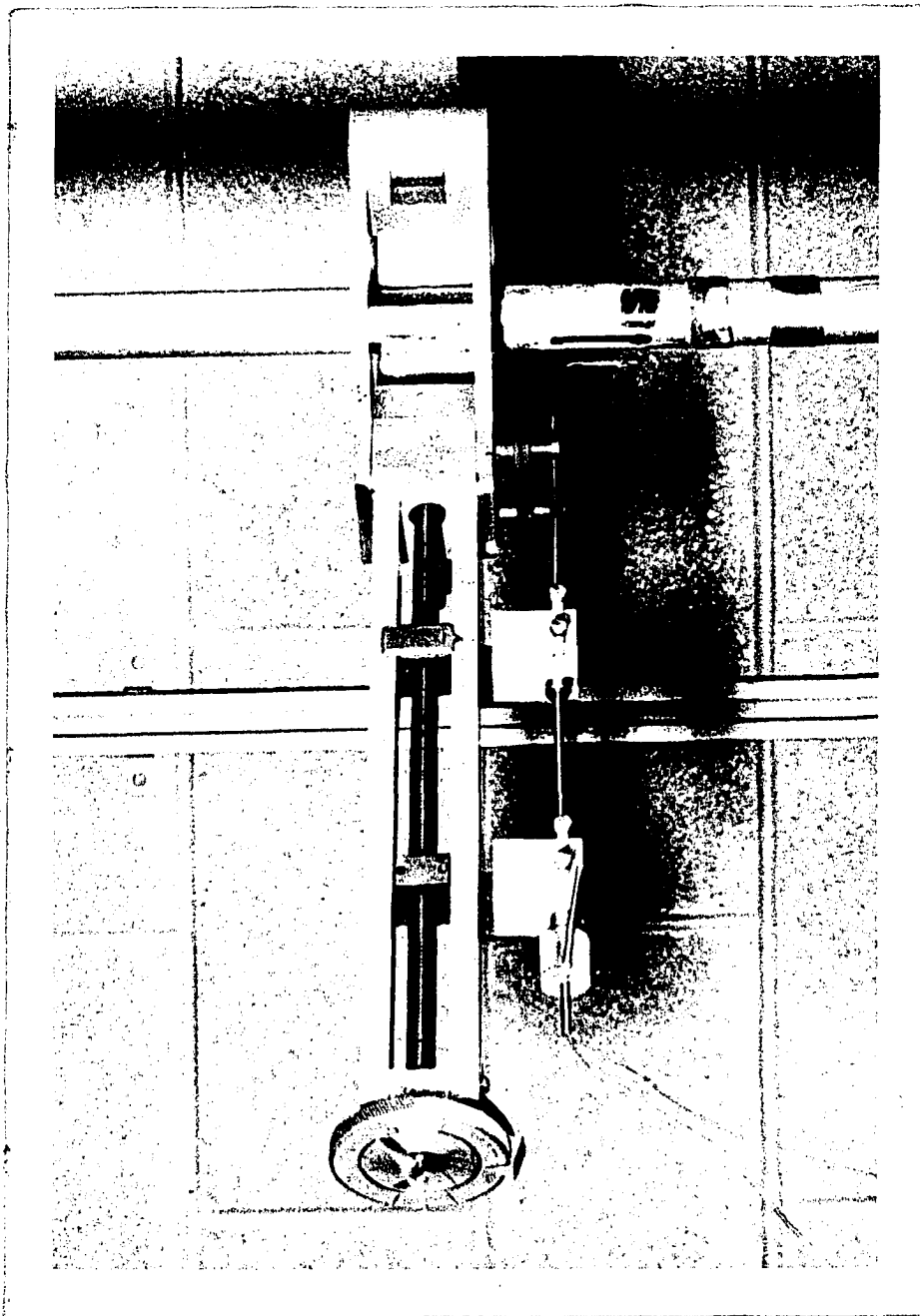


F-2. ROTAMETERS.

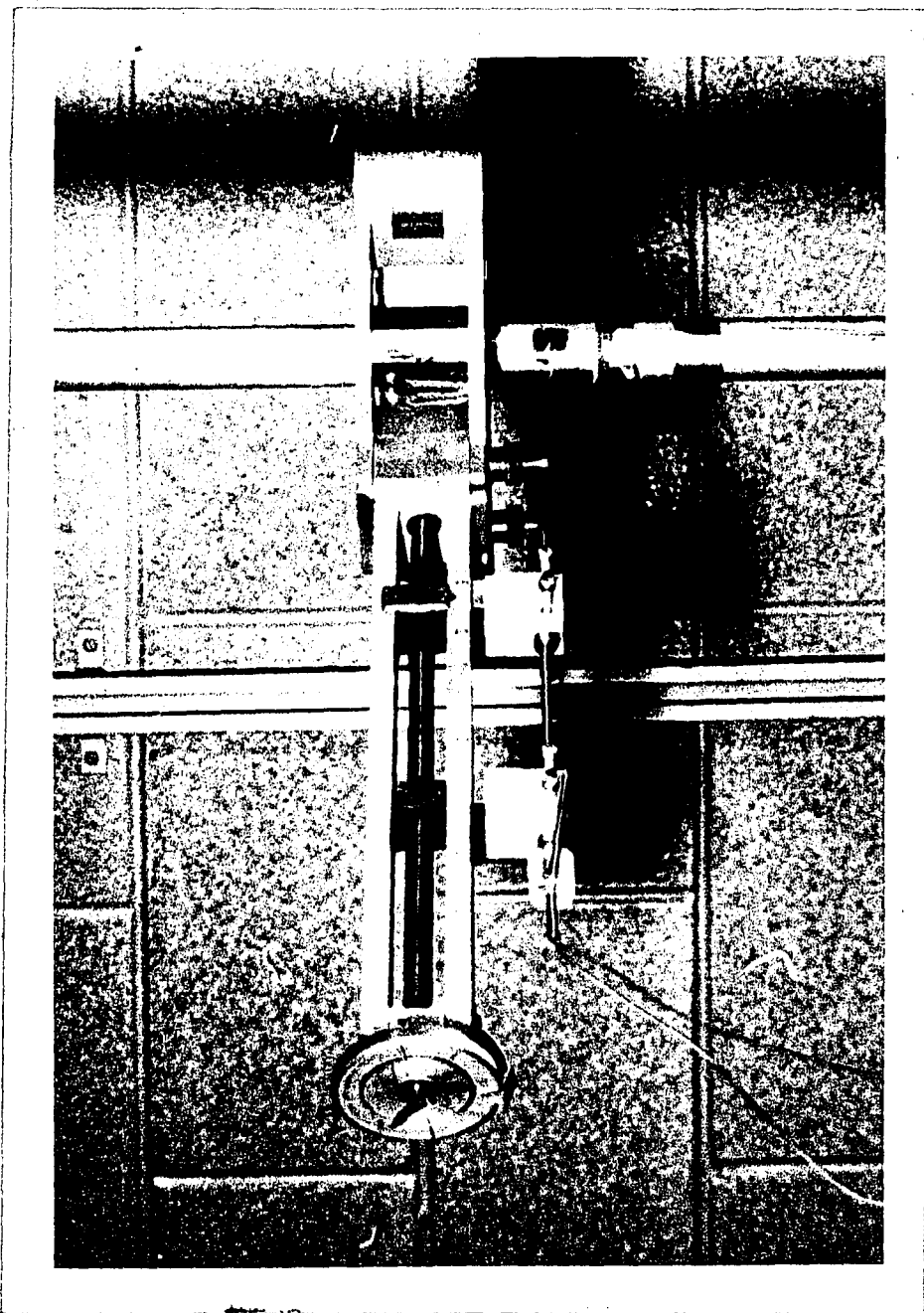
Reproduced with permission of the copyright owner. Further reproduction prohibited without permission.



F-3. TRAVERSING MECHANISM WITH THERMOCOUPLE IN POSITION.



F-4. TRAVERSING MECHANISM ON THE PIPE SHOWING THE PROBE OUT SIDE THE SLOT.



F-5. TRAVERSING MECHANISM ON THE PIPE SHOWING THE PROBE INSIDE THE SLOT.

## VITA AUCTORIS

- 1940 Born in Simla, India on Sept. 14
- 1956 Finished Higher Secondary School (Harcourt Butler Higher Secondary School, New Delhi, India)
- 1958 Finished 2nd year B Sc., Physics (Hons) (St. Stephens College, Delhi, India)
- 1962 Received the Bachelor's Degree with Honours in Mechanical Engineering from Indian Institute of Technology, Kharagpur India. Joined the engineering staff of Heavy Engineering Corporation Ltd, Ranchi, India
- 1969 Candidate for the Degree of Master of Applied Science in Mechanical Engineering at the University of Windsor, Windsor Ontario, Canada